M 2016

U.PORTO
FEUP FACULDADE DE ENGENHARIA
UNIVERSIDADE DO PORTO

DEVELOPMENT OF CHITOSAN-GRAFTED POLYCAPROLACTONE COPOLYMER FOR MUCOADHESIVE NANODELIVERY SYSTEMS

ANDREIA MARINA DE SOUSA ALMEIDA

DISSERTAÇÃO DE MESTRADO APRESENTADA
À FACULDADE DE ENGENHARIA DA UNIVERSIDADE DO PORTO EM
ENGENHARIA BIOMÉDICA

U.PORTO
FEUP FACULDADE DE ENGENHARIA UNIVERSIDADE DO PORTO

MEB - MESTRADO EM ENGENHARIA BIOMÉDICA **2015/2016**

A Dissertação intitulada

"Development of Chitosan-Grafted Polycaprolactone Copolymer for Mucoadhesive Nanodelivery Systems"

foi aprovada em provas realizadas em 27-06-2016

o júri

Presidente Prof. Doutor José Alberto Peixoto Machado da Silva
Professor Associado do Departamento de Engenharia Eletrotécnica e de Computadores da FEUP da Uporto

Prof.ª Doutora Maria Benedita Almeida Garrett de Sampaio Maia
Professora Auxiliar da Faculdade de Medicina Dentária da Uporto

Doutor Bruno Filipe Carmelino Cardoso Sarmento
Investigador do Instituto de Engenharia Biomédica da Uporto

O autor declara que a presente dissertação (ou relatório de projeto) é da sua exclusiva autoria e foi escrita sem qualquer apoio externo não explicitamente autorizado. Os resultados, ideias, parágrafos, ou outros extratos tomados de ou inspirados em trabalhos de outros autores, e demais referências bibliográficas usadas, são corretamente citados.

Autor - Andreia Marina de Sousa Almeida

Faculdade de Engenharia da Universidade do Porto

Blank page

Faculdade de Engenharia da Universidade do Porto

Development of chitosan-grafted polycaprolactone copolymer for mucoadhesive nanodelivery systems

Andreia Marina de Sousa Almeida

Dissertation for the Master Thesis in Biomedical Engineering

Supervisor: Bruno Sarmento, Ph.D.

June, 2016

Blank page

“Success is getting what you want.

Happiness is wanting what you get”

Dale Carnegie

Blank page

Resumo

Durante a última década, uma vasta gama de formulações para a administração oral de fármacos anticancerígenos tem sido utilizada na prática clínica. No entanto, este desenvolvimento é dificultado pela baixa solubilidade nos fluidos gástricos e intestinais e consequente diminuta biodisponibilidade destes fármacos. Assim, o uso de veículos transportadores de fármacos, como as micelas poliméricas, está a ser amplamente investigado como estratégia de formulação devido à sua capacidade de encapsular fármacos de forma estável e com grande eficiência, aumentando a sua solubilidade e possibilitando ainda a sua penetração nos tecidos devido ao seu pequeno tamanho. Nesta dissertação, foram produzidas micelas poliméricas à base de quitosano (CS) e policaprolactona (PCL) com o objetivo de melhorar o perfil farmacocinético do paclitaxel (PTX), após a administração oral. Copolímeros de quitosano e policaprolactona (CS-*g*-PCL) foram sintetizados através de uma reação carbodiimida por amidação sendo caracterizados por transformada de Fourier de espectroscopia de infravermelho (FTIR), análise de ressonância magnética nuclear (RMN) e ângulo de contacto. Os resultados sugerem a formação do copolímero através do aparecimento de bandas amidas no espetro de FTIR, pelo aparecimento dos picos de ambos os polímeros no espectro do novo copolímero na análise de RMN e ainda pela maior hidrofobicidade quando em contacto com a água. Averiguou-se a concentração micelar crítica (CMC) do copolímero formado pelo método condutimétrico, obtendo-se a concentração de 3.7×10^{-3} mg/mL. A caracterização morfológica das micelas foi realizada por microscopia eletrónica de transmissão (TEM) e a determinação do diâmetro médio, índice de polidispersão e carga superficial foram determinados por espalhamento de luz dinâmico (DLS) e espalhamento de luz eletroforético (ELS), respetivamente, obtendo-se valores de 408 nm, 0,335 e 30,9 mV para a formulação otimizada, escolhida para os ensaios subsequentes. A eficiência de encapsulação (82%) foi determinada por cromatografia líquida de alta performance (HPLC). O perfil de libertação do PTX encapsulado nas micelas e do PTX livre foi estudado *in vitro* em condições intestinais simuladas. Verificou-se que as micelas controlaram a libertação por até 8 h. A citotoxicidade dos polímeros CS e PCL, do copolímero, das micelas com PTX encapsulado e o PTX livre foi testada contra células epiteliais intestinais (HT29-MTX e Caco-2). Verificou-se ausência de toxicidade para os polímeros isoladamente nas concentrações testadas. O copolímero apresentou toxicidade à maior concentração testada (1 mg/mL). O aumento da concentração de PTX livre e de micelas com PTX encapsulado levaram à diminuição da viabilidade celular, contudo, o sistema micelar apresentou sempre menor toxicidade em comparação com o fármaco livre. Por fim, foi realizado o ensaio de permeabilidade para o fármaco livre e para o sistema micelar em modelo de monocultura de células Caco-2 e em modelo de co-cultura de células Caco-2/HT29-MTX. Verificou-se que o sistema micelar desenvolvido teve uma permeação superior ao fármaco livre nos dois modelos intestinais testados. Assim, o sistema micelar desenvolvido mostrou ultrapassar as barreiras fisiológicas com desempenho superior ao anticancerígeno atualmente utilizado em terapia clínica. Pode concluir-se que o sistema micelar realizado no âmbito desta dissertação apresenta potencial para ser utilizado como sistema de libertação de fármacos hidrofóbicos, nomeadamente fármacos anticancerígen

Blank page

Abstract

During the last decade, a wide range of formulations for oral administration of anticancer drugs have been used in clinical practice. However, this development is sometimes hampered by low solubility in gastric and intestinal fluids and consequent decrease in bioavailability of these drugs. Thus, the use of drug carriers, such as polymeric micelles, is being widely investigated as strategy of formulation due to its ability to encapsulate drugs in a stable way with great efficiency, increasing its solubility and also allowing tissue penetration due to their small size. In this dissertation, polymeric micelles were produced based on chitosan (CS) and polycaprolactone (PCL) in order to improve the pharmacokinetic profile of paclitaxel (PTX) after oral administration. Chitosan-grafted-polycaprolactone (CS-*g*-PCL) copolymer was synthesized through a carbodiimide reaction by amidation being subsequently, characterized by Fourier Transform Infrared Spectroscopy (FTIR), Nuclear Magnetic Resonance analysis (NMR) and contact angle. The results suggest the formation of a new copolymer by the appearance of amide bands in the FTIR spectrum, appearance of both polymers peaks in the new copolymer spectrum in NMR analysis and, also higher hydrophobicity when in contact with water. The critical micelle concentration (CMC) of the copolymer, investigated by conductimetric method, was 3.7×10^{-3} mg/mL. The micelles morphology was characterized using transmission electron microscopy (TEM) and the determination of the average diameter, polydispersity index and surface charge were determined by dynamic light scattering (DLS) and electrophoretic light scattering (ELS), respectively, obtaining values of 408 nm, 0.335 and 30.9 mV for the optimized formulation chosen for subsequent tests. The encapsulation efficiency (82%) was determined by high performance liquid chromatography (HPLC). The release profile of free PTX and PTX loaded micelles was studied *in vitro* in simulated intestinal conditions. The micelles were able to control the drug release up to 8 hours. The cytotoxicity of CS and PCL polymers, copolymer, the PTX loaded micelles and free PTX was tested against intestinal epithelial cells (HT29-MTX and Caco-2). It was observed the absence of toxicity to polymers individually for all tested concentrations. The copolymer presented toxicity at the highest concentration tested (1 mg/mL). The increase of free PTX and PTX loaded micelles led to a decreased of cell viability, however, the micellar system showed lower toxicity when compared to the free PTX. Finally, it was performed the permeability assay for the free drug and the micellar system in the Caco-2 monoculture model and Caco-2/HT29-MTX co-culture model. It was observed that the micellar system developed had superior permeation of PTX when compared to the free drug in both intestinal models tested. Thus, the micellar system developed was able to overcome the physiological barriers with better performance than the anticancer drug currently used in clinical therapy. Therefore, it can be concluded that the PTX-CS-g-PCL micelles developed in this dissertation is a potential drug carrier for the controlled release of hydrophobic drugs, particularly, anticancer agents.

Blank page

Acknowledgements

First of all, I would like to thank all my family, but particularly my parents, who always believed in me, for their unconditional love and support over all these academic years. My brother and my sister in law, by their wise advices and to my dear goddaughter, Joana, for all contagious joy, even after a hard day of work. A heartfelt thanks to João, my boyfriend, for all the help, support and care during these two years. Without you it would not be possible.

My sincere thanks to FEUP - Faculdade de Engenharia da Universidade do Porto, INEB – Instituto de Engenharia Biomédica/i3S- Instituto de Investigação e Inovação em Saúde and iinfacts – Instituto de Investigação e Formação Avançada em Ciências e Tecnologias da Saúde for having accepted me and cooperated in my dissertation.

My supervisor, Professor Bruno Sarmento, to whom I am sincerely grateful for have accepted me as a master student in his team, for all the support and guidance. Thanks to him I started in the world of research, and despite the early days were difficult, today I am grateful and happy for believing in me and for having created me a passion of doing research. It took months of professional exponential growth, but also personal. Thank you!

To all my teammates, but particularly those who worked closely with me - Rute Nunes, Ana Costa, Cassilda Reis, Flávia Sousa and Fabíola Prezotti - for all the fundamental teachings for my growth and success and, above all, for the friendship that we build. A special thanks to Daniella Souza for complicity, by working together, for the laughter and the good mood and high spirits that always brought to the lab. Thanks to all from the heart!

All of my other friends who have grown with me since childhood - Alice Ribeiro, Diana Coelho and Rita Loureiro - and the friends of the city that I bring in my heart - Ana João Nóbrega, Cláudia Montes, Beatriz Pereira, Cristiana Cabral, Sara Ferreira and Marlene Silva - by friendship, support in difficult days and the help that you have been offering me, in one way or another, over the last few years. Thank you!

And last, but far from least, Sofia Marques, friend and classmate, for all the problems, questions and concerns that we had together, for always heard me, and have a positive response to me and encouraging me. Thank you for having been part of this stage, although far but always close. Thanks for the patience, the complicity and for always being there for me.

Blank page

List of Contents

List of Figures

List of Tables

Blank page

Abbreviations and Symbols

List of abbreviations

ALP	**Alkaline phosphatase**
ATCC	**American Type Culture Collection**
ATP	**Adenosine triphosphatase**
ATR	**Attenuated total reflection**
ATR-FTIR	**Attenuated total reflection Fourier transforms infrared spectroscopy**
BCS	**Biopharmaceutic Classification System**
CAC	**Critical aggregation concentration**
$CDCL_3$	**Deuterated chloroform**
CL	**Caprolactone**
CMC	**Critical micelle concentration**
CS	**Chitosan**
CS-*g*-PCL	**Chitosan-grafted-polycaprolactone**
D_2O	**Deuterium oxide**
Da	**Dalton**
DA	**Degree acetylation**
DCC	***N*,*N*'-Dicyclohexylcarbodiimide**
DCM	**Dichloromethane**
DD	**Degree deacetylation**
DL	**Drug loading**
DLS	**Dynamic light scattering**
DMEM	**Dulbecco's Modified Eagle medium**
DMF	**Dimethylformamide**
DMSO	**Dimethyl sulfoxide**

DOX	**Doxorubicin**
DS	**Degree substitution**
EDC	**3-(3-dimethylaminopropyl) carbodiimide**
EE	**Encapsulation efficiency**
ELS	**Electrophorectic light scattering**
EPR	**Enhanced permeability and retention**
FBS	**Fetal Bovine Serum**
FDA	**Food and Drug Administration**
FTIR	**Fourier transform infrared spectroscopy**
Gal-OCMC-g-SA	**Galactosylated *O*-carboxymethyl chitosan-graft-stearic**
GI	**Gastrointestinal**
GlcN	**D-glucosamine units**
GlcNac	**N-acetyl-D-glucosamine units**
HBSS	**Hank's buffered salt solution**
HCl	**Hydrochloric acid**
HPLC	**High performance liquid chromatography**
IC50	**Inhibitory concentration**
i.v.	**Intravenous administration**
M	**Molar**
M-cells	**Microfold cells**
MTT	**3-(4,5-dimethylthiazol-2-yl)-2,5-diphenyltetrazolium bromide**
MTX	**Methotrexate**
Mw	**Molecular weight**
NEAA	**Non-essential amino acids**
NHS	***N*-hydroxisuccimide**
NMR	**Nuclear magnetic resonance**
NOCS	***N*-octyl-*O*-sulfate chitosan**
OCH	**Oleoyl-chitosan**
OCMC	***O*-carboxymethylchitosan**
OTMCS	***N*-octyl-*N*-trimethyl chitosan**
Papp	**Apparent permeability**
PBS	**Phosphate-buffered saline**
PCL	**Polycaprolactone**

PCL-NHS	**Polycaprolactone succinimide ester**
PdI	**Polydispersity index**
P-gp	**P-glycoprotein**
PTX	**Paclitaxel**
PXT-CS-*g*-PCL	**Paclitaxel loaded chitosan-grafted-polycaprolactone micelles**
ROP	**Ring-opening polymerization**
rpm	**Rotations per minute**
RT	**Room temperature**
SD	**Standard deviation**
SEM	**Scanning electron microscopy**
SOC	***N*-succinyl-*N*-octyl chitosan**
Td	**Thermal decomposition temperature**
TEER	**Transepithelial electrical resistance**
TEM	**Transmission electron microscopy**
Tg	**Glass transition temperature**
TJ	**Tight junction**
Tm	**Melting Point**
5-Fu	**5-fluorouracil**

List of Symbols

ε	**Epsilon**
η	**Eta**
μ	**Micro**
Ω	**Omega**
®	**Registered**
ζ	**Zeta**

Blank page

Chapter 1

Introduction

The field of biomedical science is in constant work trying to develop new molecules or drug products capable of performing therapeutic functions. A special regard is given to cancer therapy, as the cure for tumour diseases is far from being achieved, even with appropriate therapeutic conditions. However, much work has been devoted to this area and, gradually, the progress are beginning to be notorious.

1.1 - Context and motivation

The colorectal cancer is a leading cause of death not only in Portugal, but in the world. Although the diversity of treatment methods such as surgery, chemotherapy and radiotherapy, 50% of patients are recidivist in the disease [1]. The efficacy of well-established drugs can be improved with the support of a biomaterial that confers, for example, adequate solubility and further bioavailability. This is the case of many anti-cancer drugs, such as paclitaxel (PTX), with limited efficiency due to low solubility.

PTX is an anticancer drug used in various types of cancer, including colorectal cancer. Its mechanism of action affects the cell division, leading to hyper stabilization of microtubules that stops mitosis in G2 and M phases, leading to cell death [2]. Besides being a hydrophobic drug and, therefore, with low solubility in aqueous environment, its commercial used form, Taxol®, entails drastic side effects to patients due to the employment of organic excipients to provide suitable solubilisation. Thus, currently, the demand of a biomaterial able to encapsulate such drugs is the major focus of research.

Polymeric micelles can be spontaneously formed in aqueous solution using amphiphilic polymers, as result of hydrophobic interactions between the segments of two polymers [3]. These systems have the ability to encapsulate in their hydrophobic inner lipophilic drugs and demonstrated better response in the treatment of disease due to the capacity of the drug to remain in the systemic circulation and the reduction of side effects when compared with the free drug [4]. Moreover, the drug can be protected from adverse conditions of the body such as enzymes or biological fluids, preserving their stability [5].

Chitosan, a natural polymer, has already been described and their properties are primarily based on the fact that is biocompatible, biodegradable, non-toxic and have mucoadhesive properties, which ensures its permanence on the epithelium [6]. Besides, it is proposed here as the ideal candidate to be the hydrophilic component of polymeric micelles due to the presence of reactive groups (NH_2, OH) on its backbone. Thus, CS can be chemically modified by the addition of hydrophobic groups as moieties of polycaprolactone (PCL) allowing the preparation of CS amphiphilic derivatives that are able to self-assemble and form stable micelles [7].

Currently, it is possible to test this type of drug carriers through the intestinal *in vitro* models that mimic very closely the human intestine. These models allow the evaluation of permeability and drug absorption of these systems in order to develop a new one that will overcome all those barriers hitherto, leading to a therapeutically effective effect.

1.2 - Objectives

The main goal of this dissertation was to design a novel polymeric micelles as effective polymer-based drug delivery systems, achieving a controlled release of the encapsulated drug, PTX, in colorectal cancer cells after oral administration. This includes synthetize and characterize a new amphiphilic graft copolymer of CS and PCL with self-assembling properties in aqueous environment; produce polymeric micelles to encapsulate and enhance the solubility and stability of PTX; characterize the physical-chemical properties of micelles and drug kinetics in simulated biological media by an *in vitro* release study; evaluate their toxicity in intestinal cancer cells through the *in vitro* cytotoxicity studies; evaluate the PTX intestinal permeability formulated into polymeric micelles and free PTX in cell-based intestinal models developed by our group as an approach to improve the pharmacokinetic profile and bioavailability of PTX after oral administration.

The rationale for the overall concept of the project arises from the idea of developing a new biomaterial able to form nanosystems for the incorporation of anticancer drugs and, thus find a system capable of operating in the desired target, leading to a therapeutically effective treatment against cancer.

1.3 - Document structure

This dissertation is organised in five chapters. The first chapter is the Introduction, where the context and motivation for this work and the main goals inherent is evaluated. The second chapter is the Literature Review, which is divided into seven sections where is addressed the main problem proposed for this dissertation, the human intestine architecture as well as the models used to evaluate new formulations, a brief description of the anticancer drug used and an approach to polymeric micelles as drug carriers as well as a description the polymers that constitute them. Finally, a short review is made of the methods used to produce this type of copolymer.

Material and Methods of the all work performed is presented in chapter 3. The chapter 4 presents all the results and discussion of the work. Finally, in the last chapter is presented the main findings of this dissertation and referred to future prospects and possible improvements of this work.

Blank page

Chapter 2

Literature Review

The use of drug carriers is of upmost importance for drug delivery, being extensively investigated in pharmaceutical research. Polymer-based drug delivery systems are promising as they enable enhancing therapeutic efficiency, thus, reducing the side effects common to most drugs. This chapter will address the issues related to biomaterials used to produce nanosystems for the encapsulation of hydrophobic drugs, with special attention to anti-cancer drugs with interest on colorectal tumors.

2.1 Colorectal cancer

Cancer is a leading cause of death worldwide and the number of deaths is predictable to continue to increase in the next decades. In Portugal, deaths from cancer increased 0.6% compared to the previous year, being the second cause of death in 2013 [8]. In total, 25.920 people died of cancer in 2013 in Portugal, which corresponds to 24.3% of mortality in the country, over 162 deaths in the previous year. The colorectal cancer is the second most common type of cancer in both men and women in Portugal [8] and the third higher incidence and fourth higher mortality worldwide in both genders [9].

The change in bowel habits (diarrhea or constipation), blood in the stool, abdominal pain, loss of appetite or weight loss are some of the most common symptoms that lead to diagnosis. Carcinoma of the colon and rectum develops from mucosal epithelial cells of these organs, often from precursor or pre-malignant lesions such as polyps. The lower gastrointestinal endoscopy is the method of choice in the diagnosis of these tumors because they allow to view the lining of the rectum and colon and collect small fragments for analysis for histological confirmation.

The treatment of colorectal cancer depends on the location, size, and extent of spread of cancer, as well as the health of the patient [10]. However, the treatment is based on surgery in combination with radiotherapy and/or chemotherapeutic agents such as antimetabolites (5-fluorouracil, 5-FU), topoisomerase inhibitors (doxorubicin, DOX), platinum salts (cisplatin) or taxanes (paclitaxel, PTX) [11], which is given after surgery.

Although tumor resection by surgery and conventional chemotherapy, nearly 50% of patients with colorectal carcinoma return to develop the disease [1]. This method of treatment becomes less effective to the extent that cannot eliminate cancer cell subpopulations with highly aggressive

chemotherapy resistance, the ability to increase the heterogeneity of the tumor and metastases development [12]. Thus, there is an urgent need to develop new approaches that could improve the existing chemotherapeutic treatment.

The advances in nanotechnology have enabled the delivery of anticancer drugs or chemotherapeutic agent through nanocapsules [13], micelles [14] or nanoparticles [15]. These transport vehicles have a great potential since they can overcome some barriers, such as the reduction of systemic toxicity, improving the solubility of biomolecules, particularly hydrophobic molecules and poorly soluble in water [16]. Additionally, these carriers have the ability to prolong the half-life of the drug in systemic circulation because of the lack of functional lymphatic drainage and due to the large abnormal tumor vasculature, which makes them unable to eliminate the biomaterials that were extravagated [17]. Thus, these vehicles tend to accumulate in the tumor over time through a mechanism called enhanced permeability and retention (EPR) effect [18, 19]. Particularly, mucoadhesive nanoparticles can adhere to the mucus slowing the particle transit time in the gut, thereby increasing the time available for the entrapped drug to be released and absorbed. Therefore, is expected a larger drug doses to be directly released to the intestine epithelial cells.

2.2 Intestinal architecture and cell models for permeability studies

Currently, the pharmaceutical industry has a significant interest in the development of *in vitro* human small intestine models in order to evaluate strategies for the improvement the absorption of drugs. Thus, the determination of oral absorption is an important part in the development of new drug carriers. One approach to a simple and reproducible absorption model is to cultivate intestinal cells on permeable membranes, denominated Transwell®.

2.2.1 Anatomy and physiology of gastrointestinal system

The principal function of gastrointestinal (GI) tract is digestion and absorption of nutrients and vitamins that are ingested through food. The GI tract is arranged in order to facilitate this and others functions, being designed to prevent the entry of pathogens or undigested macromolecules. Actually, about 90% of the GI tract absorption occurs in the small intestine [20].

The intestinal tract begins after the stomach with the small intestine (duodenum, jejunum and ileum) and the large intestine (colon). Each part of the GI tract have anatomical, biochemical and physiological properties which command the parameters of digestion and absorption. Intestine wall is composed of layers that are not fully separated from each other, but are joined together by connective tissue and vascular and neuronal elements [21]. As can be seen in **Figure 2.1**, the GI tract is divided into four layers: 1) the mucosa (which is subdivided into epithelium, lamina propria, and muscularis mucosae), 2) the submucosa, 3) the muscularis propria and 4) the serosa.

Mucosa, the innermost layer, is the structural layer and functionally more complex and important because is where absorption occurs. Thus, the mucosa consists of three layers: a first coating layer comprises epithelial cells that are bathed in nutrients, commensal bacteria and mucus [22]. The epithelium is connected to the basal membrane covering the second layer, lamina propria. This layer consists of subepithelial connective tissue, blood capillaries and lymph nodes [21]. The third and deepest layer called the muscularis mucosae, which is constituted by a thin layer of smooth muscle. The submucosa lies between the mucosa and the muscularis propria. The last one is where longitudinal

and circular muscle is present with the goal of boost food through initiation of contractile peristaltic waves regulated by neuronal and hormonal form [23]. The outermost layer is referred to as the serosa which is a protective layer against spread of inflammatory and malignant processes [24].

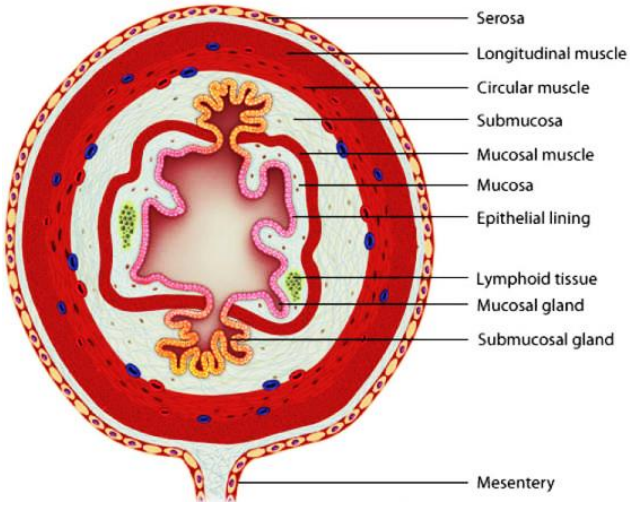

Figure 2.1 – Organization of digestive tract by layers: mucosa, submucosa, muscularis propria and serosa. Adapted from [25].

The epithelium of the small intestine consists of four different cell lines: cells that take up the villi (enterocytes, goblet cells and enteroendocrine) and differentiated cells that reside at the bottom of the crypts and secrete antimicrobial agents, Paneth cells and microfold cells (M-cells) [21, 26] (see **Figure 2.2A**). Crypts are tubular invagination of the intestinal epithelium being characterized by presenting in its base Paneth cells and stem cells, which continuously divide and are the source of all intestinal epithelial cells [26]. Already the villi are tiny finger-like projections, which increase the surface area by approximately 30-fold, being characterized by the presence of mature enterocytes, goblet cells and mucus secreting [27].

The human colon is very similar in its cellular organization and morphology to the small intestine as depicted in **Figure 2.2B**. The large intestine or colon begins in the right iliac region of the small intestine. Unlike the small intestine, the mucosa of the large intestine is not covered with villous projections but contains deep tubular pits, which increase in depth as they approach the rectum, as well as the muscularis propria and further increase the surface area for digestion and absorption by approximately 600-fold [21].

The epithelial cells of the colonic mucosa include enterocytes (absorptive cells), enteroendocrine cells, epithelial stem cells, goblet cell and microfold cells (M-cells) [21], nearly identical to cells in the small intestine.

All types of cells mentioned above have distinct functions:

a) Enteroendocrine cells: specialized endocrine cells of the gastrointestinal tract that differentiate from pluripotent stem cells with ability to coordinate the functioning of the intestine by specific hormone secretion;
b) Paneth cells: specialized cells that reside in the crypts and has a role in innate immunity through the secretion of proteins;
c) Goblet cells: produce and secrete mucins, which constitutes the mucus need for chemical and mechanical protection of the intestine;

d) Enterocytes: are columnar and highly polarized cells, and characterized by the presence of an apical brush border, which perform the around 80% of the absorption of nutrients through the epithelium [22, 28, 29];
e) M cells are specialized in transepithelial transport of macromolecules, particles and microorganisms.

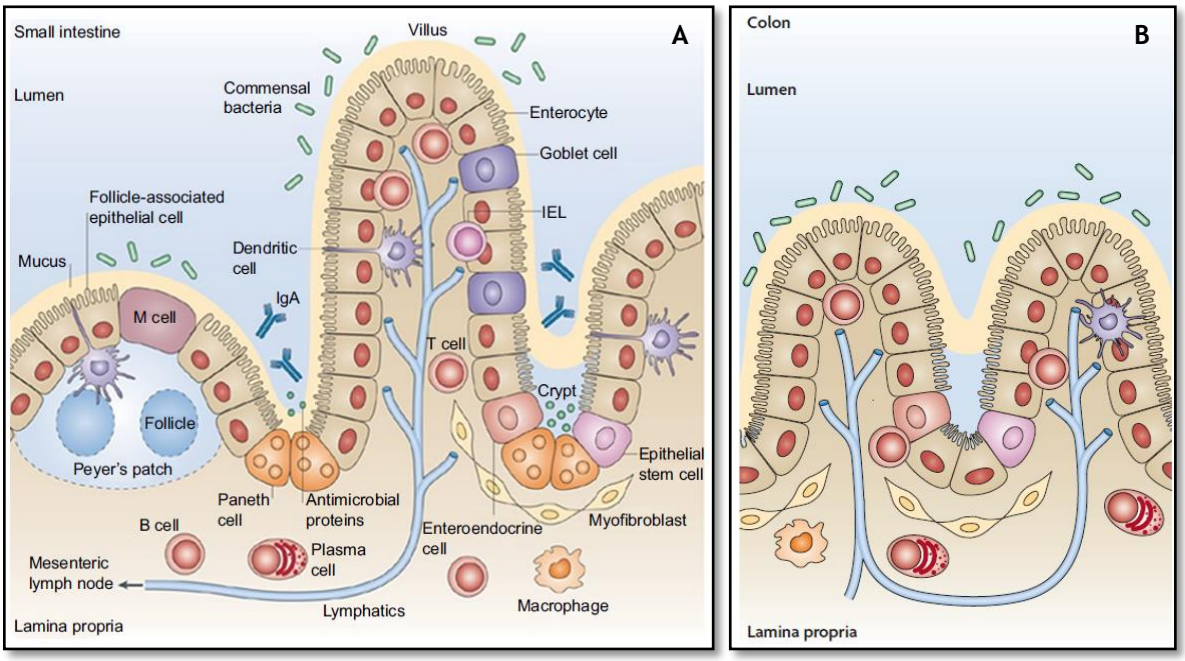

Figure 2.2 – Schematic representation of the architecture of the small intestine (**A**) and the colon (**B**) as well as all the cell types present in an intestinal villus. Adapted from [26].

2.2.2 Pathways through the intestinal epithelial barrier

Oral administration of therapeutic agents is the most common and preferred route of drug delivery for patients, in view of their ease of administration. However, drugs administered orally, as compared to those administered parenterally, are not directly available in the systemic circulation to make its therapeutic effect effective. Following oral administration of a drug, there are many barriers which the drug must pass to be absorbed by the intestine. Starting with the drastic pH changes at slightly acidic (pH 1.2-3.0) in the stomach to slightly alkaline (pH 6.5-8.0) in the end of the ileum proximal, lead to drastic changes of stability and solubility of the drug [27]. In the small intestine, which is the main site of absorption, the enzyme activity collects a number of proteolytic enzymes which may degrade the drug [27, 30]. In addition to the above parameters, molecular size, lipophilicity/hydrophilicity, site of action, efflux pathways and stability/solubility of the administered drug are others factors to be considered when considering administration of therapeutic oral agents.

There are several absorption pathways in the intestinal epithelium such as by passive diffusion, which occurs through nonspecific permeability pathways (for small amphipathic molecules), by the paracellular route (to hydrophilic molecules of low molecular weight), specialized carriers to effect the facilitated absorption of molecules (sugars and amino acids) [27], among others (see **Figure 2.3**). Since larger molecules such as peptides, proteins and anticancer drugs can be absorbed by endocytosis [31].

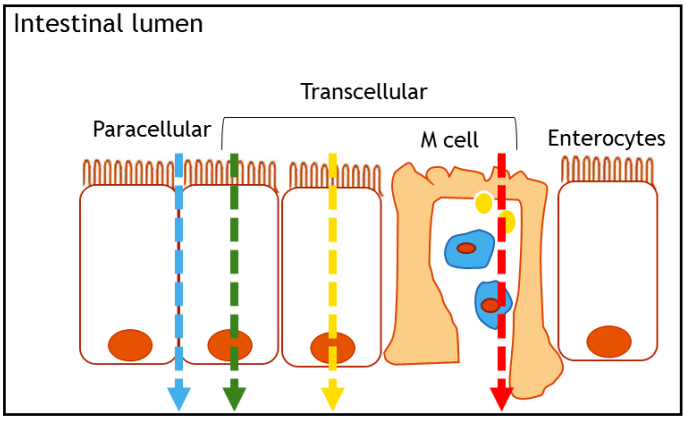

Figure 2.3 – Schematic representation of the transport across the intestinal epithelium. Molecules can across the intestinal epithelial barrier by paracellular transport (blue line) and by transcellular transport through passive diffusion (green line), transcytosis via normal enterocytes (yellow line) or via M-cells (red line).

Some reports demonstrated that particles with about 100-200 nm could be internalized by the receptor-mediated endocytosis, whereas large particles have to be phagocytized [32]. On the other hand, larger molecules must be transported by paracellular route, which corresponds to the passage of molecules across epithelial cells. Consequently, tight junctions (TJs) should open to occur this passage with biomaterials such as chitosan (CS) that have this ability [33]. Actually, the movement through the epithelium can occur the apical to basolateral side, which corresponds to the movement from the intestinal lumen to underlying tissue and circulation, and on the contrary, to the basolateral to apical side. The epithelium, reinforced by TJs and efflux transporters, exclude molecules larger than 200 Da via paracellular transport [34].

The TJs are an adhesion region between adjacent epithelium (endothelial cells) that regulates the paracellular flow. There are several proteins in this adherence area that are responsible for opening and closing it [26]. The combined role of P-glycoprotein (P-gp) which is an efflux pump family of adenosine triphosphate (ATP) binding cassette transporter and acts contrary to the absorption of drugs [35], with cytochrome P450 3A, an enzyme that metabolizes drugs has been recognized as one of the main determinants of intestinal wall absorption [36]. Still, even when administered a significant amount of drug and is carried to the intestinal epithelium, the first pass metabolism by the liver will reduce substantially the initial dose to a dose fraction which will pass, later, to the systemic circulation [37].

For these reason, the use of polymeric micelles as drug carriers is a promise to overcome these and other barriers and reach the target with less degradation and maximum quantities. The opening of the intestinal cell barrier, through a breakdown of TJs, can increase the absorption of drugs delivered orally.

2.2.3 Intestinal *in vitro* models

Since *in vivo* studies are complex and time consuming, gastrointestinal digestion and intestinal absorption *in vitro* models have been developed [22, 38, 39].

Caco-2 cells (**Figure 2.4A**), derived from human colon adenocarcinoma, are very used as model to mimic human intestinal epithelium and study intestinal absorption of drugs, as these cells suffer spontaneous enterocytic differentiation in culture and are polarized with well-established TJs [20]. Also, Caco-2 cells present apical brush border with abundant microvilli and enzymatic activity of digestive enzymes such as alkaline phosphatase (ALP) [22]. Since the permeation of drugs across monolayers of Caco-2 cells are close to the characteristics of permeation of human intestinal mucosa, this model has been suggested for predicting oral drug absorption in humans [20]. However, our group, started to use C2BBe1, a clone of Caco-2, as is described in even better mimic the enterocyte because the parental Caco-2 cells have an heterogeneous population not displaying always the brush border typical of the enterocytes [40].

Similarly, HT29 cell lines has its origin in human colorectal adenocarcinoma, and, after 21 culture can be differentiated into goblet cells, mimicking them [22]. Because of HT29 cells acquire a heterogeneous phenotype when cultured in modified medium [41], Lesuffleur established HT29-MTX cell line in a medium containing 10^{-6} M methotrexate (MTX) (see **Figure 2.4B**). This cell line grows in a monolayer of polarized goblet cells that produce mucus, it has a discrete apical brush border with intestinal hydrolases and, contrasting with Caco-2 cells, do not express P-gp and have less TJs [41]. The main physiological function of mucus includes protecting the GI epithelium itself to be degraded by stomach acid and digested by gastric and intestinal enzymes.

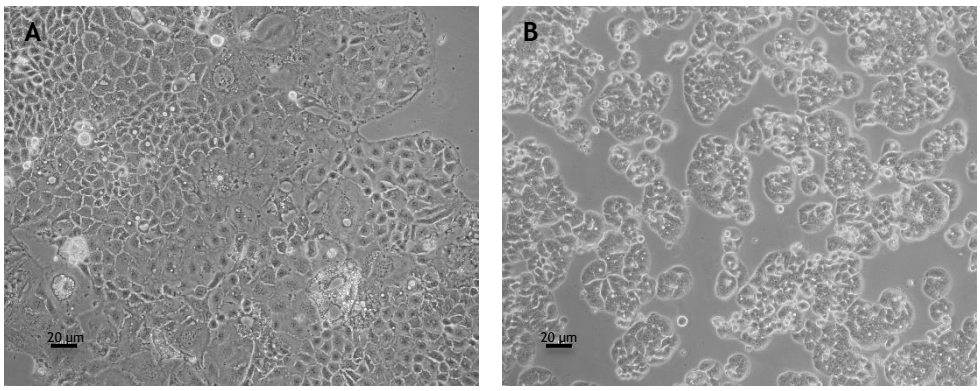

Figure 2.4 – Morphological aspect of Caco-2 cells (**A**) and HT29-MTX cells (**B**) at a resolution of 20 µm. The images were taken with Nikon TE2000-U microscope equipped with digital camera and controlled via the Nikon ACT-1 program.

The Transwell® system comprises a well of a plate with an insert inside and represents a potential *in vitro* tool for investigating intestinal permeability lumen-to-blood drug, i.e., the permeability from apical compartment to the basolateral compartment (**Figure 2.5**). It is necessary to use human cell lines, preferably several lines of cells, with the goal of reproducing the intestinal heterogeneous population, mimicking better the human intestine [22]. The insert of this system includes a 10 mm thick membrane made of polyester or polycarbonate and is available with different pore sizes.

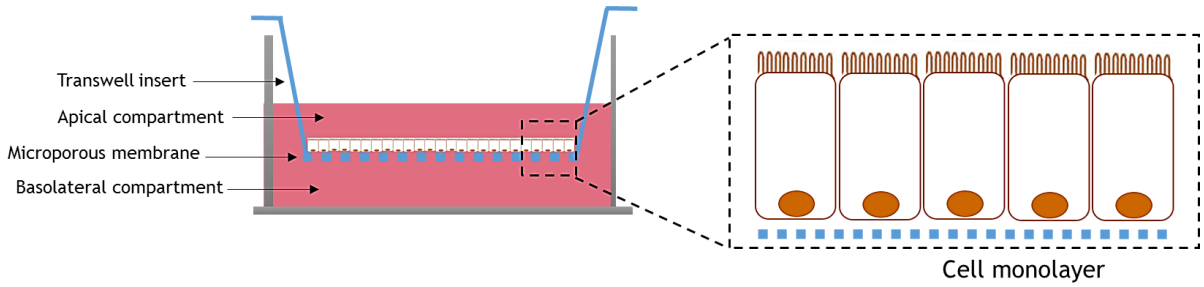

Figure 2.5 – Schematic representation of a Transwell® that consist in a well plate plus insert. The epithelial cells are seeded on the top of the membrane where the compounds are placed and the permeability occurs the apical to the basolateral compartment.

The integrity of each model can be easily monitored by measuring the transepithelial electrical resistance (TEER) which returns the absolute values of resistance per unit area [22]. The higher the value of TEER more TJs exist to modulate the transport of molecules by paracellular route.

2.2.3.1 Caco-2 model

Due to all the features described about the Caco-2 cell lines, the monoculture of these cells is the standard for the intestinal absorption in *in vitro* models.

As already mentioned, Caco-2 cells undergo spontaneous differentiation in the enterocyte, however, in the early stages of the culture (3-4 days), Caco-2 cells remain undifferentiated, showing only some apical microvilli [22]. Thus it is necessary to culture the cells as a monolayer for around 21 days to produce the differentiation into enterocytes, which are the main important cells in human intestine, able to form junctions between cells. Although they are derived from colon, they express most of the morphological and functional characteristics of the intestinal absorption cells, including enzymes typically expressed in enterocytes [22].

Some disadvantages are evident in this model, for example, no mucus production and no differentiation between cellular transport and intestinal metabolism [42], there is a high and variable P-gp expression and a low expression of metabolic enzymes [43], and the permeability of hydrophilic compounds is made by paracellular route, which makes this model less efficient because of TJs as compared with the human or animal intestine [42]. In this case, the Caco-2 model is used to investigate their utility in the study of passive absorption of drugs (**Figure 2.6**).

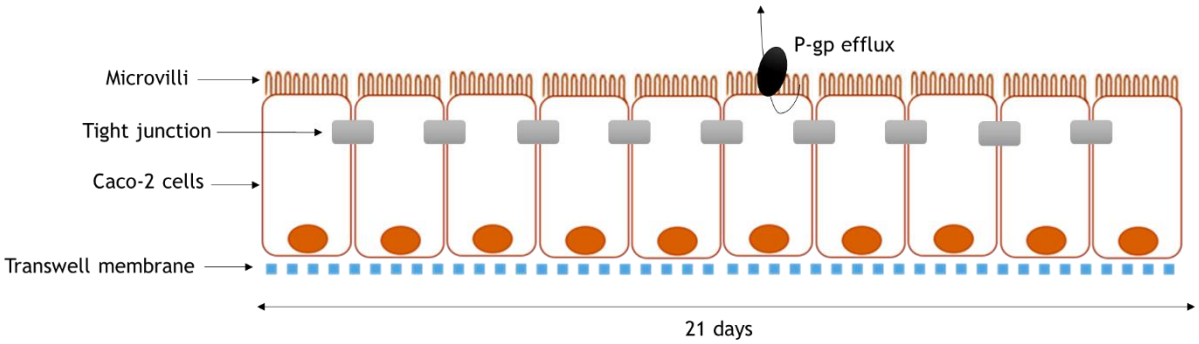

Figure 2.6 – Schematic representation of the Caco-2 monoculture model setup.

2.2.3.2 Caco-2/HT29-MTX model

To overcome some barriers of the model mentioned above, a new model was imposed. This model consists in a mixture of Caco-2 and HT29-MTX (mucus-producing) cell lines with the aim to generate more predictable results (see **Figure 2.7**).

Once HT29-MTX cells do not form TJs as tight as Caco-2 cells when cultured in monolayer, is given an increase in paracellular transport routes, making the model closer to the human intestine [44]. Also, the mucus production is important because it protects the organism against the entry of pathogens agents, however, acts as a barrier to absorption of drugs, affecting the retention time of the compound in the intestinal wall [45].

This co-culture model was studied by our group and it was found that the optimum ratio to obtain a closer mimic reality is 90% Caco-2 cells and 10% of HT29-MTX cells [38].

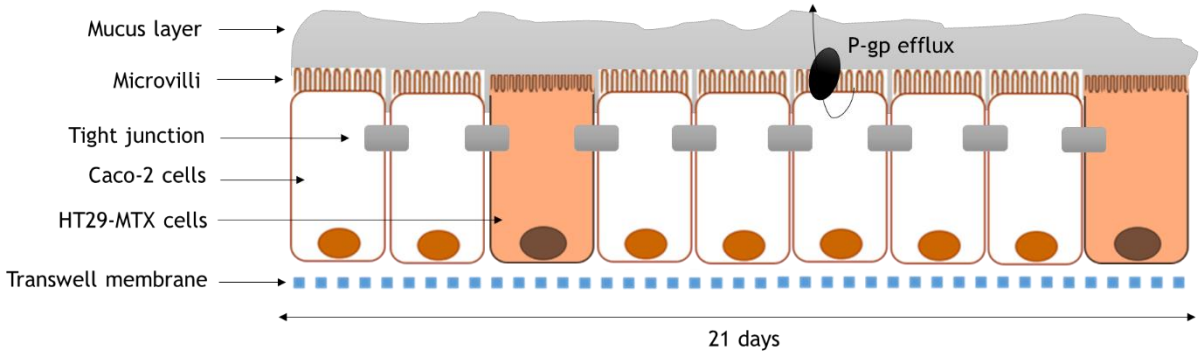

Figure 2.7 – Schematic representation of the Caco-2/HT29-MTX co-culture model setup.

2.2.3.3 Caco-2/HT29-MTX/Raji B model

A more realistic and complexed model is based on Caco-2 cells, HT29-MTX and Raji B, originally developed by our group [38, 44].

Raji B cells are derived from a human Burkitt's lymphoma, and when cultured with Caco-2 cells, these are induced to M-cell phenotype, resembling, functionally and morphologically to intestinal M-cells characterized by scarce and irregular microvilli [29] [38]. Since the presence of lymphocytes leads to the formation of cells that resemble intestinal M-cells in function and morphology, contributing to the transport of nanoparticles, and combined with the advantages of the co-culture model showed above, this model mimics even more by human intestinal epithelium.

Once M-cells are specialized in transepithelial transport of macromolecules, particles and microorganisms, this model is more complete compared to the models described above as will mimic more adequately the human intestine for development of new drugs administered orally also more suitable and closer to the *in vivo* model.

2.3 Anticancer drug model - Paclitaxel

Paclitaxel (PTX), a large antineoplastic agent isolated from the bark of Pacific Yew (*Taxus brevifolia* from family *Taxaceae)*, is characterized for its potent anti-tumor capabilities against a broad spectrum of cancers, such as metastatic breast cancer, colon cancer, ovarian cancer, among others [46]. PTX is a white to off white crystalline powder, highly hydrophobic and insoluble in water

and has the molecular formula $C_{47}H_{51}NO_{14}$ (**Figure 2.8**), which corresponds to a molecular weight (Mw) of 853 Da.

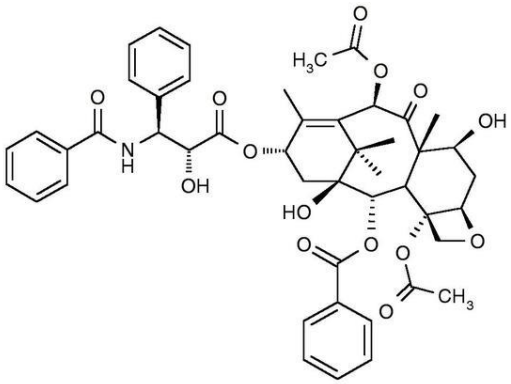

Figure 2.8 – Chemical structure of paclitaxel. Adapted from [2].

Its mechanism of action is promoted by the polymerization of tubulin and hyper stabilization of microtubules in their polymerized form, leading to cell death [47, 48]. Microtubules are an integral component of eukaryotic cells and are involved in various cellular functions including mitosis, maintaining the form and movement of the cell, organelle transport between the cell interior and spindle formation during cell division. On the other hand, tubulin is a protein that form the microtubules. PTX alter the normal balance, forcing the polymerization of tubulin dimers leading to the formation of microtubules, making them stable by preventing depolymerisation and, therefore, making them dysfunctional [48]. Consequently, interrupts cell division, since the stabilization of microtubules interferes with the G2 and M phases of the cell cycle (and these cellular activities involves microtubules), causing cell death by disrupting the normal dynamics of the tubule needed for cell division and vital interphase process [2, 48] (see **Figure 2.9**).

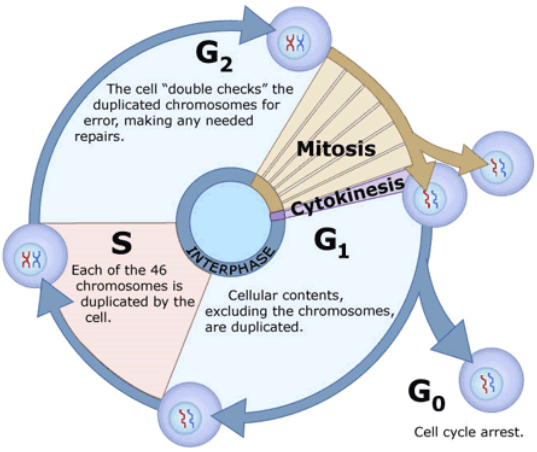

Figure 2.9 – Schematic representation of cell cycle. Adapted from [49].

PTX is poorly soluble in aqueous medium, but can be dissolved in organic solvents such as dimethyl sulfoxide (DMSO) (50 mg/mL) and methanol (50 mg/mL) [50], and acetonitrile (15 mg/mL) and ethanol (40 mg/mL) [2]. This drug is rapidly destroyed in weakly alkaline medium, methanolic solutions and in strongly acidic methanolic solutions. For instance, a sample with 0.1% acetic acid added to methanol showed no signs of degradation for 7 days at room temperature (RT) or during 3 months at

4 ºC [51]. Due to the low solubility and poor permeability of PTX, it is classified under class IV of Biopharmaceutic Classification System (BCS) [52], which means being slightly permeable by the intestinal mucosa in addition to the poor solubility, as already discussed.

The commercial form of PTX, Taxol®, is designed in a vehicle consisting of Cremophor EL (polyethoxylated castor oil) and dehydrated ethanol (50:50, v/v) [53]. This form is clinically used after dilution in isotonic saline solution before intravenous administration (i.v.). However, a drastic number of side effects are reported as hypersensitivity, peripheral neuropathy, hypotension, neurotoxicity, nephrotoxicity [54], among others. Furthermore, i.v. may cause other problems such as infections and thrombosis. Therefore, several alternatives to the use of Cremophor EL-based vehicle have been explored to reduce these and other side effects and improve the therapeutic efficacy of PTX. One such alternative is polymeric micelles [55] to be administered orally as it is the most cost-effective treatment method due to less need for visits and remained in the hospital staff and for the preparation and administration of the treatment.

The half maximal inhibitory concentration (IC50) is a measure of the effectiveness of a substance in inhibiting a specific biological or biochemical function by half. The IC50 of PTX is in the range of 2.5-7.5 nM [56]. It is important to have knowledge of this value because it indicates the amount of PTX required to inhibit a particular biological process by half, in this case, to inhibit cell division. Clinically, the dose generally accepted is 200-250 mg/m^2 [2].

Studies conducted in HeLa cells (from human cervical cancer origin) and fibroblasts using PTX (0.25-10 mM) showed that PTX blocked cells in the G2 and M phase of the cell cycle [57]. Already in human colorectal cell lines (HCT116) at PTX concentration of 3-10 nM, there was inhibition of mitosis leading to cell death [58].

In general, the PTX *in vitro* activity is greater than the activity of cisplatin, DOX, and 5-Fu against human tumors and equal to or less than docetaxel [46].

2.4 Polymeric micelles as drug delivery vehicles

Polymeric micelles are amphiphilic polymers that could be self-assembled into a core-shell nanostructure based on hydrophobic and hydrophilic segments with a range of diameters of 10-200 nm [59, 60]. This micellar system has the advantage of improve stability in the bloodstream, large capacity encapsulation, despite the reduced size, are not toxic and yet have a controlled release of the drug [61]. The time of drug circulation in the blood is higher [18, 19], providing better permeability to anticancer drugs by improving its delivery from the deep blood vessels to tumors [17]. Additionally, these carriers are typically accumulated in extensive vasculature sites, such as solid tumors and sites of inflammation, due to EPR effect [18, 19], as already mention above.

The fact that these systems are organized in core-shell type structures, make them selected for drug delivery applications. The stability of these processes is given by the decrease of the Gibbs free energy, which makes these systems thermodynamically more stable, this process is called self-assembly [62, 63]. For being an amphiphilic system, the hydrophobic moiety is protected from the aqueous medium, and therefore the hydrophilic part is in contact therewith (see **Figure 2.10**). The hydrophobic core provides space for the encapsulation of hydrophobic drugs such as PTX or DOX, and the hydrophilic shell allows the inclusion of hydrophobic drugs and it also provides stability, protecting from biological environment [64]. Taking in account these properties, polymeric micelles have become a promising carriers of hydrophobic drugs. They are not easily absorbed in the GI tract,

providing the reduction of the side effects and they are protected from environmental stimuli such as enzymes and gastric pH [16, 65].

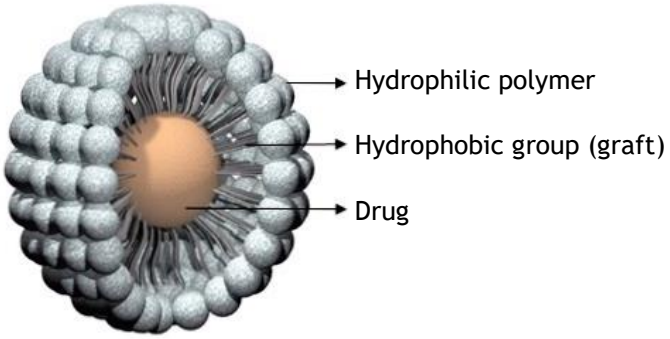

Figure 2.10 – Schematic representation of drug encapsulation from self-assembled nanosystems.

Chemical modifications of polymers are the most efficient and well-known method to create self-assembled systems. These changes lead to the formation of amphiphilic polymer derivatives by the addition of hydrophobic groups, such as alkyl and acyl groups, to the hydrophilic polymer backbone. These target drug delivery systems are developed to prevent drug degradation, as well as their loss, to avoid the harmful side effects and to increase the bioavailability of the drug in the required site of interest [16].

If the external components of micelles are usually comprised by hydrophilic polymers as polyethyleneglicol (PEG) or chitosan (CS), to form the micellar core, it has been used various polyesters such as poly (L-lactide), poly(glycolic acid-lactide) and PCL [65]. The latter have advantages over others polyesters by always keeping elastic at RT, which makes it highly permeable [66, 67], and decomposes more slowly, being optimal for controlled release drugs [3].

There are two concepts that have to be explained about micelles: the first is the critical micelle concentration (CMC), which is the minimum concentration required for a given polymer to form micelles by self-assembly. The second is the critical aggregation concentration (CAC), which is the minimum concentration required for a given polymer to aggregate. Typically, the CMC values are higher than the CAC value [68]. The CMC of the polymer-based micelles depends on the hydrophobic character of the molecule [69] and a Mw of the blocks [70]. There are several methods to calculate the CMC, such as by conductivity measurements, interfacial tension or fluorescence spectroscopy [64]. However, in the case of polymer-based micelles, the CMC is very low, being the fluorescence spectroscopy the best choice because of its high sensitivity [64].

The hydrodynamic diameter of polymeric micelles is possible to be determined by dynamic light scattering (DLS) method [71] and the morphology of the micelles can be visualized by transmission electron microscope (TEM) and by scanning electron microscope (SEM) methods [60]. Differing the composition and size of the micelles of hydrophobic segments and hydrophilic of the materials that compose them, it is possible to regulate the properties of the micelles as the size and loading capacity [60].

2.5 Chitosan and amphiphilic derivatives

Polysaccharides are widely distributed in nature and, among them, CS is receiving increasing attention. CS is a linear polysaccharide prepared from chitin, which is the second most abundant natural polymer in the world, after cellulose [72, 73]. Chitin can be found in the exoskeleton of

insects, crustaceans and some cell wall of fungi. CS, derivatived from chitin, can be obtained by alkaline deacetylation or enzymatic hydrolysis [73]. The reaction product is CS only when the average degree of acetylation (DA), is equal to or less than 50%. The DA is used to characterize the average content of *N*-acetyl-D-glucosamine units (acetylated unit) while degree of deacetylation (DD) is the number of D-glucosamine units (deacetylated unit) [7, 72]. Thus, CS is constituted by N-acetyl-D-glucosamine (GlcNAc units) and of D-glucosamine units (GlcN units), linked by glycosidic linkages ß-(1,4) (**Figure 2.11**) [6, 72-74].

This polymer shows solubility in moderately acidic medium. Its solubility in acidic medium occurs due the protonation of the NH_2 functional group on the C-2 position of the D-glucosamine repeating unit [72, 74, 75].

CS has one amino group and two hydroxyl groups in the repeating glycosidic residue, providing reactive sites for a variety of reactions, which is an advantage over other polymers [76]. Several types of CS can be obtained and with different physicochemical properties such solubility, pK_a and viscosity, which depend on parameters like DD and Mw [73, 77, 78].

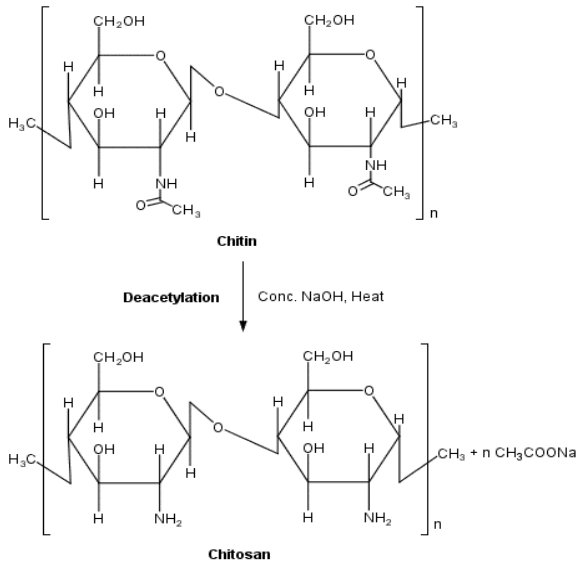

Figure 2.11 – Deacetylation of chitin to chitosan.

The DD and the Mw are two of the most important physicochemical properties of this polymer. An increase on the DD, leads to an increase of its viscosity, due to high and low deacetylated CSs having different conformations in aqueous solutions [79]. Additionally, the CS solution viscosity can be also affected by factors as temperature and concentration [79]. For example, when CS concentration increases or the temperature of the solution decreases, the viscosity increases.

CS is a polycation whose charge density depends on DA and pH. Due to the progressive amine protonation of pendant groups, the solubility is pH dependent. Therefore, CS is only soluble at pH values of approximately 6 or less [6, 75, 80]. This feature turns CS into biopharmaceutical of interest, along with its properties of mucoadhesiveness and ability to open epithelial TJs [33]. In fact, at low pH (<6), CS amine groups are protonated and become positively charged, leading to polycationic behavior [7, 81]. By contrast, at a higher pH value (above around 6), CS amines are deprontonated and reactive (**Figure 2.12**).

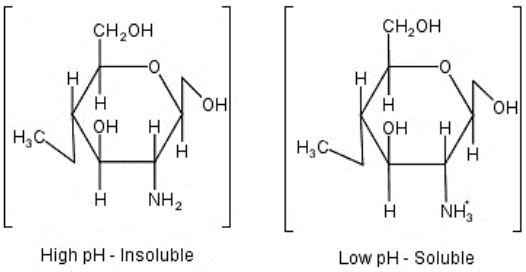

Figure 2.12 - The soluble–insoluble transition of chitosan occurs at about pH 6.

To improve CS solubility in physiological media, its biological properties and expand its potential applications, CS derivatives have been synthesized [13-15, 55, 82-84]. Indeed, macromolecules with amphiphilic character have become a subject of great interest over the last years.

2.5.1 Biological properties of chitosan

CS is a polymer of great interest in pharmacy, medicine and tissue engineering due to its biological activities such as non-toxicity [85-88], antimicrobial activity [72, 73, 89-92], biocompatibility [7, 93, 94], biodegradability [7, 95-97], mucoadhesiveness and ability to open, temporarily, the tight junctions of the epithelium [94, 98, 99], thereby facilitating the permeation of drugs [6, 100-103]. These properties may double the therapeutic effects making CS a polymer with pronounced potential for biomedical and biopharmaceutical applications, especially for drug delivery.

The presence of NH_2 groups in CS is the reason why it exhibits much higher potential as compared with chitin [7] and what makes it an excellent polymer for pharmaceutical applications. Also, as shown in **Table 2.1,** it is possible understand the CS biological properties and the relationship between its structural characteristics (DD and Mw). For instance, the lower the DD and Mw, the higher the CS biodegradability [7, 95-97]. Moreover, CS plays a role in hemostasis, but independently of the coagulation cascade [96]. Okamoto and colleagues showed that CS reduces clotting time in a dose-dependently manner, with the ability to aggregate platelets [104].

Table 2.1 — Biological and structural properties of chitosan.

Property	Structural characteristics[a]	References
Biodegradability	↓ DD, ↓ Mw	[7, 95-97]
Biocompatibility	↑ DD	[7, 93, 94]
Cytocompatibility	↑ DD	[7, 93]
Mucoadhesion	↑ DD, ↑ Mw	[94, 98, 99]
Hemostatic action	↑ DD	[73, 105, 106]
Analgesic action	↑ DD	[107, 108]
Antimicrobial activity	↑ DD, ↑ Mw	[72, 73, 89-92]
Antioxidant activity	↑ DD, ↓ Mw	[72, 109-111]

[a] ↑ - Directly proportional to property; ↓ - inversely proportional to property.

The properties of CS mentioned above make the CS an exciting and promising excipient for the pharmaceutical industry, with a large margin for development. However, CS amphiphilic derivatives have, indeed, attracted the particular attention among researchers working in biomedical engineering, and particularly, in drug delivery, given the fact that they improve physical and chemical properties of CS when used alone [77].

2.5.2 Chitosan amphiphilic derivatives

A large number of CS amphiphilic derivatives have been reported in the literature over the past years. CS amphiphilic derivatives result from the attachment of hydrophobic structures to the hydrophilic CS backbone due to the presence of hydroxyl and amine groups, and can be achieved by using different methodologies such as alkylation [112-115] and acylation [62, 116-123] . Generally, the chemical derivatization of CS can be regioselective due to the presence of reactive sites C2-amine, C3-hydroxyl and C6-hydroxyl. The properties of products of the regioselective reactions are strongly influenced by the distribution of substituents groups along the polymer chain and, therefore, it is possible to obtain *N*-substituted, *O*-substituted or *N*,*O*-substituted CS derivatives. In general, the reaction products of an amphiphilic CS are, among others, *N*-alkyl chitosan, acyl-chitosan and graft derivatives. Interestingly, the introduction of a hydrophobic molecule on CS backbone modifies its rheological behavior, being therefore used as rheological modifiers in pharmaceutical industries [124]. However, such substitutions may be controlled over the reaction conditions applied [68, 113], as is shown here.

2.5.2.1 Alkylation

The alkylation is one of the most frequent modifications of CS. Alkylation reactions occur through the grafting of alkyl chains in the structure of the CS. In other words, alkyl CS is obtained by the introduction of alkyl groups on the amine groups of CS by reductive amination of CS [125]. Generally, this substitution reaction is carried out in heterogeneous conditions and owing to the semi-crystalline character of CS, amorphous regions will be more accessible than ordered ones, giving rise to substituted products displaying block distribution patterns.

The hydrophobic character of alkylated CS is dependent on the length of the chains, i.e., the longer the alkyl chains, the higher the polymer hydrophobicity [126]. Additionally, the higher the average degree of substitution (DS), the more hydrophobic will be the modified CS.

Desbrieres *et al.*, [125], developed a procedure to obtain alkylated derivatives of CS from its swollen structure and modified after precipitation by neutralization, which improves the accessibility to the reactive sites. Generally, aldehydes and ketones are employed as alkylating agents and the Schiff bases resulting from reaction with CS are converted to *N*-alkyl CS derivatives by reduction with sodium borohydride ($NaBH_4$) or sodium cyanoborohydride ($NaBH_3CN$) (**Figure 2.13**), the reaction efficiency depending on the choice of the reducing agent [68]. Indeed, $NaBH_3CN$ is commonly used because it is more reactive and selective, but it is highly toxic [68].

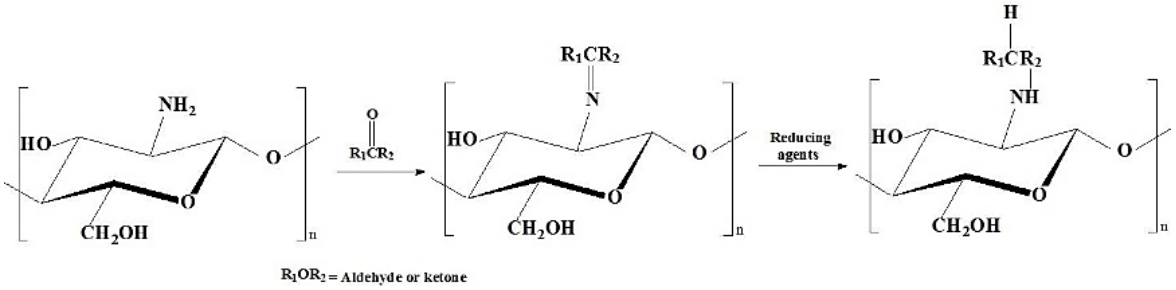

Figure 2.13 - Reaction scheme to obtain *N*-alkyl derivatives of chitosan.

CS modifications can dramatically alter its properties, therefore, it is necessary to characterize the properties and medical safety of these new derivatives [127]. Indeed, the presence of hydrophobic interactions between the alkyl chains improves the properties of modified CSs: the C12 is the minimum length of the alkyl chain for the hydrophobic behavior be effective; the solutions of such CS derivatives are usually non-Newtonian, mainly when the length of alkyl chains increases; also de C12 alkyl chain length proved to be more efficient to improve film formation and mechanical properties; the efficiency of this modification increases with increasing DS [126].

Apart from their properties, alkyl chitosan derivatives have been widely used in drug delivery. In **Section 2.5.3**, examples are given of this modification.

2.5.2.2 Acylation

The addition of hydrophobic groups is also carried out by acylation reactions. Acylated CS was proposed as a drug carrier for drug delivery, essentially due to its hydrophobic association that promotes self-assembly of nanoparticles or micelles. The advantage of the acylation of CS over its alkylation occurs because the acylation allows the introduction of new groups in sites C2-amine, C3-hydroxyl and C6-hydroxyl [68]. In the case of *O*-acylation, the presence of the ester bond in the structure of the resulting CS derivative permits its degradation by the action of lipase enzymes, making it a biodegradable polymer [68].

The acylation of CS makes possible its solubilization in organic solvents due to the introduction of hydrophobic groups in the polymer. However, the solubility of acylated CS in water depends on the acyl chain length and on DS [68, 128]. This means that short acyl chains and relatively low DS result in water soluble CS derivatives but increasing the DS will dramatically decrease the water solubility.

2.5.2.2.1 *N*-acylation

The *N*-acylation of CS may be achieved by activation of carboxylic acids through reaction with carbodiimides as well as by using reactive carboxylic acid derivatives, such as anhydrides and acyl chlorides.

Carbodiimide reactions are carried out by activation of carboxylic acids in the presence of 1-ethyl-3-(3-dimethylaminopropyl) carbodiimide (EDC). This reaction gives rise to the intermediate *O*-acylisourea, which is capable of undergoing nucleophilic attack of the primary amine groups, such as those present in GlcN units of CS [68]. The primary amine connects to the carboxyl group through an amide bond and release the by-product urea derivative, isourea. The reaction scheme is shown in **Figure 2.14**.

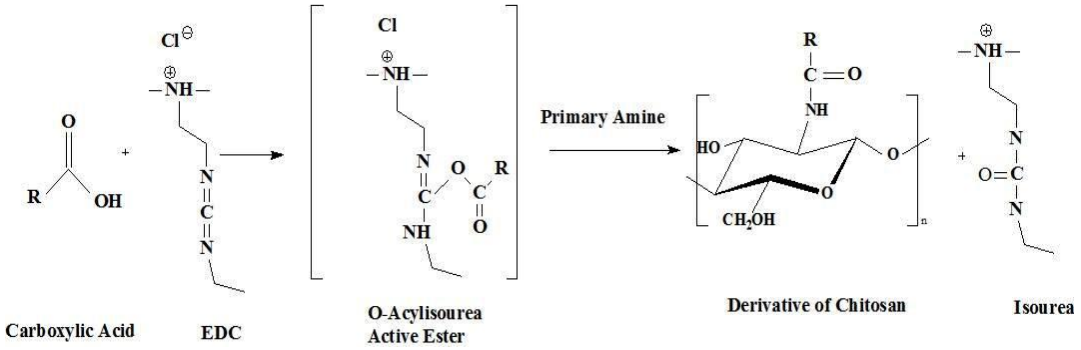

Figure 2.14 - Acylation modification by carbodiimide reaction.

In carbodiimide reactions it has been commonly used *N*-hydroxisuccimide (NHS) or its water-soluble sulfo-NHS with the EDC. Adding this, the efficiency of the reaction is improved through the formation of an amine-reactive intermediate that is more stable than the *O*-acylisourea. The reaction scheme addition of NHS is shown in **Figure 2.15**.

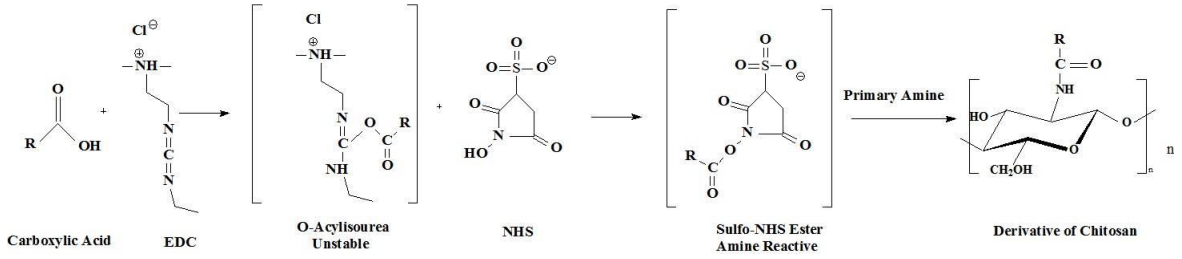

Figure 2.15 - Acylation synthesis from the use of EDC and NHS.

Lee *et al*. [129], carried out the CS modification with EDC and it is possible to verify that with an increase in the amount of deoxycholic acid and EDC there is an increase of the DS. However, the DS ranges from 2.8 to 5.1 per 100 anhydroglucosamine units of CS, concluding that the limited solubility of deoxycholic acid in the reaction medium affected the achievement of derivatives with higher DS. The same was observed in the reaction with linoleic acid, the resulting DS attaining only 1.8% [130].

Other methodology for obtaining acylated CS is by reaction with anhydrides, which results in selective *N*-substitution. This reaction can be carried out in homogeneous [131] or heterogeneous [132] conditions. The reaction scheme is shown in **Figure 2.16**.

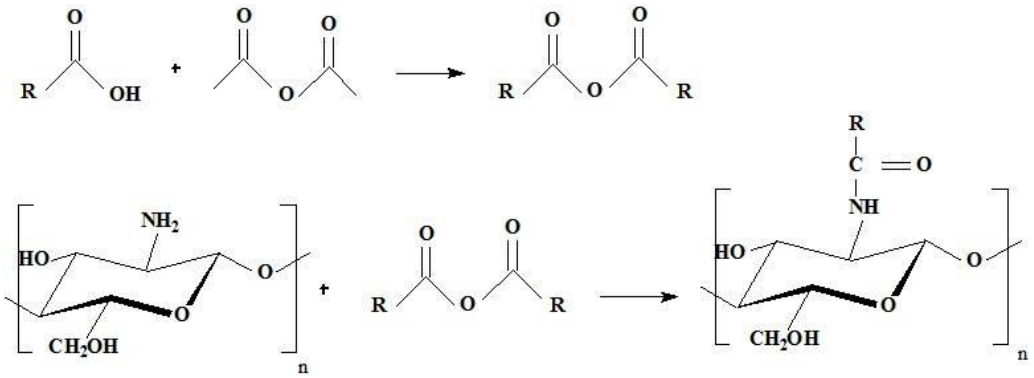

Figure 2.16 - *N*-acyl chitosan reaction by anhydrides.

2.5.2.2.2 *O*-acylation

The reactions presented above aim to produce the *N*-acylation of CS. However, the *O*-acylation reactions may also occur, as many of these reactions are not fully selective for amine groups. Thus, the preparation of derivatives with well-defined structures can be achieved through the control of reaction conditions, allowing the preparation of advanced functional materials from CS.

Since amine groups are stronger nucleophiles as compared to primary and secondary hydroxyl groups, the preparation of *N*-phthaloyl CS derivative is a promising advance as besides being a regioselective reaction, it is easily carried out under mild conditions. The phthaloyl group is commonly used as protector of amine groups and after protection; *O*-substitution reactions are carried out. Finally, the phthaloyl group is removed by reaction with hydrazine, regenerating the amine groups [133]. **Figure 2.17** shows the phthaloyl protecting group and reaction of *O*-acylation.

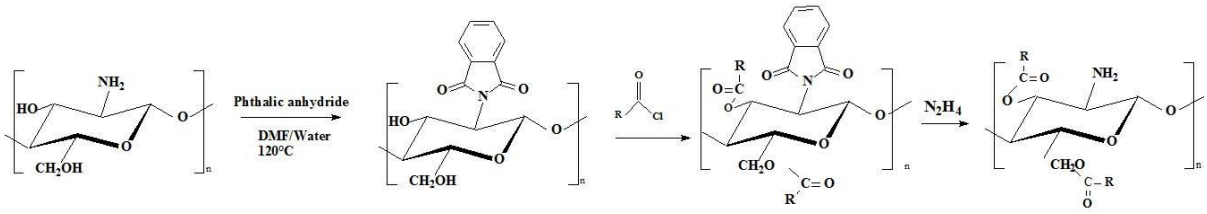

Figure 2.17 - Reaction of protection through the phthaloyl group.

In spite of the reactions with phthaloyl be effective, this approach needs several steps, including the protection and deprotection of the amine groups, favoring the occurrence of side-reactions as well as low reaction yield. Therefore, a new method was developed using methanesulfonic acid (CH_3SO_3H) to protect the amine groups, allowing the occurrence of selective *O*-acylation by reaction with acyl chlorides [68]. As a strong acid, methanesulfonic acid is able to protonate the amine groups through the formation of salts, resulting in the substitution preferentially on the hydroxyl groups of CS, as shown in **Figure 2.18**.

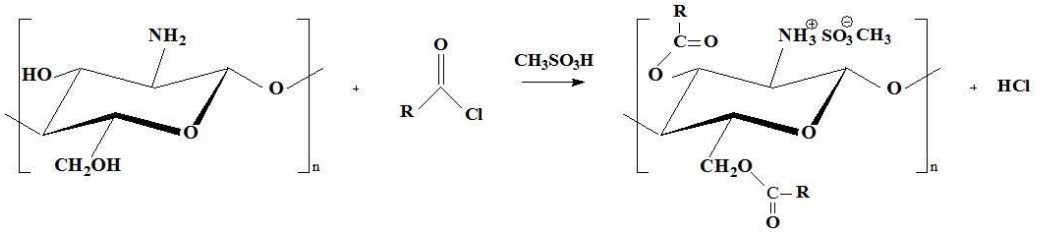

Figure 2.18 - Reaction of *O*-substitution through the protection of amine groups with CH_3SO_3H.

2.5.3 Chitosan derivatives in drug delivery of anticancer drugs

Currently, new chemical formulations for drugs are developed, but the low solubility in aqueous media and unacceptable levels of toxicity for drugs or excipients in the formulation has been a limitation. The first formulations developed had in its composition solubilizing agents [134]. However, it exhibited secondary effects. Thereby, the advance of studies in this area led to the development of new types of formulations, such as systems based in nanoparticles and micelles, with the aim of avoid the use of such solubilizing agents [135]. Polymer-based micelles and nanoparticles produced from CS derivatives have been considered as promising carriers for bioactive molecules. Accordingly, some applications are presented below for these amphiphilic derivatives of CS in drug delivery systems.

Amphiphilic CS derivatives have already proven to be excellent systems for drug delivery when loaded with anticancer agents such as PTX, camptothecin or DOX.

The derivatives *N*-succinyl-*N*-octyl chitosan (SOC) were synthesized by *N*-substitution reaction in the presence of sodium borohydride. The three derivatives obtained had DS ranging between 28.6-52.5% and CMC values were 3.1×10^{-5}, 2.4×10^{-5} and 5.9×10^{-6} g/mL [14]. The CMC decreases with increasing DS of octyl content. The encapsulation of doxorubicin DOX was achieved by dialysis and was affected by the amount of octyl groups, increasing in function of DS [14]. Additionally, the average size of these micelles was dependent on the amount of the octyl chains, ranging between 100-200 nm. These results showed a sustained release pattern, also dependent on the amount of the octyl chains and drug loading (DL) content: the higher drug content had the slower drug release [14]. Additionally, these polymer-based micelles exhibit more toxicity than the free drug, which may be useful as a carrier DOX drug in anticancer treatment.

Zhang *et al*. [82], developed *N*-octyl-*N*-trimethyl chitosan derivatives (OTMCS) by introducing the octyl group in chitosan backbone followed by *N*-methylation, resulting in a derivative possessing average degree of substitution of 8% and 54% for octyl and trimethyl substituents, respectively [82]. This new derivative, OTMCS, can form micelles by self-assembly and is capable of encapsulate hydrophobic drugs such 10-hydroxycamptothecin, enhancing their solubility in aqueous media. The results showed an average particle size ranging between 24-278 nm and DL content between 4.1-32%, depending of the DS [82]. Additionally, the results showed a sustained-release behavior of the drug and good stability of the system. Concluding, these micelles could be promising carriers for hydrophobic drugs, improving their solubility, stability and release.

In another example from the same author, *N*-octyl-*O*-sulfate chitosan (NOCS) was prepared via reductive amination. NOCS micelles have been used to study the release of PTX. The loading of PTX and formation of micelles occur via dialysis using ethanol and water as solvent selected [55]. The solvents used to dissolve both, the polymer and the drug, and the feed weight ratio of PTX to the

polymer, significantly affected the encapsulation efficiency (EE), ranging between 37.6-59.1% [55]. However, the highest EE was observed when the feed weight ratio of PTX to the polymer was 1:1.5–1:1.7 [55]. The PTX-loaded micelles presented sizes around 250 nm and spherical shape without aggregation with high PTX loading, about 25% [55], which still is a promise nanocarrier for hydrophobic drugs. Therefore, the authors used these same micelles for *in vivo* studies [136]. The biodistribution study revealed that the drug retention was higher in the liver, followed by kidney and lung 15 minutes after administration. However, after 8 hours, the concentration of PTX became higher in the spleen, liver, lung and kidney [136]. Still, the brain and spinal cord were exposed to low concentrations of PTX. The antitumor efficacy in different animal tumor models of PTX-loaded micelles seems to be more efficient in inhibition of tumor growth at certain concentrations than when used Taxol®. However, at the concentration of 10 mg/kg both have similar behaviors. Regarding toxicity, only the Taxol® shows toxic effects [136]. These results indicate that the use of NOCS loaded with PTX is more beneficial than the conventional system containing Cremophor EL, overcoming the limitations and providing the necessary therapeutic efficacy.

The galactosylated *O*-carboxymethyl chitosan-graft-stearic acid (Gal-OCMC-g-SA) was synthesized by coupling the carboxyl group of stearic acid (SA) with the amine group of *O*-carboxymethylchitosan (OCMC) in the presence of EDC and NHS [83]. This derivative was synthesized for liver targeting delivery of DOX and has a DS of stearic groups ranging from 4.6% to 12.6% and galactose DS from 13.1%. Also, the particle size and polydispersity index decreased with increasing DS, through a non-linear relation [83]. These results indicated that the nanoparticles with spherical shape had a DL content around 13% and an EE around 77%, depending on the DS. The *in vitro* release studies, showed that the DOX loaded Gal-OCMC-*g*-SA nanoparticles had a pH-dependent release of DOX, which may be beneficial to the accumulation of drug in tumor tissues [83]. Additionally, the hemolysis test showed good safety of these micelles in blood-contacting applications, which indicate that material as potential application for the treatment of cancer, specially, for liver targeting.

Balan *et al*. [13], used different amounts of hydrophobic groups of palmitoyl chloride (PC) to prepare, through a nucleophilic acyl substitution reaction, a novel amphiphilic derivative, where free amine groups of chitosan are able to react with the carboxyl groups of acyl halides to form an amide bond. *N*-palmitoyl CS and magnetite were used to load DOX into magnetic nanocapsules, using a double emulsion method. Magnetic nanocapsules exhibited suitable magnetic saturation, superparamagnetic behavior and good ability to incorporate a chemotherapeutic agent [13], properties which can be exploited in many different areas of biomedicine. These magnetic nanocapsules showed a DS directly related with molar ratio. At 1/0.5, 1/1 and 1/2 chitosan/PC molar ratio, the DS (%) was 7.69±0.42, 12.35±1.60 and 25.57±2.33, respectively. Consequently, due to the fact that part of amine groups have been substituted, the zeta potential decreases because there are fewer amines [13]. These systems showed a narrow size distribution of 215±23.33 nm, EE of 73% and DL of 1.54%. Also, *in vitro* drug release exhibited a biphasic drug release with an initial burst effect in the first 6 hours, followed by a constant release up to 6 days [13]. The cytotoxicity studies revealed that the empty magnetic nanocapsules do not have cytotoxicity at the highest concentration tested, which is a good evidence to be used as drug delivery system.

Oleoyl chloride has been used to synthesize oleoyl-chitosan (OCH) and this CS derivative was applied to load nanoparticles with DOX. In this research, the DS of the OCH derivative was 11% and the diameters of empty and loaded with DOX nanoparticles were 255.3 nm and 315.2 nm, respectively [15]. The results showed that these nanoparticles had EE around 53% and the drug release was fast and complete at pH 3.8, whereas at pH 7.4 there was a sustained release after a burst release.

Additionally, the toxicity of OCH nanoparticles was investigated by MTT assay and the results showed low toxicity of the material at all concentrations as well as the hemolysis test showed a non-toxic level. Finally, the inhibition of DOX-OCH nanoparticles to human cancer cells *in vitro* have shown inhibitory effects on the growth of four cancer cell lines (A549, Bel-7402, HeLa, and SGC-7901) at most concentration levels (1000 μg/mL) than that of DOX. [15].

Gu *et al*. [84], produced chitosan-graft-poly(ε-caprolactone) (CS-*g*-PCL) through acylation modification to encapsulate 5-Fu as anticancer system. The polymer-based micelles prepared had a particle size in the range 61.4-108.6 nm depending on the DS with spherical shape after introduction the drug and, the EE was above 90% for a DL content of 14.8% [84]. The *in vitro* drug release of 5-Fu loaded micelles occurred in a sustained manner and had the controlled release behavior. Additionally, the cytotoxicity test made by MTT assay showed no cytotoxicity against A549 and MCF-7 cells for empty micelles and the loaded micelles as well. However, the latest present lower toxicity when compared with free drug [84].

All of the examples presented above appear to be quite promising systems for loading and delivery of hydrophobic drugs, particularly anticancer drugs. There is still much research to be done until it can take each of these systems in the treatment of human cancer.

Table 2.2 - Overview of amphiphilic chitosan derivatives used to encapsulate anticancer drugs.

Chitosan derivative	Modification	System	Active agent	Reference
SOC	Alkylation	Micelles	Doxorubicin	[14]
OTMCS	Alkylation	Micelles	10-hydroxycamptothecin	[82]
NOCS	Alkylation	Micelles	Paclitaxel	[55]
Gal-OCMC-g-SA	Acylation	Nanoparticles	Doxorubicin	[83]
N-palmitoyl chitosan	Acylation	Nanocapsules	Doxorubicin	[13]
OCH	Acylation	Nanoparticles	Doxorubicin	[15]
CS-*g*-PCL	Acylation	Micelles	5-fluorouracil	[84]

2.6 Polycaprolactone

Polycaprolactone (PCL) was extensively used in the biomaterial's field and a number of drug delivery devices during the resorbable-polymer-boom of the 1970s and 1980s increased [3]. In recent years, PCL, that is prepared by ring-opening polymerization (ROP) of ε-caprolactone (ε-CL) [137], has been used again due to their rheological, viscoelastic properties, excellent mechanical strength and nontoxicity superior to many of their counterparts of aliphatic polyesters [138] (see **Table 2.3**), which makes it easy to manufacture and to handle for a wide variety of implants and devices [3, 139, 140]. It is known to their biocompatibility and biodegradability, which make it a useful material in resorbable sutures, scaffolds in tissue engineering and recently in bone graft substitutes [141-144]. However, the drug delivery field has been extensively explored. Unlike most aliphatic polyesters, PCL is always in a rubbery state at RT which makes it highly permeable for many therapeutic drugs [66, 67].

PCL is a hydrophobic and semi-crystalline polymer approved by the U. S. Food and Drug Administration (FDA) [3], having a glass transition temperature (T_g) of -60 ºC and it is crystallinity

tends to decrease with the increasing of Mw [145]. The good solubility of PCL, its a low melting point (T_m) (59-64 ºC) and exceptional blend-compatibility has stimulated extensive research into it is a potential application in the biomedical field [145]. It has a thermal decomposition temperature (T_d) of 350 ºC, which is much higher than that of other aliphatic polyesters (235-255 ºC) [138, 146]. These and other characteristics are summarized in **Table 2.3**.

Table 2.3 - Summary of the polycaprolactone features.

Feature		Reference
Crystallinity (%)	67 %	[145]
Glass transition temperature (T_g)	T_g= -60 ºC	[67, 145]
Melting Point (T_m)	T_m= 59 ºC to 65 ºC	[67, 145]
Thermal decomposition temperature (T_d)	T_d= 350 ºC	[138, 146]
Young's modulus (MPa)	197	[67, 145]
Water permeability at 25 ºC (g/m^2/day)	177	[145]

This polymer is soluble in chloroform, dichloromethane, benzene, toluene and cyclohexanone at RT [147, 148]. By contrast he has a low solubility in acetone, 2-butanone, ethyl acetate, DMF and acetonitrile and is insoluble in alcohol, petroleum ether and diethyl ether [147, 148].

As already mentioned, PCL can be prepared by ROP of the cyclic ε-CL monomer [149] (**Figure 2.19**). The ε-CL consists of 5 nonpolar methylene groups and single relatively polar ester group which gives it unique properties outlined above [66]. The synthesis of PCL by ROP goes according to four different mechanisms: cationic, anionic, activated monomers and coordination of polymerization of the opening of ε-CL ring [67].

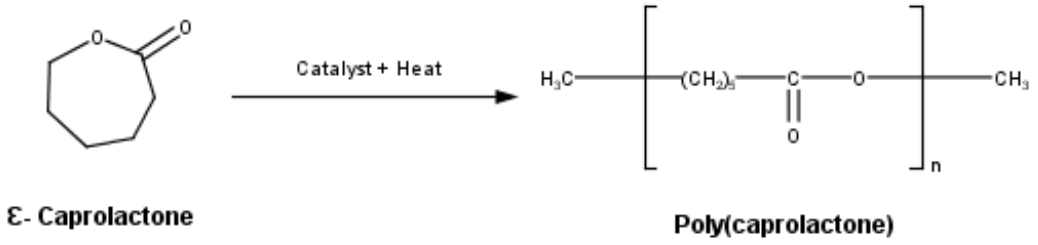

Figure 2.19 - Synthesis of polycaprolactone from ε-caprolactone by ring-opening polymerization.

PCL degrades more slowly than polyglycolide and poly D,L-lactide, and for this reason, is used in drug-delivery devices that remain in the body for over a year [3]. Furthermore, the fact of being biocompatible and hydrophobic makes PCL a polymer of excellence.

A promise to this material is the development and synthesis of PCL-based amphiphilic block copolymers [150]. Since the administration of therapeutic compounds may be hampered by its low solubility in water, this problem can be solved when combined with another biomaterial, for example, the CS. In this case, the combination of the hydrophobic PCL with the hydrophilic CS lead to self-assembly micelles. These, in turn, are capable of increasing the solubility of hydrophobic molecules, as already mention above.

2.7 Chitosan-grafted-polycaprolactone (CS-*g*-PCL)

Over the past few years, research into biomaterials for drug delivery has been long. Particularly, polymers for drug delivery has been explored because the improvement solubility of therapeutic molecules. As PCL degrades more slowly than other aliphatic polyesters, by having a rubber behavior at RT, and due to other properties already discussed above, it is one of the major polymers chosen for drug delivery. Thus, synthetize a hybrid biomaterial by grafting CS and PCL is a big deal because their problems of solubility well known.

Besides overcome the solubility problems through the PCL graft CS [151], hydrophilicity of CS enhances the wettability and permeability of PCL by accelerating the hydrolytic degradation of PCL [137]. Moreover, the distribution of the hydrophobic chains of PCL by the hydrophilic phase of CS, promotes cell attachment and adsorption of proteins [152].

Several methods of synthesis of these polymers have been performed. However, combining CS and PCL by grafting is considered the most effective method to form a biofunctional biomaterial by the combination of the excellent properties of both polymers [153]. There are several grafting methods to produce this excellent biomaterial. For example, Cai et al., [154] used stoichiometric sodium dodecyl sulfate-CS complex as an intermediate and the grafting level of PCL could be modulated by adjusting the PCL and sulfate-CS complex weight ratio. Already Yu et al., [151] used *N*-phthaloyl CS as an intermediate to synthetize CS-*g*-PCL. This reaction is called protection-grafting-deprotection route. In this situation, the amino groups of CS are protected and just the hydroxyl groups at C-3 and C-6 are remained as active initiating points for grafting. After that, the phthaloyl groups are deprotected to regenerate free amino groups, as already described above.

On the other hand, ROP of ε-CL through CS is a method that allows a high grafting level of PCL polymer [155]. Usually, this reaction is developed with 4-dimethylamino-pyridine as a catalyst and water as a swelling agent [84, 156] or methanesulfonic acid as solvent and catalyst [5, 155] or using stannous octoate as a catalyst [153].

Another approach is also possible. To synthesize CS-*g*-PCL, Liu *et al.*, [157] used ROP of ε-CL onto phthaloyl-protected CS in the presence of tin (II) 2-ethylhexanoate catalyst via a protection-grafting-deprotection route in the presence of toluene [157].

In this dissertation, to reach CS-*g*-PCL a carbodiimide reaction by amidation was employed. From PCL modified with a terminal carboxyl group it is possible graft PCL onto CS backbone using amine coupling agent DCC/NHS at an alkaline pH, reacting the carboxyl end groups of PCL with the amine groups of CS. The product of this reaction, CS-*g*-PCL, is a CS amphiphilic derivative modified by *N*-acylation (see **Section 2.5.2.2.1**). PCL with a terminal carboxyl group is activated with DCC which is then stabilized with NHS, forming PCL succinimide ester (PCL-NHS). After removing the insoluble by-product, dicyclohexylurea, PCL-NHS activated is added to the CS solution is comprised of acetic acid and sodium hydroxide to a pH of 7-8. The reaction between two polymers continued at 50 ºC for 24 h.

Blank page

Chapter 3

Material and Methods

3.1 Chemical material

To assess the degree of acetylation (DA) and de molecular weight (Mw) of chitosan (CS, Sigma Aldrich), N-acetyl-D-glucosamine from Sigma Aldrich was used. Acetic acid and sodium acetate were from Panreac.

Polycaprolactone (PCL) was purchased from Polyscitech (PCL, 1-5 KDa). The carboxylic end groups of the PCL were activated by *N*,*N*'-Dicyclohexylcarbodiimide (DCC, Alfa Aesar) and *N*-Hydroxysuccinimide (NHS, Sigma Aldrich) for direct conjugation with CS by amidation reaction. Dichloromethane (DCM, Merck Millipore) and dimethylformamide (DMF, Merck Millipore) was used to solubilize PCL.

Paclitaxel (PTX) was kindly provided by Indena SpA – Milano, and the centrifugal filters (Amicon® Ultra-15, 100 kDa) were used to separate the unencapsulated drug of the micelles. To perform the *in vitro* release study was used 10 KDa cut-off dialysis membrane (Thermo Scientific), phosphate-buffered saline (PBS) and Tween®-80 (Sigma Aldrich).

3.2 Cell culturing

Colorectal cancer cell lines, C2BBe1 Clone of Caco-2 was obtained from American Type Culture Collection (ATCC, USA), and HT29-MTX cell line was kindly provided by Dr. T. Lesuffleur (INSERMU178, Villejuif, France). Dulbecco's modified Eagle medium (DMEM, Lonza), was supplemented with 10% (v/v) fetal bovine serum (FBS, Merck Millipore), 1% (v/v) penicillin (100 U/mL, Merck Millipore), streptomycin (100 µg/mL, Merck Millipore) and 1% (v/v) non-essential amino acids (NEAA, Merck Millipore). 3-(4,5-dimethylthiazol-2-yl)-2,5-diphenyltetrazolium bromide (MTT) and dimethyl sulfoxide (DMSO) were obtained from Sigma Aldrich, Triton X-100 1% from Spi-Chem, and culture flasks, 96-well tissue culture plates and Transwell® plates were purchased from Corning Inc., USA. The plates were read in microplate spectrophotometer (Biotek Synergy 2, USA) and cells were maintained in an incubator (ESCO CelCulture® CO_2 Incubator, Singapore) at 37 ºC temperature and 5% CO_2 in a water saturated atmosphere.

3.3 Methods

3.3.1 Degree of acetylation

The spectrophotometer UV/Vis spectrometer (UNICAM) used to determine the DA of CS was utilized in the spectrum range of 190 to 240 nm. Three solutions of acetic acid at of 0.01, 0.02 and 0.03 M were prepared and recorded the first derivative spectra, against water. The superposition of the three spectra shows the zero crossing point (H, at 203 nm), that is when all the acetic acid spectra share a common point. The zero crossing point is close to the N-acetyl-D-glucosamine maximum on the wavelength axis what makes the N-acetyl-D-glucosamine determination independent of the acetic acid concentration in the concentration [158].

Then were prepared 5 references of N-acetyl-D-glucosamine in the range 0.5 – 3.5 mg (0.5 mg, 1 mg, 1.5 mg, 2.5 mg and 3.5 mg) in 100 mL of acetic acid 0.01 M and record the spectra as before. For the spectrum of CS was dissolved 500 mg in 50 mL of 0.1 M acetic acid and then dilute to 500 mL with water.

The determination of DA of chitosan by ^{1}H NMR were also performed. Approximately, 6 mg of CS was dissolved in 1 mL of hydrochloric acid/deuterium oxide 1% (HCl/D_2O, v/v) under constant magnetic stirring for 24 hours at RT. The resulting solution was transferred into quartz tube (Noreli 507-HP) and the conditions employed in spectrum acquisition were: a) water suppression pulse sequence to 1-1 with an interval of 3 s between the pulses suppression; b) accumulation of 32 scans; c) 7s relaxation interval; d) 80 ºC; e) spectral window of 10.0 ppm.

This method consists in using the area under the peak at 2 ppm region assigned to the methyl of hydrogen nuclei of the acetamide group (ACH_3) and the area of peak attributed to the proton attached to 2-carbon of the glucosamine ring (AH_2-H_6) as it has already been described [159]. The areas were obtained from the ACD/ChemSketch software. Then, the DA is obtained from the following equation:

$$\%DA = \frac{\frac{A(CH_3)}{3}}{\frac{A(H_{2-6})}{6}} \times 100 \quad (3.1)$$

3.3.2 Molecular weight

To determine the Mw was used the Ubbelohde capillary viscometer (Kapillar-Viskosimeter, Schott). First, a solution of acetic acid 0.5 M in 500 mL of distilled water was prepared. Then, CS was dissolved in acetic acid 0.5 M/sodium acetate 0.2 M at 3 different concentrations (0.01 g/dL, 0.02 g/dL and 0.04 g/dL).

The viscometer was immersed in a constant temperature bath at 25 $\pm$ 0.1°C. The flow time (t) was recorded and this procedure was repeated five times for each concentration. The average of Mw was obtained from Mark-Houwink equation: $\eta = KM_v{}^a$, where [η] is the intrinsic viscosity, M_v is the average of Mw of the solution and **K** and **a** are the Mark-Houwink constants specific for a given polymer [160].

To reach the intrinsic viscosity, the following equations were calculated:

$$\eta_r = \frac{t}{t0} \quad (3.2)$$

$$\eta_{sp} = \eta_r - 1 \quad (3.3)$$

$$\eta_{sp\,red} = \frac{\eta_{sp}}{C} \quad \textbf{(3.4)}$$

$$\eta_{in} = \frac{\ln \eta_r}{C} \quad \textbf{(3.5)}$$

$$[\eta] = \frac{\eta_{sp}}{C}_{C=0} \quad \textbf{(3.6)}$$

where, η_r is the relative viscosity, t is the solution flow time in the viscometer; $t0$ is the time flow of the pure solvent in the viscometer; η_{sp} is the specific viscosity; $\eta_{sp\,red}$ is the reduced specific viscosity, also known by the Huggins equation; η_{in} is the inherent viscosity, also known by the Kraemer equation; C is the concentration of polymer in g/dL; $[\eta]$ is the intrinsic viscosity in dL/g and is calculated extrapolating ($C = 0$) the linear regression obtained by plotting $\frac{\eta_{sp}}{C}$ against *C*, according to Huggins equation.

3.3.3 Synthesis of chitosan-grafted-polycaprolactone

The synthesis of chitosan-grafted-polycaprolactone (CS-*g*-PCL) was carried out based on the work done by Elkhooly *et al*. [161]. Briefly, 2% (w/v) chitosan solution was prepared by dissolving in 2% (v/v) acetic acid in a glass beaker with moderate stirring until the complete dissolution of CS. The pH of the supernatant was adjusted with 3M NaOH to 7-8. The deprotonation of CS amine groups is essential step to improve the efficiency of conjugation, because of the activated succinimide ester reacts with primary amines at physiologic to slightly alkaline conditions (pH 7.2 - 9). PCL (1 g) was dissolved in 50 mL of 1:1 (v/v) DMF/DCM. After complete dissolution of PCL, 2.5 mmol of DCC and 2.5 mmol NHS was added to the solution. The activation reaction of the carboxyl group of the PCL (which will react with the amine groups of CS) through NHS using DCC as a catalyst was carried out for 12 h at RT. The insoluble by-product of this reaction, dicyclohexylurea, was removed by centrifugation for 20 minutes at 15 ºC and 4300 rpm (Thermo Scientific Heraeus Megafuge 1.0R). The obtained solution was further filtered under vacuum. To remove the excess of reagent DCC/NHS, the activated PCL solution was dialyzed against 10 fold volume of DMF/DCM using 10 KDa cut-off dialysis membrane (Thermo Scientific) for 2 days with two changes of volumes. Finally, 12.5 mL of activated PCL (PCL-NHS) solution was added into 50 mL of CS solution (pH= 7-8) and stirred for 24 h at 50 ºC.

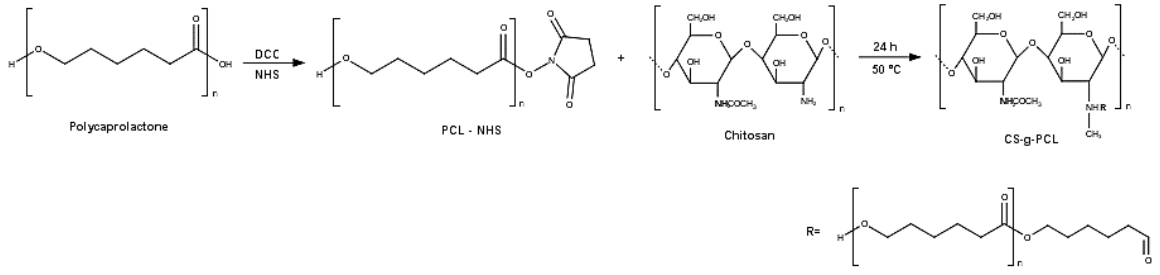

Figure 3.1 - Synthesis scheme the reaction of chitosan with polycaprolactone through chitosan modification by *N*-acylation.

3.3.4 Characterization of chitosan-grafted-polycaprolactone

Nuclear magnetic resonance (NMR, Bruker Avance III 400) was performed in order to confirm the formation of the new copolymer. Approximately, 6 mg of samples were dissolved in 1 mL of HCl/D_2O 1% (v/v) for chitosan, $CDCl_3$ for polycaprolactone and HCl/D_2O 1% (v/v) for graftcopolymer under constant magnetic stirring for 24 hours at RT. The resulting solution was transferred into quartz tube (Noreli 507-HP) and the conditions employed in spectrum acquisition were: a) water suppression pulse sequence to 1-1 with an interval of 3 s between the pulses suppression; b) accumulation of 32 scans; c) 7s relaxation interval; d) 80 ºC; e) spectral window of 10.0 ppm.

Attenuated total reflection Fourier transforms infrared spectroscopy (ATR-FTIR) spectra of each sample were generated by ABB MB3000 FTIR spectrometer from ABB (Zurich, Switzerland) equipped with a MIRacle single reflection attenuated total reflectance (ATR) accessory from PIKE Technologies (Madison, WI, USA). All spectra were collected with 256 scans and a 4 cm^{-1} resolution in the region of 4000-600 cm^{-1}.

Contact angle of the copolymer and the commercial chitosan were measured on an optical contact angle measuring device (OCA15, Dataphysics Instruments Co. Ltd, German) to determine the hydrophilicity/hydrophobicity of the new polymer obtained. For this test, 200 mg of each sample was subjected to vacuum during 2 minutes followed by 8 tons for 30 seconds, in order to form a tablet. For the drop, 4 µL of distilled water are released from a needle (0.50 mm) falling on the tablet. Contact angles are measured using the Laplace-Young method with brightness of 96 and contrast of 511 at 15 seconds after the fall of the drop, focused by a high performance CCD camera.

The critical micelle concentration (CMC) of CS-*g*-PCL was determined by a conductimetric titration (Consort C863, Spain) carried out at 25 ºC. The procedure consists of measuring the conductivity of various copolymer concentrations (1 mg/mL - 1×10^{-6} mg/mL). Then, the concentration values used are used in logarithmic values with the respective values previously found and, the CMC was obtained by the meeting of two lines of the graph of conductivity against concentration.

3.3.5 Preparation of paclitaxel-loaded chitosan-grafted-polycaprolactone micelles

The paclitaxel-loaded chitosan-grafted-polycaprolactone (PTX-CS-*g*-PCL) micelles were prepared by evaporation method. First, 5 mg of copolymer was dissolved in 5 mL of acetic acid 0.1M and DMF (1:1) (v/v). Then, to the homogeneous mixture was added dropwise 250 µL, 125 µL, 50 µL or 25 µL of PTX solution at concentration of 1 mg/mL (for different PTX loading), dissolved in 70% ethanol, which corresponds to a drug mass compared to the mass of copolymer of 5.0%, 2.5%, 1.0% and 0.5%, respectively. The mixture was allowed under stirring for 4 h to evaporate the solvent. After 4 h, the solution was sonicated for 5 minutes in iced bath. Then, the solutions was centrifuged through Amicon® Ultra-15 100 kDa at 5000 rpm during 10 minutes to remove the unencapsulated drug. After filtration, PTX-CS-*g*-PCL polymeric micelles were collected. In **Figure 3.2** is possible observe a schematic representation of the method used to produce PTX-CS-*g*-PCL micelles.

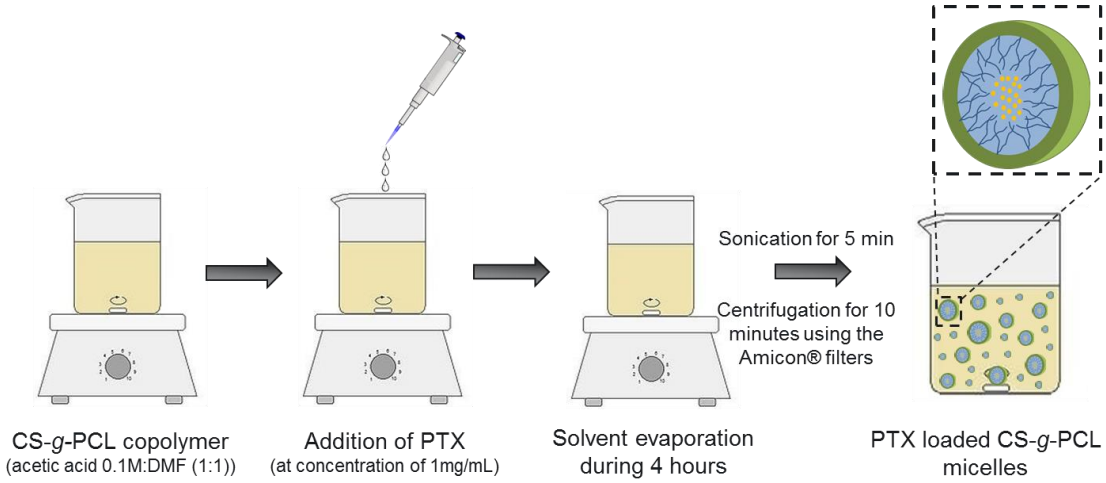

Figure 3.2 – Schematic representation of the method used to prepare PTX loaded CS-*g*-PCL micelles.

3.3.6 Characterization of paclitaxel-loaded chitosan-grafted-polycaprolactone micelles

The average diameter, polydispersity index and surface charge were determined by dynamic light scattering (DLS) and electrophoretic light scattering (ELS) (ZetaSizer Nano ZS, Malver, UK), respectively. All measurements were performed with three independent batches of micelles, with three runs each.

The PTX encapsulation efficiency (EE) and drug loading (DL) of micelles were assessed indirectly by assaying the amount of drug recovered in supernatants resulting from centrifugation by high performance liquid chromatography (HPLC, Merck-Hitachi 7000). The HPLC analysis of PTX samples was achieved on a LiChrospher® 100 RP-18 (5 µm) (Merck Millipore) with guard column with a mobile phase consisting of methanol and water (65:35, v/v) at a flow rate of 1.0 mL/min. The sample injection volume was 20 µL, and the absorbance wavelength was set at 227 nm in an UV detector. The EE and DL was calculated using the following formula, respectively:

$$EE\% = \frac{initial\ paclitaxel - recovered\ paclitaxel}{initial\ paclitaxel} \times 100 \quad (3.7)$$

$$DL\% = \frac{initial\ paclitaxel - recovered\ paclitaxel}{micelles\ weight} \times 100 \quad (3.8)$$

The morphological features of the micelles were observed by transmission electron microscope (TEM). Samples were prepared by placing 10 µL of micellar solution obtained after centrifugation on 300 mesh nickel grids, and after 2 minutes the excess of suspension was removed with filter paper and, examined under a JEOL JEM 1400 TEM (Tokyo, Japan). Images were digitally recorded using a Gatan SC 1100 ORIUS CCD camera (Warrendale, PA, USA).

3.3.7 *In vitro* paclitaxel release studies

The *in vitro* release profiles of free PTX and the PTX-CS-*g*-PCL micelles were studied by dialyzing the drug-loaded micellar solution against 40 mL of PBS (pH 7.4, 0.1% (w/v) Tween®-80). From the

micellar solution obtained, 2.5 mL were placed in a dialysis membrane (10 KDa cut-off, Thermo Scientific). The membrane was then immerged into the release medium. Each sample was gently agitated at 100 rpm at 37°C (IKA KS 4000i Control). At predetermined time intervals (0.25, 0.5, 075, 1, 2, 4, 6 and 8 h), 2 mL of release medium was removed, and the same volume of medium was refreshed. The amount of PTX released was determined by HPLC analysis, as described below.

In order to compare the release profile of the PTX encapsulated in micelles with the free PTX, 156 µL of PTX at concentration of 1 mg/mL was added at release medium to perform a volume of 2.5 mL. Then, this solution was placed in a dialysis bag was conducted under the same conditions described. The release experiments were conducted in triplicate and the mean was calculated.

Tween®-80 was included in the release medium to increase the solubility of PTX as well as to prevent binding of the PTX to the dialysis membrane, maintaining the sink conditions [162]. One requirement for achieving a suitable drug dissolution test is to use a sufficient volume of dissolution medium or release medium that should be able to dissolve the expected amount of drug released. This ability to dissolve the expected amount of drug is known as a sink conditions.

3.3.8 Cytotoxicity studies

Potential cytotoxicity of CS, PCL, empty micelles, free PTX and PTX-CS-*g*-PCL micelles was tested against Caco-2 (C2BBe1 clone) and HT29-MTX cells, colorectal cancer cells, using MTT reagent. Caco-2 (passage 51-74) and HT29-MTX (passage 41-63) cells grew separately in culture flasks in a complete medium consisting of DMEM supplemented with 10% (v/v) FBS, 1% (v/v) L-glutamine, 1% (v/v) NEAA, and 1% (v/v) antibiotic-antimitotic mixture (final concentration of 100 U/ml Penicillin and 100 U/ml Streptomycin). The culture medium was replaced every other day. Cells were seeded (200 µL) into wells of 96-well tissue culture test plates with 1×10^4 cells/well for HT29-MTX cell line and 2×10^4 cells/well for Caco-2 and incubated at 37ºC in a 5% CO_2 air atmosphere for 24 hours. Then, medium was removed and cells are washed twice with 200 µL of PBS. Then was replaced fresh warm medium (200 µL) with different concentrations (0.01 - 0.1 – 1 – 10 – 100 – 1000 µg/mL) of CS, PCL, empty micelles, PTX-CS-*g*-PCL micelles and free PTX (the latter two were not performed cytotoxicity at the two highest concentrations). A negative control (Triton X-100 1%) and positive control (medium with cell incubation) was included. After 4 h and 24 h of incubation at 37 ºC in 5% CO_2 atmosphere, the medium was discarded and cells were washed twice with 200 µL of PBS. Finally, was added 200 µL of MTT solution per well (final concentration of 0.5 mg/mL) and was incubated for 4 h in dark. After 4 h, was removed and discard the MTT solution, and was added 200 µL of DMSO to dissolve the MTT formazan crystals. The plates were placed in orbital shaker for 15 min in the dark, at RT and the absorbance was measured using a microplate spectrophotometer at 570 nm and 630 nm. The results was analysed according to the following equation:

$$Viability\ (\%) = \frac{experimental\ value - negative\ control}{positive\ control - negative\ control} \times 100 \qquad (3.9)$$

The MTT assay is a colorimetric assay used to assess the cellular metabolism and inference on cellular viability, measuring the activity of cellular enzymes that reduce the thiazolyl blue tetrazolium bromide (MTT) substrate, to form insoluble formazan crystals, resulting on a dark purple colour [163].

3.3.9 Permeability studies

For the permeability experiments, 1×10^5 cells/cm^2 in monocultures of Caco-2 cells and co-cultures of Caco-2:HT29-MTX in a proportion of 90:10 were seeded in 12-Transwell® cell culture inserts (pore diameter 3.0 µm) and were allowed to grow and differentiate for 21 days with medium replacement every other day, as previously optimized by our group [38, 44].

Before permeability experiments, DMEM was removed from both chambers and the Transwell membrane was washed twice with pre-warmed Hank's buffered salt solution (HBSS), then replaced by new HBSS and allowed to equilibrate for 30 min at 37 ºC. Permeability studies were run at 37 ºC during 3 h and with 0.5 mL of PTX-CS-*g*-PCL 2.5% micelles and free PTX at concentration of 50 µg/mL, both prepared in HBSS, were placed in the apical side and 1.5 mL of HBSS in the basolateral side. At different time points (15, 30, 45, 60, 90, 120 and 180 minutes), 200 µL of each samples were taken from the basolateral side of the inserts and the same volume of fresh HBSS was added to replace the withdrawn volume. At the end of the experiment, all volume (0.5 mL) of the apical compartment was removed for further analysis. The sample concentrations were quantified by HPLC analysis of PTX samples as already described above.

The integrity of the cell monolayers was checked before the permeability experiment by measuring the transepithelial electric resistance (TEER) using Millicell® Electrical Resistance System (Millipore, USA). The values were normalized by subtracting the resistance value of the empty insert and expressed in ohm per area of the insert (Ω.cm^2). The permeability results were expressed in percentage of release and apparent permeability (P_{app}). P_{app} was calculated using the following equation:

$$P_{app} = \frac{\Delta Q}{A \times C_0 \times \Delta t} \quad (3.10)$$

, where C_0 is the initial concentration in the apical compartment (µg/mL), A is the surface area of the insert (cm^2), Δt is the time during which experiment occurred (seconds) and ΔQ is the amount of compound detected in the basolateral side (µg).

3.3.10 Statistical analysis

All the experiments were performed in triplicate and are represented as mean ± standard deviation (SD). A one-way and two-way analysis of variance (ANOVA) with Bonferroni Multiple/Post Hoc Group Comparisons (GraphPadPrism software Inc., USA) was used to analyse the data. The level of significance was set at probabilities of *p < 0.05, **p < 0.01, and ***p < 0.001.

Blank page

Chapter 4

Results and Discussion

4.1 Chitosan characterization

CS is a polysaccharide obtained by partial or complete deacetylation of chitin, and its molecular structure and properties are largely affected by the DD. Important properties of biological impact are biocompatibility, biodegradation, mucoadhesion, adsorption enhancing, antioxidant capacity, hemostatic effect and cell response [160, 164]. Important to notice is that the DD can be replaced by the DA, where $\boldsymbol{DA = 100 - DD}$.

4.1.1 Degree of acetylation

CS is composed of two far UV chromophoric groups, N-acetyl-D-glucosamine (GlcNAc) and D-glucosamine (GlcN) [165]. Because of these groups show no evidence of interacting within the polymer in a manner that would affect absorption of UV radiation, the monomer units contribute in a simple way to the total absorbance of the material, at a particular wavelength [165].

Determination of the DA of CS by UV spectrophotometry using dual standards is a simple, convenient and accurate method to determine the DA of chitosan. However, another method is already widely used, which is the first derivative of the UV spectrophotometry offering a simple and fast measurement of DA value with good accuracy and precision [158]. Although UV spectra of the zero order can be used to measure DA, the first derivative of the spectra is less affected by background noise and impurities [166], and so as suggested method [167].

The degree of acetylation of the chitosan was determined according to the first derivative ultraviolet spectrophotometry method. The spectra of GlcNAc and acetic acid solutions were superposed from it is the first derivative (**Figure 4.1**).

By overlaying all spectra obtained it is possible to measure the **H**, in the ordinate axis, which is found measuring the distance between the zero crossing point to each GlcNAc concentration, and draw a linear calibration curve and determine the equation, linearity and confidence limits (**Figure 4.2**). Thus, a linear calibration curve was obtained by plotting the H values against the correspondent GlcNAc concentration.

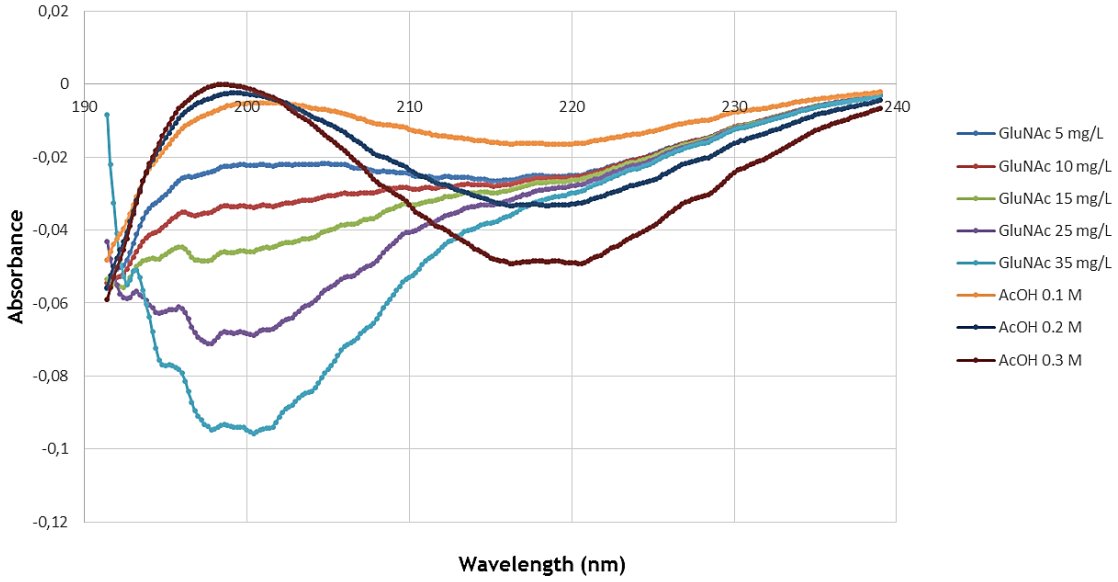

Figure 4.1 – First derivative UV-spectra for various concentrations of acetic acid and N-acetyl-D-glucosamine. The point where all the acetic acid spectrum cross is the zero crossing point.

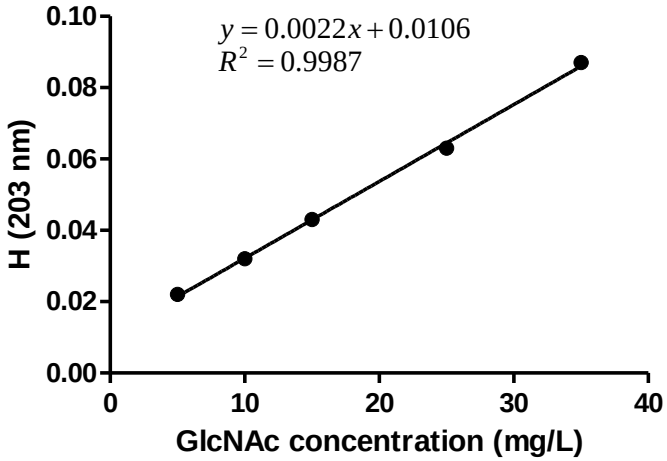

Figure 4.2 – H values as a function of GlcNAc concentration.

In **Figure 4.3** it can be seen the CS spectra plotted overlapped on the **Figure 4.1**. By measuring the value of the CS spectra at 203 nm (zero crossing point), the concentration of GlcNAc in the analysed CS sample can be determined by substituting the correspondent H by Y in the obtained equation (**Figure 4.2**). So, the achieved concentration of N-acetyl-D-glucosamine in mg/L is equal to the degree of acetylation in wt.% (only valid if the chitosan sample dissolved is exactly 500 mg) [167].

The DA value (19.27%) can be seen in **Table 4.1** as well as the DD, which was calculated through the following equation:

$$DD = 100 - DA \quad \textbf{(4.1)}$$

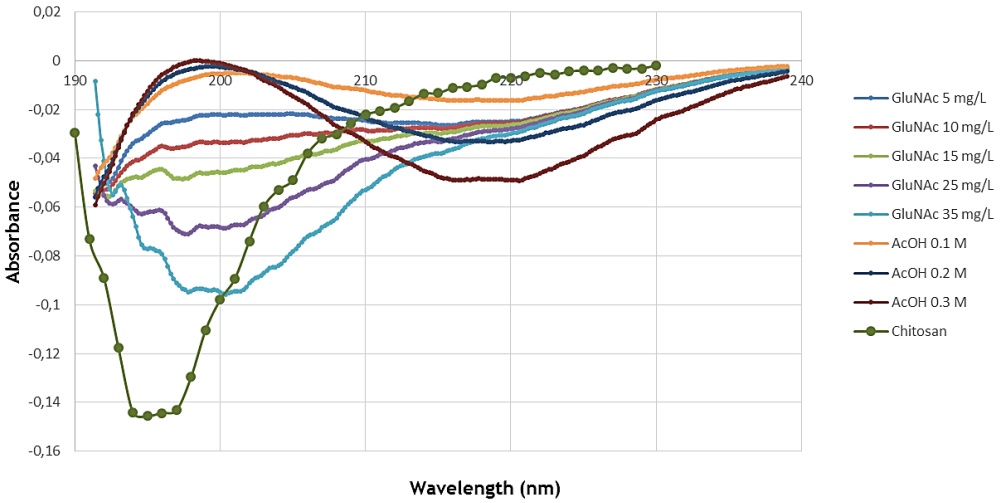

Figure 4.3 – First derivative UV-spectra for a chitosan sample and various concentrations of acetic acid and N-acetyl-D-glucosamine.

To confirm the results obtained by the previous technique, DA was also determined by NMR spectroscopy.

In the ^{1}H NMR analysis is possible to find the DA by CH_3 (GlcNAc) and H_2-H_6 (GlcNAc and GlcN) areas from the CS spectrum, as can be seen in **Figure 4.4**, since the NMR shows the complete structure of CS. This method consists in using the area under the peak at 2 ppm region assigned to the methyl of hydrogen nuclei of the acetamide group (ACH_3) and the area of peak attributed to the proton attached to C-2 of the glucosamine ring (AH_2-H_6) as it has already been described [159]. Then, the DA was obtained through the substitution of the areas in the **Equation 3.1**. The DA obtained was 18.48%.

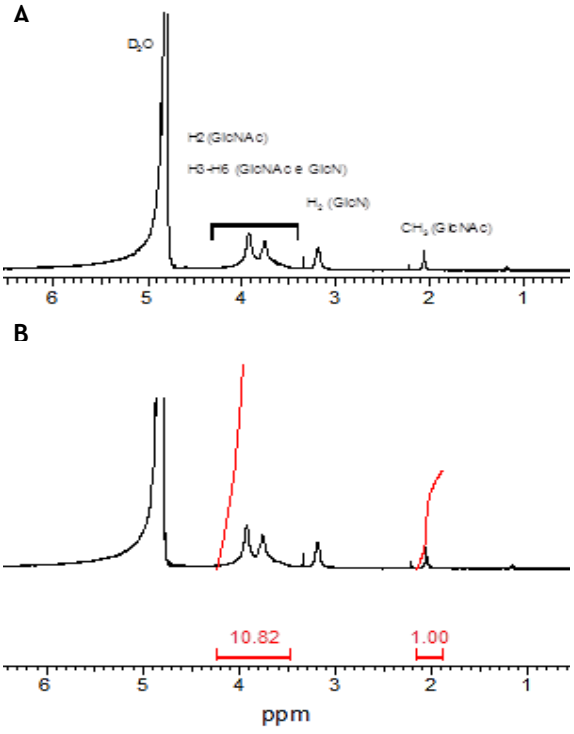

Figure 4.4 – ^{1}H NMR chitosan spectrum with group's identification (**A**) and with calculated areas (**B**).

This means that DD is 81.52%. **Table 4.1** summarizes the DD for the chitosan obtained by First derivative UV-spectra and ^{1}H NMR.

Table 4.1 — Degree of deacetylation (DD) and degree of acetylation (DA) of chitosan calculated through the first derivative spectra and ^{1}H NMR analysis.

	First derivative	^{1}H NMR
DD (%)	80.73	81.52
DA (%)	19.27	18.48

Through the analysis of the results, it can be conclude that both techniques had similar results. Thus, during this dissertation, the DD of the CS used is about 81%.

The use of the DD on this range of values is common to other similar studies performed where the DD was 85% [84, 168]. As mentioned before, the DD and Mw are important CS features that must be known in order to predict physicochemical characteristics such as biocompatibility or biodegradability. Besides that, the higher the DD, more free amino groups will be to react with other molecules. In this particular case, it is important that the CS had a high DD for free amino groups react with the carboxylic groups of PCL.

4.1.2 Molecular weight

The Mw of CS was determined by viscometric method [169] at 25 ± 0.1ºC. The relative viscosity, η, of CS samples was measured using Ubbelohde capillary viscometer and the intrinsic viscosity [η] of CS was calculated using both the Huggins and the Kraemer equations.

As mentioned earlier, the average of Mw was determined based on the Mark-Houwink equation: $\eta = K{M_v}^{a}$, where $k = 3.5 \times 10^{-4}$ and $a = 0.76$ [158].

The intrinsic viscosity was assumed to be the average between the values obtained from Huggins and Kraemer equations. For CS the intrinsic viscosity was 1.993 and based on the Mark-Houwink equation, the M_v determined was 87,371 Da, approximately 87 kDa. In **Figure 4.5**, it is shown the Huggins and Kraemer equations with their equations, used to calculate the Mw of CS.

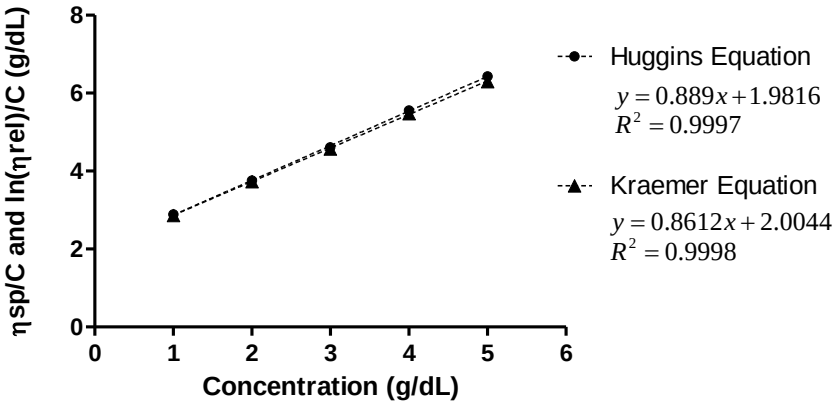

Figure 4.5 – Plots of the $\eta sp/C$ and $ln(\eta rel)/C$, from Huggins and Kraemer equations, respectively, versus concentration of the chitosan samples.

A study performed by Schipper *et al*. [94], used several types of CS varying their Mw and DD to assess how this variation had influence on the absorption of drugs through human epithelial cells. Permeability was evaluated in monoculture Caco-2 model. The results showed that CS with low Mw (<22 kDa) and high DA (<35%) had little improvement in the absorption of molecules. On the other hand, CS with low DA and high Mw increased epithelial permeability [94].

It can be concluded that, besides the physical and chemical characteristics dependent of these two factors, the improvement of drug absorption by the intestinal epithelium is also dependent of them. So, based on these facts, the CS used in this work seems to be the one with the ideal characteristics to be as drug carrier in the intestinal epithelium.

4.2 Synthesis and characterization of chitosan-grafted-polycaprolactone

A carbodiimide reaction by amidation was made to reach chitosan-grafted-polycaprolactone (CS-*g*-PCL) as shown in **Figure 3.1**. As described above, from modified PCL with a terminal carboxyl group it is possible to graft PCL onto CS backbone using amine coupling agent DCC/NHS at an alkaline pH. PCL, with a terminal carboxyl group, is activated with NHS, which is catalyzed with DCC, forming polycaprolactone succinimide ester (PCL-NHS). After removing the insoluble by-product, dicyclohexylurea, PCL-NHS activated is added to the CS solution is comprised of acetic acid and sodium hydroxide to a pH of 7-8. The reaction between two polymers continued at 50 ºC for 24 h.

4.2.1 NMR analysis

The chemical structure of CS-*g*-PCL was verified by ^{1}H NMR analysis. In **Figure 4.6A**, **4.6B** and **4.6C**, it was observed the ^{1}H NMR spectra of CS-*g*-PCL, PCL and CS, respectively. Four characteristic peaks of PCL emerged at 1.4, 1.6-1.7, 2.3, 4.1 ppm, which corresponded to the γ, ß and δ, α and ε signals of the graft segment in CS-*g*-PCL copolymer, respectively. The peaks at 3.4-4.0 and 2.05 ppm were assigned to 3, 4, 5, 6, 6' and 7 of pyranose repeat units in CS, respectively.

The chemical structure of CS-*g*-PCL was clearly confirmed by the presence of the characteristic peaks of CS and PCL in the ^{1}H NMR spectrum [151]. So it could be concluded that CS-*g*-PCL were successfully prepared through carbodiimide reaction by amidation.

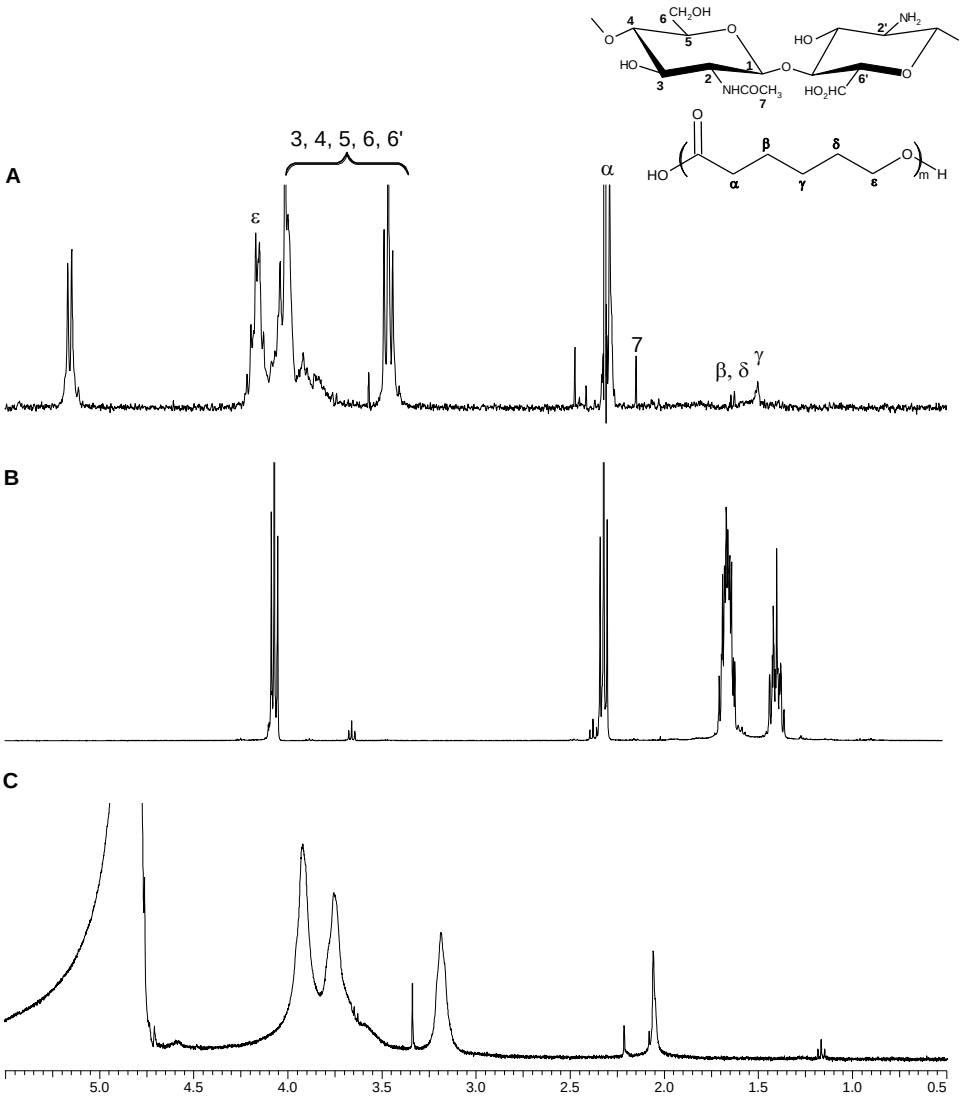

Figure 4.6 - ^{1}H NMR spectra of (**A**) CS-*g*-PCL in HCl/D_2O 1% (v/v), (**B**) PCL in $CDCl_3$ and (**C**) CS in HCl/D_2O 1% (v/v).

4.2.2 FTIR analysis

The activation of the terminal carboxylic end groups of the PCL is followed by the formation of secondary amide bonds (O=C–NH) between PCL and CS.

The broad band around 3389 cm^{-1} corresponded to the contribution of the O–H stretching from intra/inter molecular hydrogen bonding and N–H stretching of CS (**Figure 4.7C**). The peaks at 890 cm^{-1} until 1094 cm^{-1} was assigned to ether groups of the saccharine structures of CS [170]. The peak at 1590 cm^{-1} belongs to the N–H deformations of amino group. The activation of the terminal carboxylic end groups of the PCL is followed by the formation of amide bonds (O=C–NH) between PCL and CS. For this reason, secondary amide bands were detected at 1650 cm^{-1} (–C=O stretching) (**Figure 4.7A**) [171]. On the other hand, several characteristic bands for PCL (–CO–O–C–) vibrations (**Figure 4.7B**) are located at 1725 (–C=O stretching) and the broad band at 2800-3000 cm^{-1} (**Figure 4.7B**).

The grafted copolymer presented characteristic bands of both CS and PCL and, more importantly, is shown the appearance of the new amide bands, result of the reaction of the two polymers, which implied the success of the carbodiimide reaction by amidation.

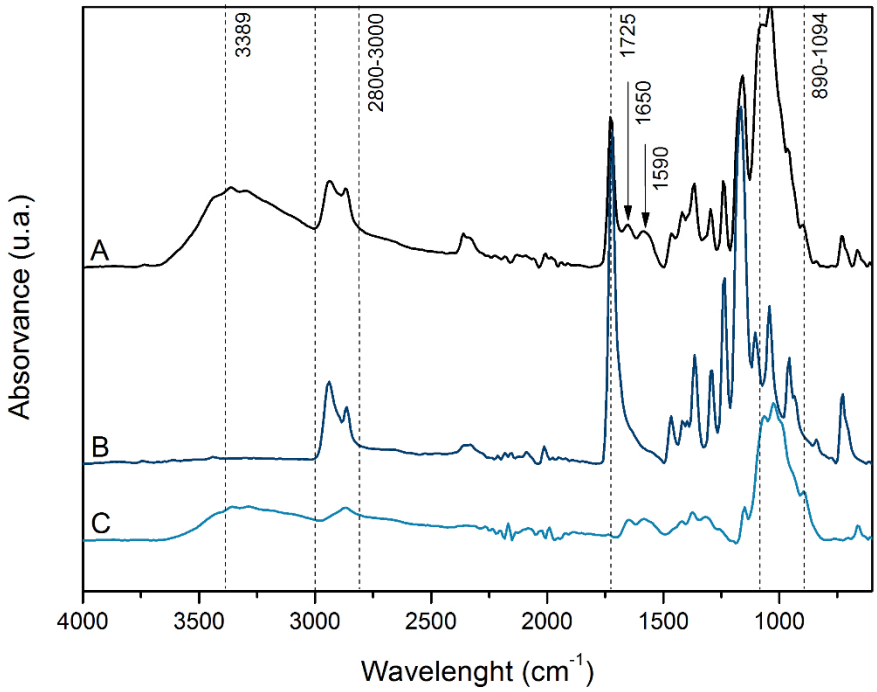

Figure 4.7 - ATR-FTIR absorbance spectra for detection of surface functional groups. (**A**) CS-*g*-PCL copolymer, (**B**) PCL and (**C**) CS.

NMR and FTIR analysis were performed in order to confirm the formation of the new copolymer. The NMR analysis is the most sensitive technique used to determine the structure of a substance. In this case, NMR was used in the identification of hydrogen groups of the copolymer. On the other hand, FTIR spectroscopy is based on the particular vibrations that each molecule is subjected, corresponding to an energy level. This energy depends on factors such as molecular geometry or the mass of atoms which is given as an indication of chemical groups presented in a substance [172]. Thus, FTIR analysis was used as complementary characterization since it is possible to observe the appearance of the new chemical bonds, in this case, the amide bands, result of the reaction of CS amine groups with carboxyl groups of PCL.

4.2.3 Contact angle

Another technique used to conform the reaction between these two polymers is the contact angle. Contact angle technique consists of the measurement of the angle that the drop surface makes with a solid, when they contact. The larger the angle is more hydrophobic the surface. An angle of 90-120º is considered a hydrophobic surface and an angle greater than 150º is considered a super hydrophobic surface. On the other hand, the contact angle low to 90º are considered hydrophilic.

As can be seen in **Figure 4.8**, the contact angle of CS is lower than the copolymer and therefore more hydrophilic. As expected, the contact angle of the copolymer is greater than the contact angle of the CS, which indicates the presence of the PCL hydrophobic groups in the new copolymer. However, this difference is not very strong, which may indicate a low DS of the copolymer. Still, these results are in agreement with the literature, where the contact angle of the copolymer is similar to the contact angle found by Gu *et al.*, for an average of ε-CL per glucosamine unit in CS of 21.3 [84].

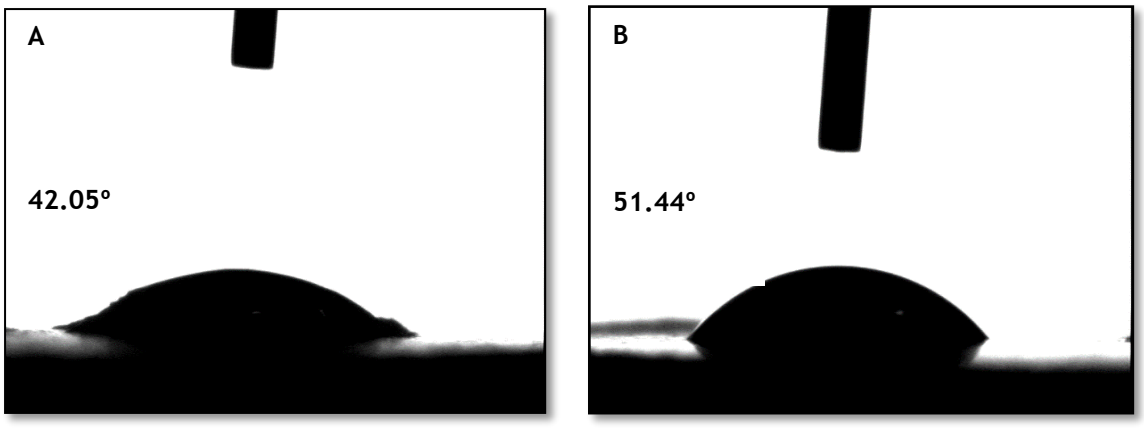

Figure 4.8 – Water contact angle of chitosan (**A**) and CS-*g*-PCL copolymer (**B**) after 15 seconds of analysis.

4.2.4 Critical micelle concentration

Due to the hydrophobic nature of the PCL and hydrophilic nature of the CS, CS-*g*-PCL has the ability to spontaneously form micelles in aqueous environment. To calculate the concentration at which copolymer can form micelles spontaneously, the conductimetric method was employed. The CMC was obtained by the meeting point of two lines of the graph of conductivity against the logarithmic concentration (**Figure 4.9**). The CMC obtained was 3.7×10^{-3} mg/mL, which is a result according to the literature [5].

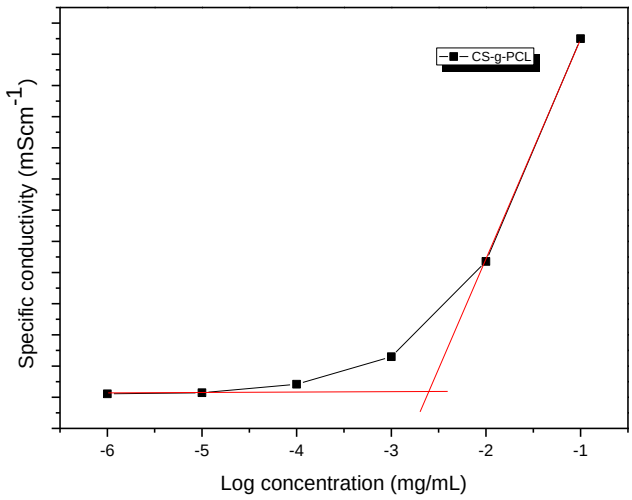

Figure 4.9 - Conductivity curve as a function of the log concentration of the copolymer.

4.3 Characterization of paclitaxel loaded chitosan-grafted-polycaprolactone

The properties and characteristics of the micelles affect the formulation stability, and can influence its future interactions with cells and tissues. Thus, aiming to predict the *in vivo* behavior of the developed micelles, their physical-chemical characteristics such as size, polydispersity index (PdI), zeta potential, encapsulation efficiency, drug loading and morphology were evaluated.

4.3.1 Particle size, size distribution and zeta potential

Several drug masses were tested for the same mass copolymer. Only for the formulation with 5% of PTX showed large size when compared with the others. Regarding the PdI and the zeta potential, no significant differences were observed when the drug addiction was altered.

As shown in **Table 4.2**, for all formulations tested, the size of the micelles varies from a high range 408-529 nm. Furthermore, the size of the micelles presented does not vary in proportion to the amount of drug added to the formulation and the values presented were high. However, the size of the micellar system is not a problem, since the micelles are not internalized by the cells [173].

Regarding the PdI, were presented high values in almost all formulations. However, these values can be explained by the fact of being micelles mostly made of a natural polymer, CS, where the size of the chains cannot be controlled and, therefore, the size of the micelles is very variable.

All micelles formulations showed positive zeta potential, indicating that micelles were properly coated with positively-charged CS. Consistent with previous published data [174, 175], the presence of PTX compared with free-drug nanocarriers did not significantly affect the average size and zeta potential of the micelles.

Table 4.2 - The particle size, polydispersity index (PdI), ζ-potential and theoretical drug loading of PTX-CS-*g*-PCL micelles and CS-*g*-PCL micelles (empty micelles). Each value represents the mean ± SD of three independent measurements ($n = 3$).

Sample	Theoretical drug loading (%)	Size (nm)	PdI	ζ-Potential (mV)
CS-*g*-PCL	-	435±25	0.546±0.160	27.5±1.1
PTX-CS-*g*-PCL	0.5	436±35	0.471±0.017	31.7±8.2
PTX-CS-*g*-PCL	1.0	427±64	0.501±0.135	33.1±4.1
PTX-CS-*g*-PCL	2.5	408±40	0.335±0.021	30.9±3.1
PTX-CS-*g*-PCL	5.0	529±33	0.451±0.041	33.3±2.1

4.3.2 Paclitaxel encapsulation efficiency

In order to quantify the amount of drug encapsulated in each micelle formulation, as indicated above, the quantification was carried out by HPLC.

A calibration curve to verify the feasibility of the method proposed for this drug analysis was run. The patterns for the calibration curve were prepared taking into account the mobile phase of the method and also, the solution in which the micelles were prepared. Thus, the preparation of patterns

was performed with a total volume of 1 mL, which 80% of volume was methanol and 20% was acetic acid 0.1M. The drug concentration used in each pattern ranged from 0.5 µg/mL to 100 µg/mL. In **Figure 4.10** is possible to observe the calibration curve found. As it can see, the calibration curve present a R^2=0.9991, which means the method is in perfect conditions, thus feasible to move forward in quantification.

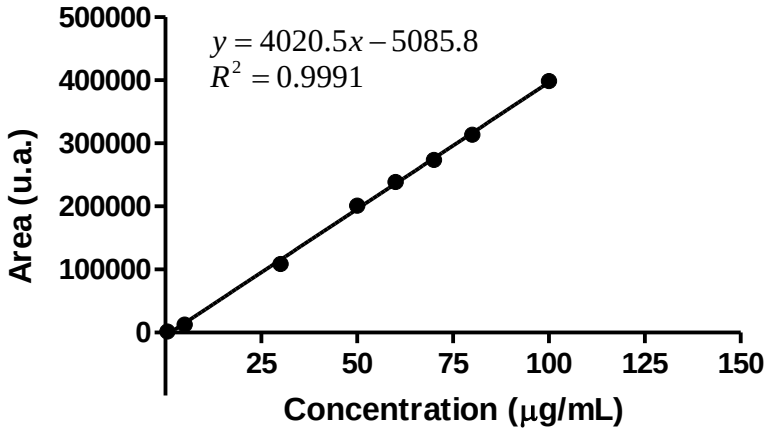

Figure 4.10 - Standard curve calibration for paclitaxel quantification using HPLC.

After the achievement of the calibration curve it was started by injecting the micelles with methanol in an attempt to destroy them. However, no peak was observed, indicating no destruction. So, it was tried with other solvents such as acetonitrile and chloroform, but remained intact micelles. Exhausted the alternatives for quantifying the EE by the direct method, it was moved to the indirect method. It means that it was used the resulting supernatants of centrifugation of the micelles, where only the non-encapsulated drug were present. Thus, the supernatants were injected and the peaks related to PTX appeared.

The average retention time of PTX is 7.9 minutes. For each peak found, its area was calculated. The area value obtained was substituted in calibration curve equation presented above, thereby obtaining the concentration of PTX. The EE was calculated from **Equation 3.7** and the DL was calculated from the **Equation 3.8**. **Table 4.3** presents the theoretical and practical values of DL as well as the efficiency of encapsulation.

Table 4.3 - The theoretical and practical drug loading of PTX-CS-*g*-PCL micelles. Each value represents the mean ± SD of three independent measurements ($n = 3$).

Sample	Theoretical drug loading (%)	Drug loading (%)	Encapsulation efficiency (%)
PTX-CS-*g*-PCL	0.5	0.401±0.004	80.6±0.9
PTX-CS-*g*-PCL	1.0	0.791±0.062	79.9±6.2
PTX-CS-*g*-PCL	2.5	1.995±0.034	81.8±1.4
PTX-CS-*g*-PCL	5.0	3.585±0.162	75.3±3.2

As can be seen in the table above, the increase of DL was not proportional to the increase of the EE. The results indicate that for a range of 0.5-2.5% of the EE is quite similar at around 80%. However, when increased DL to 5.0%, the EE decreased slightly, probably due to saturation of the micellar system. These results may indicate that due to the degree of substitution for this copolymer, the system is not capable to encapsulate more than 2.5-5.0%.

4.3.3 Transmission electron microscopy

TEM images (**Figure 4.11**) were taken to corroborate with micelle size and PdI, as well as assess the micellar morphology and PTX encapsulation. TEM microphotographs showed a variability in micelles size, justifying the high value of PdI, previously measured by DLS. However, is possible to see that most of the micelles found presents sizes smaller than 400 nm.

These microphotographs also confirms the uniform spherical shape of the micelles before and after encapsulation of PTX. The presence of the PTX in micelles did not affect their size as it was had already concluded with DLS analysis.

It is evident the presence of PTX in **Figure 4.11B** due to the blackening of the inside of the micelles, unlike **Figure 4.11A**, that had a completely white interior. This result confirm the EE described above, which is a very good result.

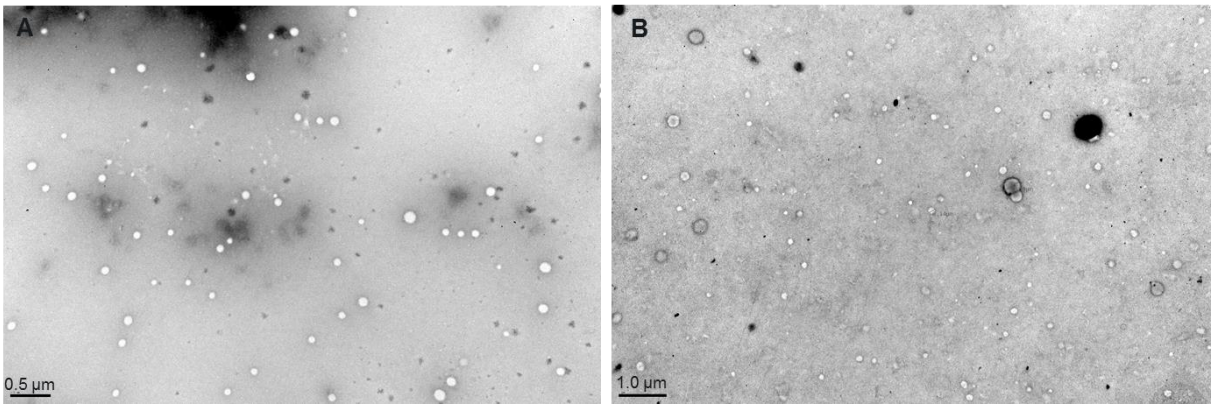

Figure 4.11 – Transmission electron microscopy images of CS-*g*-PCL free drug micelles (**A**) and PTX-CS-*g*-PCL micelles (**B**) with a scale bar corresponding to 0.5 µm and 1 µm, respectively.

Based on the results obtained in **Table 4.2** and **4.3**, was chosen drug concentration of 2.5% for the subsequent work since it is that presents more advantages in micellar system for drug delivery such as smaller size and lower PdI and higher EE.

4.4 In vitro release studies

The *in vitro* release profile of free PTX and PTX-CS-*g*-PCL micelles was investigated in 0.1% Tween®-80 containing PBS (pH 7.4, w/v) at 37 ºC, assuring sink conditions. The cumulative percentage release is shown in **Figure 4.12**.

As can be observed, 59% of the encapsulated PTX was released from the CS-*g*-PCL micelles in the first hour, despite the difficulty of release in the first time points. This is consistent with other works, where is suggested that the drug was entrapped and uniformly distributed in the matrix and thus, have more difficult to be released and, consequently, it takes longer [176].

When compared the release profile of PTX this micellar system with other drug carrier vehicles, it appears that the system developed had a controlled release profile in the first hours, unlike other works, where there was a burst release of PTX from the nanoparticles [174, 177]. Also, after 8 hours almost all PTX was released from the CS-*g*-PCL micelles. Already in other works carried out, the PTX carrier system used was not able to release all PTX encapsulated [174, 178]. Thus, this system appears to be a good approach for controlled release of PTX.

On the other hand, the release of the free PTX in the first hour is equivalent to 70.8% of the initial amount of PTX placed in the dialysis bag. The amount released is quite similar to the total amount of free PTX released (73.9%). As described in the literature [179], the total dissolution of free PTX occurs within the first hour of the experiment. However, the same did not happen in this study, probably because the sink conditions were not ensured effectively leading to an incomplete dissolution of PTX in the medium.

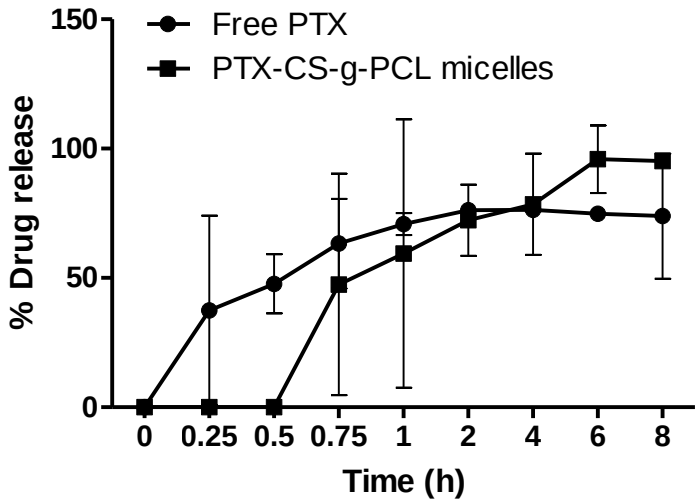

Figure 4.12 - Cumulative *in vitro* release of PTX-CS-*g*-PCL micelles (▪) and free paclitaxel (●) in 0.1% Tween®-80 containing phosphate-buffered saline (pH 7.4, w/v) at 37 ºC ($n = 3$, mean ± SD).

4.5 Cytotoxicity studies

In order to evaluate the intestinal safety and biocompatibility of polymers CS, PCL, the new copolymer formed (CS-*g*-PCL), empty micelles and PTX-CS-*g*-CPL micelles, *in vitro* experiments using Caco-2 and HT29-MTX intestinal epithelial cells were performed. Samples of the above-mentioned formulations, and controls of free PTX were incubated with cells for 4 and 24 h and cell viability was assessed by MTT assay.

As depicted in **Figure 4.13A** and **4.13B**, the CS and PCL have no apparent toxicity when incubated for 4h in both cell lines at all concentrations. Although there is a slight decrease at the highest concentration, it is not biologically relevant. The same trend was observed after incubation for 24 h (**Figure 4.13C** and **4.13D**). Regarding to new copolymer, a similar safety profile was observed during 4h of incubation. Some toxicity was present at concentration of 1000 µg/mL, more evident in HT29-

MTX cells. After 24 h of incubation, the overt toxicity becomes particularly significant at concentration of 1000 µg/mL, reaching a very low level of viability (**Figure 4.13C** and **4.13D**).

In general, it seems that the concentration had some effect on toxicity only for the copolymer, with toxicity for higher concentrations. Similarly, the effect of the incubation time can be evaluated, which for 4 h the viability remained similar for all concentrations (except for the highest) and at 24 h of incubation, the toxicity is more evident for the last three highest concentrations. Regarding the potential application of polymeric micelles, and correspondent PTX loading capacity (approximately 10% w/w), it is not expected significant impact on cell viability. Still, to plan future permeability and potential efficacy experiments, it is accept the overall CS-*g*-PCL concentrations lower than 100 µg/mL.

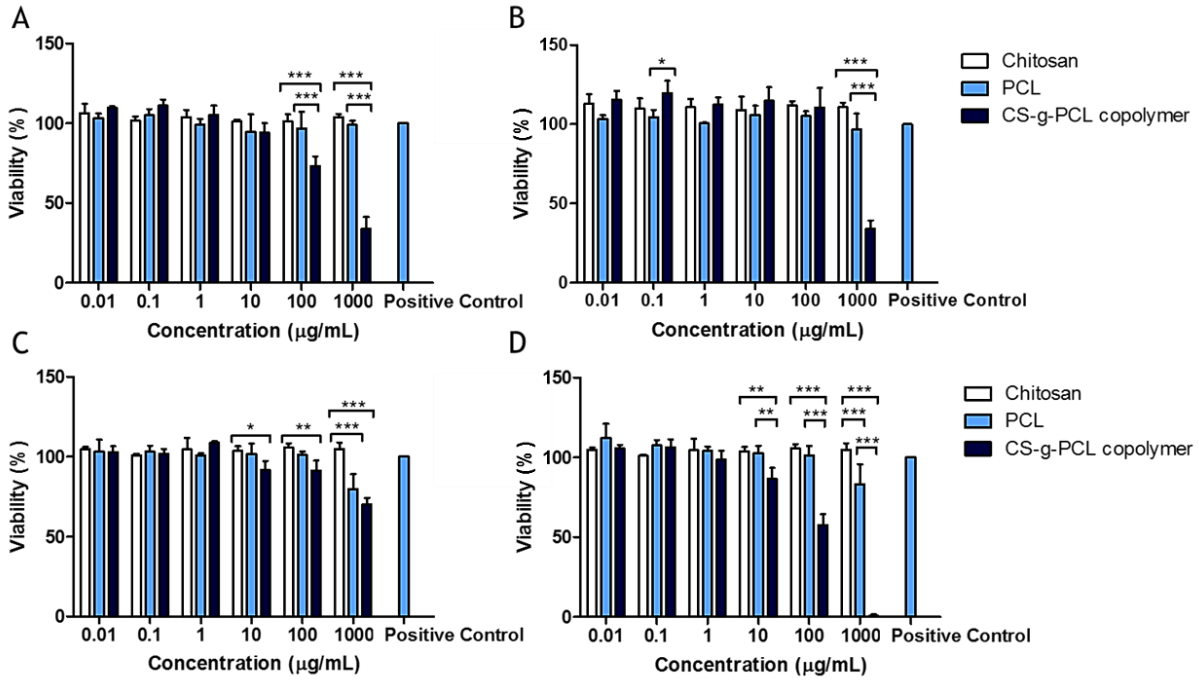

Figure 4.13 – Cell viability of chitosan, PCL and CS-*g*-PCL against Caco-2 (**A** and **C**) and HT29-MTX (**B** and **D**) cell lines, respectively, at concentrations of 0.01-1000 µg/mL after incubation for 4 h (**A** and **B**) and for 24 h (**C** and **D**). Values were reported as mean ± SD ($\boldsymbol{n = 8}$). (*), (**), and (***) denotes a significant difference ($p<0.05$, $p<0.01$ and $p<0.001$), respectively.

As empty micelles demonstrated some toxicity at concentration of 1000 µg/mL, it was decided to test the drug loaded micelles at concentrations of 0.01-10 µg/mL range. Additionally, this range of concentrations is in line with PTX concentration used in clinic protocols and the plasma levels of the drug acceptable for humans [180]. Also, it is noteworthy that this test has not been conducted to evaluate the antitumor efficacy of PTX loaded micelles or free PTX, but to assess the safety of materials in presence of intestinal cells. Moreover, these tests were performed at very short incubation times (4 h and 24 h), which is insufficient time for cell division and, therefore there is no intervention of PTX in mitosis.

Regarding the toxicity at 4 h to either the free drug or loaded micelles (**Figure 4.14A** and **4.14B**) no apparent toxicity is shown, despite the small significance found between loaded micelles and free drug in Caco-2 cell line (**Figure 4.14A**). However, after 24 h of incubation (**Figure 4.14C** and **4.14D**), there is evidence of decrease in cell viability for PTX concentration higher than 0.1 µg/mL, presenting

viability values close to 50% at the highest concentration (10 µg/mL). This result is consistent with other works performed [174, 181]. The loaded micelles demonstrated better safety profiles in comparison with the free drug, achieving viability values near from 70% to Caco-2 cells and 60% in HT29-MTX cells.

In summary, the viability decreases with increasing concentration for the both free PTX and PTX-loaded CS-*g*-PCL micelles, wherein free drug present more toxicity. Regarding the incubation time, there are significant viability difference presented at 4h and 24h. Thus, it is clear that CS-*g*-PCL micelles provide a better safety profile of PTX compared to PTX in solution.

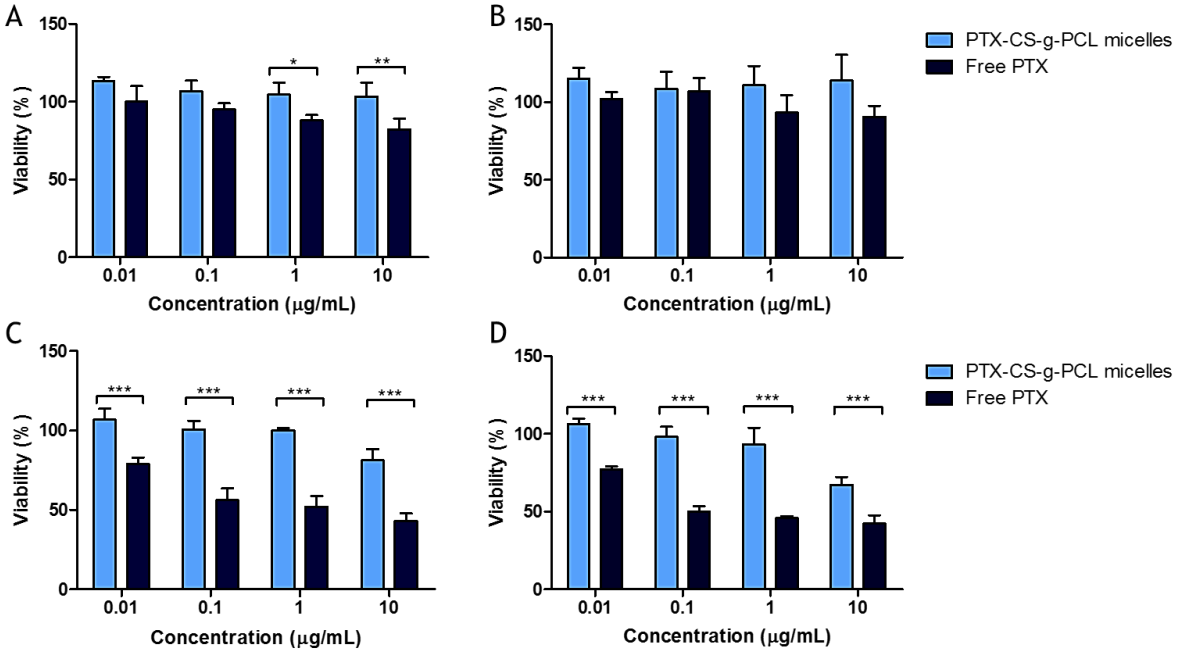

Figure 4.14 – Cell viability of loaded micelles and free PTX against Caco-2 (**A** and **C**) and HT29-MTX (**B** and **D**) cell lines, respectively, at concentrations of 0.01-10 µg/mL after incubation for 4 h (**A** and **B**) and for 24 h (**C** and **D**). Values were reported as mean ± SD ($\boldsymbol{n = 8}$). (*) and (***) denotes a significant difference ($p<0.05$ and $p<0.001$), respectively.

4.6 Permeability studies

One approach to enhance the bioavailability of PTX is to improve its permeability across the intestinal barrier. The objective of this set of experiments was to investigate and demonstrate the effect of PTX-CS-*g*-PCL micelles on enhancing the oral absorption of PTX focused on Caco-2 monoculture model and Caco-2/HT29-MTX co-culture model at physiological proportions (90/10).

As mentioned previously, cells were seeded for both models and allowed to grow for 21 days. On the day of the experiment (day 21), the measurement of TEER was made before the experiment (**Table 4.4**), in order to assess the integrity of the monolayer. Also, the TEER values reflects the quality of the TJs. A decrease of TEER manifests opening tight junctions, which means an increase of the paracellular permeability [182]. As can be seen in **Table 4.4**, the TEER values of Caco-2/HT29-MTX co-culture model had lower values compared with Caco-2 monoculture model. This data indicate that the presence of HT29-MTX cells enhance the permeability promoting TJs less tight and, consequently, lower TEER values. Thus, the TEER values obtained before the experiment showed that

the integrity of the cell monolayers was attained, so are fulfil the conditions necessary to start the test.

Table 4.4 - TEER values before the permeability experiment. Each value represents the mean ± SD of three independent measurements ($\boldsymbol{n = 3}$).

$TEER_{Caco\text{-}2}$ ($\Omega.cm^2$)		$TEER_{co\text{-}culture\ model}$ ($\Omega.cm^2$)	
CS-*g*-PCL micelles	Free PTX	CS-*g*-PCL micelles	Free PTX
112±1	101±3	83±2	72±2

The permeability profile of PTX loaded micelles and free PTX are shown in **Figure 4.15** for Caco-2 monoculture and in **Figure 4.16** for Caco-2/HT29-MTX co-culture models. Also, in **Figure 4.17** it is possible to compare the permeability of the micelles for both models in an attempt to better discussion of results.

As can be observed in **Figure 4.15**, the permeability of PTX encapsulated in the micelles started somewhat later, probably due to the delay in release PTX from micelles. This delay in in agreement with the simulated *in vitro* release profile (Figure 4.12). Nonetheless, the permeability was increased to a maximum of 13% permeation, compared to the maximum of 10% obtained to PTX in solution. Although the permeability of free PTX was continuous, permeating the epithelium around 7%, increasing to nearly 10%. The increased permeability of the PTX-micellar system is also probably due to solubility increasing effect provided by nanoencapsulation. The free PTX permeability corresponds to a $\boldsymbol{Papp = 4.2 \times 10^{-6} cm/sec}$, which is in the same range of permeability values founded in literature for this cell model [183, 184].

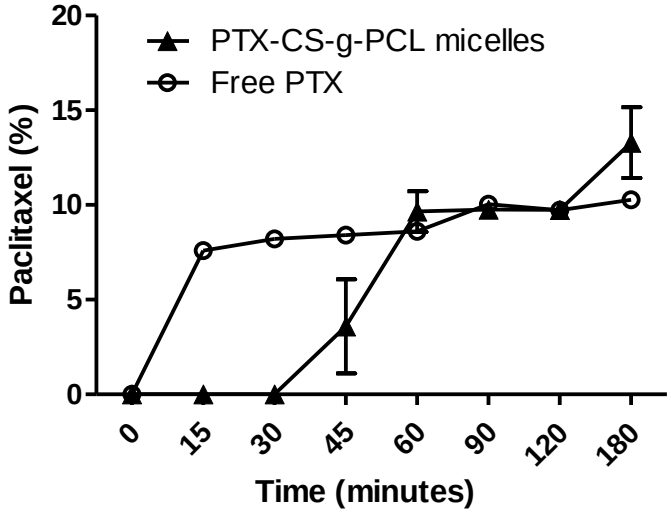

Figure 4.15 – *In vitro* cumulative permeability profiles of paclitaxel loaded micelles (▲) and free paclitaxel (○) across Caco-2 monoculture model. All experiments were conducted from the apical to basolateral compartment in HBSS at 37 ºC. Error bars represent mean ± SD ($\boldsymbol{n = 3}$).

Despite initial delay on the permeability of PTX loaded micelles, it was an increase of the micelles permeability in the last time point. Perhaps, if the test continued for longer, would verify an increase in permeability due to the adhesive nature of the micelles to intestinal cells. In a work developed by Mo *et al.*, with micelles based in CS, the Papp $\boldsymbol{8.55 \pm 0.90 \times 10^{-6}}$ cm/s, which was approximately

2-fold improved in comparison with free PTX [182]. The authors relate this increase to the mucoadhesive CS character as well as the positive charge of the micelles which promotes the opening of tight junctions [185].

In an attempt to evaluate the effect of mucus in the permeation of PTX in the intestinal epithelium a Caco-2/HT29-MTX co-culture model, previously developed by our group, was used to compare the permeability profiles of PTX compare to enterocytes monolayer. As can be seen in **Figure 4.16**, the permeation of PTX for both samples had a similar profile reaching a permeability of 17% and 15% for PTX encapsulated and for free PTX, respectively. In general, can be concluded that the co-culture model enhances the permeation of either the drug-loaded micelles or the free drug as would be expected for this model since, the presence of HT29-MTX cells promote TJs less tight than in Caco-2 monoculture model [186], thus allowing a permeation slightly higher.

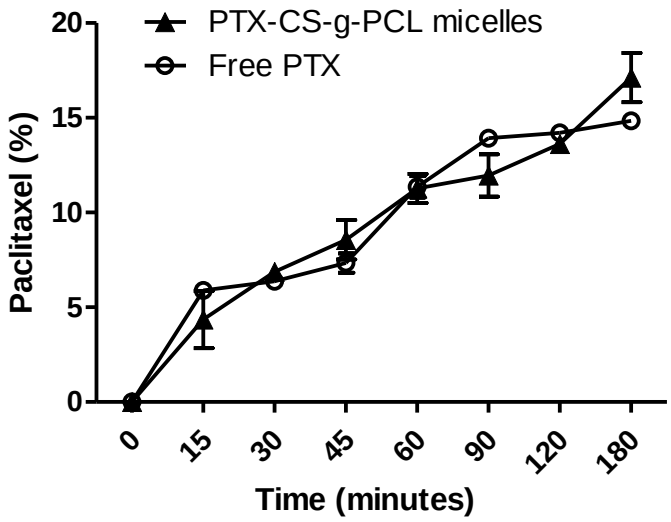

Figure 4.16 – *In vitro* cumulative permeability profiles of paclitaxel loaded micelles (▲) and free paclitaxel (○) across Caco-2/HT29-MTX co-culture model. All experiments were conducted from the apical to basolateral compartment in HBSS at 37 ºC. Error bars represent mean ± SD ($\boldsymbol{n = 3}$).

As can be seen in Figure 4.17, in this model did not occurs a delay in permeation of PTX from the micelles, probably due to the presence of mucus, which provided a deeper and faster interaction of micelles with epithelial cells. In other words, the mucoadhesive character of CS present in these micelles promoted adherence to the mucosal layer of the model, favouring the immediate permeation of PTX. Furthermore, it is possible to conclude that the co-culture model presented had the faster and higher permeability. As mentioned before, this model is more realistic compared with the human intestine through the mucus production, but also due the formation of TJs less tight as Caco-2 monolayer [38], which means an increase of the paracellular permeability [182].

At the end of the experiment, the volume of the apical compartment was also collected for later analysis. As can be seen in **Table 4.5**, after analysis by HLPC and PTX quantitation, it was found that about 6% of drug present in the micelles was not permeated for the monoculture model and about 7% was not permeate the model co-culture. The remaining about 84% of drug to the monoculture model and about 76% for the co-culture model must have been retained in the cell layer, adhering to the cells.

Regarding to the free PTX, about 27% of free drug was not permeated for the monoculture model and about 25% for the co-culture model. The remaining about 60% of free drug should probably have been retained in the cell monolayer, adhering to the cells.

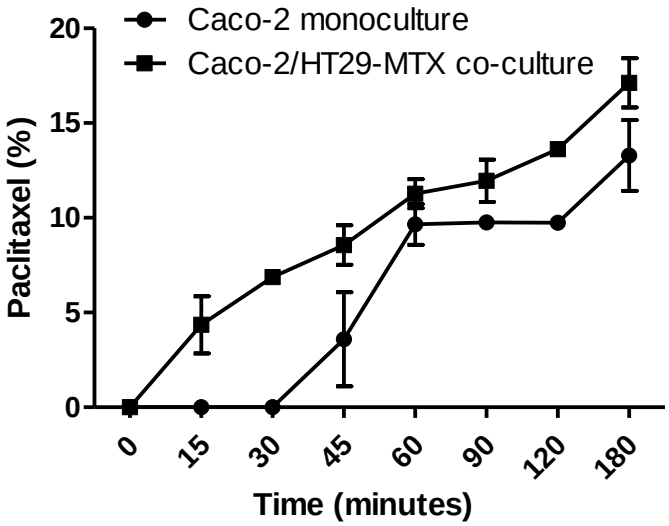

Figure 4.17 – *In vitro* cumulative permeability profiles of paclitaxel loaded micelles across Caco-2 monoculture model (●) and across Caco-2/HT29-MTX co-culture model (■). All experiments were conducted from the apical to basolateral compartment in HBSS at 37 ºC. Error bars represent mean ± SD ($n = 3$).

Table 4.5 - Apical compartment paclitaxel quantification (%). Each value represents the mean ± SD of three independent measurements ($n = 3$).

Apical compartment paclitaxel quantification (%)			
Caco-2 monoculture model		Caco-2/HT29-MTX co-culture model	
CS-*g*-PCL micelles	Free PTX	CS-*g*-PCL micelles	Free PTX
5.96±0.99	26.87±1.15	6.91±0.66	25.08±9.77

Indeed, micellar system had more PTX absorbed to cells than free PTX. This possible adhesion can be explained by the absorption of the micelles to the cells due to the mucoadhesive character of chitosan. These chitosan-based micelles place the anti-cancer drug in deeper contact with cancer cells, which may be more effective for the anti-tumor activity.

Blank page

Chapter 5

Conclusion

In this work a new copolymer based on chitosan and polycaprolactone was synthetized with ability to form micelles by self-assembly. Both polymers were chosen because of their properties, but especially chitosan due to its biocompatibility, non-toxicity and mucoadhesion properties. The chemical synthesis was a success based on the results of FTIR, NMR and contact angle prove.

The characterization of the micelle passed through the measurement of average size, which for the chosen formulation was 408 ± 40 nm with a polydispersity index of 0.335 ± 0.021, which is quite high because the micelles are composed mainly of chitosan, which is a natural polymer and where the length of their chains cannot be chosen. The zeta potential showed positive charge of 30.9 ± 3.1 mV, according to the literature. The determination of the encapsulation efficiency of PTX was achieved by an indirect method, since there was no possibility to destroy the micelles. Was obtained an encapsulation efficiency of about 82% which is a very good result for a theoretical drug loading of 2.5%. Also, the morphology of the micelles was evaluated and was found a uniform spherical, even in the presence of PTX, when compared to the empty micelles.

For the *in vitro* tests carried out, it was found that the release profile of PTX in intestinal conditions is consistent with the literature. Since the release profile of the micellar system only begins 30 minutes after contact with the release medium. This may be explained by the fact that the PTX have some difficulty to break free of the micelles. The same could have happened in permeability studies in Caco-2 monoculture model, where the drug permeated only appears after 30 min. However, in both models tested, the micelles have a greater permeation. Furthermore, the Caco-2/HT29-MTX coculture model had a greater permeation for the micellar system and for the free drug, which is in line with the expected results. Thus, it is expected that the micellar system is a promise, since can encapsulate enough amount of drug able to release and can across through the intestinal barrier more effectively.

Finally, the cytotoxicity studies did not show overt toxicity after 4h to either the PTX loaded micelles and for the free drug. After 24h, it was found that the viability of both cell lines decreases with increasing concentrations of PTX loaded micelles and free PTX. However, the free PTX presents higher toxicity, and therefore, the micellar system more suitable for applications in drug delivery.

In conclusion, the micellar system produced presents diameters and encapsulation efficiency convenient to be used as a drug delivery system and assays performed *in vitro* demonstrate that

produced micellar system has a better performance in terms of release in intestinal conditions, greater intestinal permeability and even lower toxicity in colorectal cancer cells compared to free drug.

It can, therefore, be assumed that the system may hold promise as a vehicle of drug delivery. However, there is always room for improvement, and further, more comprehensive studies must be conducted in order to make this system a reality in clinical practice for colorectal cancer therapy.

5.1 Future perspectives

Despite all the work, there are always things that can be done in an attempt to improve the system under development. The ninhydrin assay is used to determine the degree of substitution of chitosan in the copolymer formed. This test is important because the degree of substitution of chitosan by hydrophobic groups has an influence in several characteristics, such as micelle size and superficial charge. Also, production of micelles varying the chitosan/polycaprolactone ratio may be a good approach. Besides the features mentioned above, it has been described that the higher the ratio of hydrophobic groups, the higher the encapsulation efficiency [5].

Other characterizations of the micelles may also be performed, such as scanning electron microscopy or atomic force microscopy to examine the surface morphology of the micelles. This micellar system could also be evaluated for their antitumor activity, verifying the efficiency of the PTX loaded micelles and the free PTX to interfere with the cell cycle and to induce apoptosis due to stabilization of microtubules. Another alternative would be to study the effectiveness of this system when encapsulated with other types of drugs such as camptothecin and doxorubicin.

Finally, the *in vivo* study for the assessment of biodistribution, safety and therapeutic efficiency of this system will be essential to proceed for clinical therapy.

Blank page

References

[1] T. C. Wehler, S. Hamdi, A. Maderer, C. Graf, I. Gockel, I. Schmidtmann, *et al.*, "Single-agent therapy with sorafenib or 5-FU is equally effective in human colorectal cancer xenograft—no benefit of combination therapy," *International journal of colorectal disease,* vol. 28, pp. 385-398, 2013.

[2] A. K. Singla, A. Garg, and D. Aggarwal, "Paclitaxel and its formulations," *International journal of pharmaceutics,* vol. 235, pp. 179-192, 2002.

[3] M. A. Woodruff and D. W. Hutmacher, "The return of a forgotten polymer—Polycaprolactone in the 21st century," *Progress in Polymer Science,* vol. 35, pp. 1217-1256, 2010.

[4] B. Khorsand, G. Lapointe, C. Brett, and J. K. Oh, "Intracellular drug delivery nanocarriers of glutathione-responsive degradable block copolymers having pendant disulfide linkages," *Biomacromolecules,* vol. 14, pp. 2103-11, Jun 10 2013.

[5] K. Duan, X. Zhang, X. Tang, J. Yu, S. Liu, D. Wang, *et al.*, "Fabrication of cationic nanomicelle from chitosan-graft-polycaprolactone as the carrier of 7-ethyl-10-hydroxy-camptothecin," *Colloids Surf B Biointerfaces,* vol. 76, pp. 475-82, Apr 1 2010.

[6] A. Sosnik, J. das Neves, and B. Sarmento, "Mucoadhesive polymers in the design of nano-drug delivery systems for administration by non-parenteral routes: a review," *Progress in Polymer Science,* vol. 39, pp. 2030-2075, 2014.

[7] M. Dash, F. Chiellini, R. M. Ottenbrite, and E. Chiellini, "Chitosan—A versatile semi-synthetic polymer in biomedical applications," *Progress in polymer science,* vol. 36, pp. 981-1014, 2011.

[8] (2015, May 2016). Available: https://www.ine.pt/xportal/xmain?xpgid=ine_main&xpid=INE

[9] (2012, May 2016). Available: http://globocan.iarc.fr/Default.aspx

[10] E. Fernandes, J. A. Ferreira, P. Andreia, L. Luís, S. Barroso, B. Sarmento, *et al.*, "New trends in guided nanotherapies for digestive cancers: A systematic review," *Journal of Controlled Release,* vol. 209, pp. 288-307, 2015.

[11] A. S. Thakor and S. S. Gambhir, "Nanooncology: the future of cancer diagnosis and therapy," *CA: a cancer journal for clinicians,* vol. 63, pp. 395-418, 2013.

[12] P. Ramos and M. Bentires-Alj, "Mechanism-based cancer therapy: resistance to therapy, therapy for resistance," *Oncogene,* vol. 34, pp. 3617-3626, 2015.

[13] V. Balan, G. Dodi, N. Tudorachi, O. Ponta, V. Simon, M. Butnaru, *et al.*, "Doxorubicin-loaded magnetic nanocapsules based on N-palmitoyl chitosan and magnetite: Synthesis and characterization," *Chemical Engineering Journal,* vol. 279, pp. 188-197, 2015.

[14] X. Xiangyang, L. Ling, Z. Jianping, L. Shiyue, Y. Jie, Y. Xiaojin, *et al.*, "Preparation and characterization of N-succinyl-N′-octyl chitosan micelles as doxorubicin carriers for effective anti-tumor activity," *Colloids and Surfaces B: Biointerfaces,* vol. 55, pp. 222-228, 2007.

[15] J. Zhang, X. G. Chen, Y. Y. Li, and C. S. Liu, "Self-assembled nanoparticles based on hydrophobically modified chitosan as carriers for doxorubicin," *Nanomedicine: Nanotechnology, Biology, and Medicine,* vol. 3, pp. 258-265, 2007.

[16] W. Xun, H.-Y. Wang, Z.-Y. Li, S.-X. Cheng, X.-Z. Zhang, and R.-X. Zhuo, "Self-assembled micelles of novel graft amphiphilic copolymers for drug controlled release," *Colloids and Surfaces B: Biointerfaces,* vol. 85, pp. 86-91, 2011.

[17] G. S. Kwon and K. Kataoka, "Block copolymer micelles as long-circulating drug vehicles," *Advanced drug delivery reviews,* vol. 16, pp. 295-309, 1995.

[18] K. Kazunori, Y. Masayuki, O. Teruo, and S. Yasuhisa, "Block copolymer micelles as vehicles for drug delivery," *Journal of Controlled Release,* vol. 24, pp. 119-132, 1993.

[19] G. S. Kwon and M. L. Forrest, "Amphiphilic block copolymer micelles for nanoscale drug delivery," *Drug development research,* vol. 67, pp. 15-22, 2006.
[20] P. V. Balimane and S. Chong, "Cell culture-based models for intestinal permeability: a critique," *Drug discovery today,* vol. 10, pp. 335-343, 2005.
[21] R. N. Jaladanki and J.-Y. Wang, "Regulation of gastrointestinal mucosal growth," in *Colloquium Series on Integrated Systems Physiology: From Molecule to Function*, 2011, pp. 1-114.
[22] C. Pereira, F. Araújo, C. C. Barrias, P. L. Granja, and B. Sarmento, "Dissecting stromal-epithelial interactions in a 3D *in vitro* cellularized intestinal model for permeability studies," *Biomaterials,* vol. 56, pp. 36-45, 2015.
[23] R. K. Montgomery, A. E. Mulberg, and R. J. Grand, "Development of the human gastrointestinal tract: twenty years of progress," *Gastroenterology,* vol. 116, pp. 702-731, 1999.
[24] B. Gannon, "The vasculature and lymphatic drainage," *Gastrointestinal and oesophageal pathology. Edinburgh: Churchill Livingstone,* vol. 129, 1995.
[25] (2015, April 2016). Available: http://www.myvmc.com/anatomy/gastrointestinal-system/
[26] M. T. Abreu, "Toll-like receptor signalling in the intestinal epithelium: how bacterial recognition shapes intestinal function," *Nature Reviews Immunology,* vol. 10, pp. 131-144, 2010.
[27] A. L. Daugherty and R. J. Mrsny, "Transcellular uptake mechanisms of the intestinal epithelial barrier Part one," *Pharmaceutical science & technology today,* vol. 2, pp. 144-151, 1999.
[28] L. G. Van der Flier and H. Clevers, "Stem cells, self-renewal, and differentiation in the intestinal epithelium," *Annual review of physiology,* vol. 71, pp. 241-260, 2009.
[29] M. A. Clark, M. A. Jepson, and B. H. Hirst, "Exploiting M cells for drug and vaccine delivery," *Advanced drug delivery reviews,* vol. 50, pp. 81-106, 2001.
[30] Y. Yun, Y. W. Cho, and K. Park, "Nanoparticles for oral delivery: targeted nanoparticles with peptidic ligands for oral protein delivery," *Advanced drug delivery reviews,* vol. 65, pp. 822-832, 2013.
[31] P. W. Swaan, "Recent advances in intestinal macromolecular drug delivery via receptor-mediated transport pathways," *Pharmaceutical research,* vol. 15, pp. 826-834, 1998.
[32] K. Y. Win and S.-S. Feng, "Effects of particle size and surface coating on cellular uptake of polymeric nanoparticles for oral delivery of anticancer drugs," *Biomaterials,* vol. 26, pp. 2713-2722, 2005.
[33] M. Garcia-Fuentes and M. J. Alonso, "Chitosan-based drug nanocarriers: where do we stand?," *Journal of Controlled Release,* vol. 161, pp. 496-504, 2012.
[34] M.-C. Chen, K. Sonaje, K.-J. Chen, and H.-W. Sung, "A review of the prospects for polymeric nanoparticle platforms in oral insulin delivery," *Biomaterials,* vol. 32, pp. 9826-9838, 2011.
[35] T. R. Stouch and O. Gudmundsson, "Progress in understanding the structure–activity relationships of P-glycoprotein," *Advanced drug delivery reviews,* vol. 54, pp. 315-328, 2002.
[36] X. Zhang and W. Wu, "Ligand-mediated active targeting for enhanced oral absorption," *Drug discovery today,* vol. 19, pp. 898-904, 2014.
[37] A. S Darwich, S. Neuhoff, M. Jamei, and A. Rostami-Hodjegan, "Interplay of metabolism and transport in determining oral drug absorption and gut wall metabolism: a simulation assessment using the "Advanced Dissolution, Absorption, Metabolism (ADAM)" model," *Current drug metabolism,* vol. 11, pp. 716-729, 2010.
[38] F. Araújo and B. Sarmento, "Towards the characterization of an *in vitro* triple co-culture intestine cell model for permeability studies," *International journal of pharmaceutics,* vol. 458, pp. 128-134, 2013.
[39] F. Araújo, N. Shrestha, M.-A. Shahbazi, P. Fonte, E. M. Mäkilä, J. J. Salonen, *et al.*, "The impact of nanoparticles on the mucosal translocation and transport of GLP-1 across the intestinal epithelium," *Biomaterials,* vol. 35, pp. 9199-9207, 2014.
[40] M. D. Peterson and M. S. Mooseker, "Characterization of the enterocyte-like brush border cytoskeleton of the C2BBe clones of the human intestinal cell line, Caco-2," *J Cell Sci,* vol. 102, pp. 581-600, 1992.
[41] T. Lesuffleur, A. Barbat, E. Dussaulx, and A. Zweibaum, "Growth adaptation to methotrexate of HT-29 human colon carcinoma cells is associated with their ability to differentiate into columnar absorptive and mucus-secreting cells," *Cancer Research,* vol. 50, pp. 6334-6343, 1990.
[42] P. Artursson, "Cell cultures as models for drug absorption across the intestinal mucosa," *Critical reviews in therapeutic drug carrier systems,* vol. 8, pp. 305-330, 1990.

[43] S. Mouly and M. F. Paine, "P-glycoprotein increases from proximal to distal regions of human small intestine," *Pharmaceutical research,* vol. 20, pp. 1595-1599, 2003.
[44] F. Antunes, F. Andrade, F. Araújo, D. Ferreira, and B. Sarmento, "Establishment of a triple co-culture *in vitro* cell models to study intestinal absorption of peptide drugs," *European Journal of Pharmaceutics and Biopharmaceutics,* vol. 83, pp. 427-435, 2013.
[45] I. Behrens, A. I. V. Pena, M. J. Alonso, and T. Kissel, "Comparative uptake studies of bioadhesive and non-bioadhesive nanoparticles in human intestinal cell lines and rats: the effect of mucus on particle adsorption and transport," *Pharmaceutical research,* vol. 19, pp. 1185-1193, 2002.
[46] C. M. Spencer and D. Faulds, "Paclitaxel. A review of its pharmacodynamic and pharmacokinetic properties and therapeutic potential in the treatment of cancer," *Drugs,* vol. 48, pp. 794-847, Nov 1994.
[47] M. F. Carlier and D. Pantaloni, "Taxol effect on tubulin polymerization and associated guanosine 5'-triphosphate hydrolysis," *Biochemistry,* vol. 22, pp. 4814-4822, 1983.
[48] P. B. Schiff, J. Fant, and S. B. Horwitz, "Promotion of microtubule assembly *in vitro* by taxol," 1979.
[49] (April 2016). *The cell cycle, mitosis and meiosis*. Available: http://www2.le.ac.uk/departments/genetics/vgec/schoolscolleges/topics/cellcycle-mitosis-meiosis
[50] Paclitaxel Product Information [Online]. Available: https://www.sigmaaldrich.com/content/dam/sigma-aldrich/docs/Sigma/Product_Information_Sheet/t1912pis.pdf
[51] S. L. Richheimer, D. M. Tinnermeier, and D. W. Timmons, "High-performance liquid chromatographic assay of taxol," *Analytical chemistry,* vol. 64, pp. 2323-2326, 1992.
[52] N. A. Kasim, M. Whitehouse, C. Ramachandran, M. Bermejo, H. Lennernäs, A. S. Hussain, *et al.*, "Molecular properties of WHO essential drugs and provisional biopharmaceutical classification," *Molecular pharmaceutics,* vol. 1, pp. 85-96, 2004.
[53] D. M. Vyas, "3 Paclitaxel (taxol®) formulation and prodrugs," *Pharmacochemistry Library,* vol. 22, pp. 103-130, 1995.
[54] J. Szebeni, C. R. Alving, and F. M. Muggia, "Complement activation by Cremophor EL as a possible contributor to hypersensitivity to paclitaxel: an *in vitro* study," *Journal of the national cancer institute,* vol. 90, pp. 300-306, 1998.
[55] C. Zhang, P. Qineng, and H. Zhang, "Self-assembly and characterization of paclitaxel-loaded N-octyl-O-sulfate chitosan micellar system," *Colloids and Surfaces B: Biointerfaces,* vol. 39, pp. 69-75, 2004.
[56] J. Liebmann, J. Cook, C. Lipschultz, D. Teague, J. Fisher, and J. Mitchell, "Cytotoxic studies of paclitaxel (Taxol) in human tumour cell lines," *British journal of cancer,* vol. 68, p. 1104, 1993.
[57] P. Schiff and S. B. Horwitz, "Taxol stabilizes microtubules in mouse fibroblast cells," *Proceedings of the National Academy of Sciences,* vol. 77, pp. 1561-1565, 1980.
[58] D. e. a. Guenard, *Current Pharmaceutical Design,* vol. 1, 1995.
[59] X. Huang, Y. Xiao, and M. Lang, "Self-assembly of pH-sensitive mixed micelles based on linear and star copolymers for drug delivery," *Journal of colloid and interface science,* vol. 364, pp. 92-99, 2011.
[60] V. P. Torchilin, "Micellar nanocarriers: pharmaceutical perspectives," *Pharm Res,* vol. 24, pp. 1-16, Jan 2007.
[61] Z. Ahmad, A. Shah, M. Siddiq, and H.-B. Kraatz, "Polymeric micelles as drug delivery vehicles," *RSC Advances,* vol. 4, p. 17028, 2014.
[62] C. Le Tien, M. Lacroix, P. Ispas-Szabo, and M.-A. Mateescu, "N-acylated chitosan: hydrophobic matrices for controlled drug release," *Journal of Controlled Release,* vol. 93, pp. 1-13, 2003.
[63] M. Ishihara, M. Fujita, S. Kishimoto, H. Hattori, and Y. Kanatani, "Biological , Chemical , and Physical Compatibility of Chitosan and Biopharmaceuticals," in *Chitosan-Based Systems for Biopharmaceuticals: Delivery, Targeting and Polymer Therapeutics*, ed, 2012, p. 500.
[64] Z. Ahmad, A. Shah, M. Siddiq, and H.-B. Kraatz, "Polymeric micelles as drug delivery vehicles," *Rsc Advances,* vol. 4, pp. 17028-17038, 2014.
[65] S. Biswas, P. Kumari, P. M. Lakhani, and B. Ghosh, "Recent advances in polymeric micelles for anti-cancer drug delivery," *Eur J Pharm Sci,* Dec 31 2015.

[66] A. R. Sarasam, "Chitosan- polycaprolactone mixtures as biomaterials - influence of surface morphology on cellular activity," Bachelor of Science in Chemical Engineering, Jawaharlal Nehru Technological University, 2001.
[67] M. Labet and W. Thielemans, "Synthesis of polycaprolactone: a review," *Chemical Society Reviews,* vol. 38, pp. 3484-3504, 2009.
[68] I. Aranaz, R. Harris, and A. Heras, "Chitosan Amphiphilic Derivatives . Chemistry and Applications," pp. 308-330, 2010.
[69] V. P. Torchilin, "Micellar nanocarriers: pharmaceutical perspectives," *Pharmaceutical research,* vol. 24, pp. 1-16, 2007.
[70] S. Biswas, P. Kumari, P. M. Lakhani, and B. Ghosh, "Recent advances in polymeric micelles for anti-cancer drug delivery," *European Journal of Pharmaceutical Sciences,* 2015.
[71] G. Kwon, M. Naito, M. Yokoyama, T. Okano, Y. Sakurai, and K. Kataoka, "Block copolymer micelles for drug delivery: loading and release of doxorubicin," *Journal of Controlled Release,* vol. 48, pp. 195-201, 1997.
[72] H. Honarkar and M. Barikani, "Applications of biopolymers I: chitosan," *Monatshefte für Chemie-Chemical Monthly,* vol. 140, pp. 1403-1420, 2009.
[73] H. Silva, K. Dos Santos, and E. I. Ferreira, "Quitosana: derivados hidrossolúveis, aplicações farmacêuticas e avanços," *Química Nova,* vol. 29, p. 776, 2006.
[74] F. Araújo, N. Shrestha, P. L. Granja, J. Hirvonen, H. A. Santos, and B. Sarmento, "Safety and toxicity concerns of orally delivered nanoparticles as drug carriers," *Expert opinion on drug metabolism & toxicology,* vol. 11, pp. 381-393, 2015.
[75] I. Aranaz, R. Harris, and A. Heras, "Chitosan amphiphilic derivatives. Chemistry and applications," *Current Organic Chemistry,* vol. 14, p. 308, 2010.
[76] P. Agrawal, G. J. Strijkers, and K. Nicolay, "Chitosan-based systems for molecular imaging," *Advanced drug delivery reviews,* vol. 62, pp. 42-58, 2010.
[77] N. Alves and J. Mano, "Chitosan derivatives obtained by chemical modifications for biomedical and environmental applications," *International journal of biological macromolecules,* vol. 43, pp. 401-414, 2008.
[78] S. K. Shukla, A. K. Mishra, O. A. Arotiba, and B. B. Mamba, "Chitosan-based nanomaterials: A state-of-the-art review," *International journal of biological macromolecules,* vol. 59, pp. 46-58, 2013.
[79] E. Khor and L. Y. Lim, "Implantable applications of chitin and chitosan," *Biomaterials,* vol. 24, pp. 2339-2349, 2003.
[80] F. Andrade, F. Goycoolea, D. A. Chiappetta, J. das Neves, A. Sosnik, and B. Sarmento, "Chitosan-grafted copolymers and chitosan-ligand conjugates as matrices for pulmonary drug delivery," *International Journal of Carbohydrate Chemistry,* vol. 2011, 2011.
[81] Y.-W. Cho, J. Jang, C. R. Park, and S.-W. Ko, "Preparation and solubility in acid and water of partially deacetylated chitins," *Biomacromolecules,* vol. 1, pp. 609-614, 2000.
[82] C. Zhang, Y. Ding, L. L. Yu, and Q. Ping, "Polymeric micelle systems of hydroxycamptothecin based on amphiphilic N-alkyl-N-trimethyl chitosan derivatives," *Colloids and Surfaces B: Biointerfaces,* vol. 55, pp. 192-199, 2007.
[83] H. Guo, D. Zhang, C. Li, L. Jia, G. Liu, L. Hao, *et al.*, "Self-assembled nanoparticles based on galactosylated O-carboxymethyl chitosan-graft-stearic acid conjugates for delivery of doxorubicin," *International Journal of Pharmaceutics,* vol. 458, pp. 31-38, 2013.
[84] C. Gu, V. Le, M. Lang, and J. Liu, "Preparation of polysaccharide derivates chitosan-graft-poly (ε-caprolactone) amphiphilic copolymer micelles for 5-fluorouracil drug delivery," *Colloids and Surfaces B: Biointerfaces,* vol. 116, pp. 745-750, 2014.
[85] M. A. Hernández-valdepeña, J. Pedraza-chaverri, I. Gracia-mora, R. Hernández-castro, F. Sánchez-bartez, J. Nieto-sotelo, *et al.*, "Suppression of the tert -butylhydroquinone toxicity by its grafting onto chitosan and further cross-linking to agavin toward a novel antioxidant and prebiotic material," vol. 199, pp. 485-491, 2016.
[86] A. S. Berezin and Y. a. Skorik, "Chitosan-isoniazid conjugates: Synthesis, evaluation of tuberculostatic activity, biodegradability and toxicity," *Carbohydrate Polymers,* vol. 127, pp. 309-315, 2015.
[87] L. Yu, X. Yue, R. Yang, S. Jing, and L. Qu, "A sensitive and low toxicity electrochemical sensor for 2, 4-dichlorophenol based on the nanocomposite of carbon dots, hexadecyltrimethyl ammonium bromide and chitosan," *Sensors and Actuators B: Chemical,* vol. 224, pp. 241-247, 2015.

[88] S. Shukla, A. Jadaun, V. Arora, R. K. Sinha, N. Biyani, and V. K. Jain, "In vitro toxicity assessment of chitosan oligosaccharide coated iron oxide nanoparticles," *Toxicology Reports,* vol. 2, pp. 27-39, 2015.

[89] X. Fei Liu, Y. Lin Guan, D. Zhi Yang, Z. Li, and K. De Yao, "Antibacterial action of chitosan and carboxymethylated chitosan," *Journal of Applied Polymer Science,* vol. 79, pp. 1324-1335, 2001.

[90] I. Helander, E.-L. Nurmiaho-Lassila, R. Ahvenainen, J. Rhoades, and S. Roller, "Chitosan disrupts the barrier properties of the outer membrane of Gram-negative bacteria," *International journal of food microbiology,* vol. 71, pp. 235-244, 2001.

[91] E. I. Rabea, M. E.-T. Badawy, C. V. Stevens, G. Smagghe, and W. Steurbaut, "Chitosan as antimicrobial agent: applications and mode of action," *Biomacromolecules,* vol. 4, pp. 1457-1465, 2003.

[92] T. Kean and M. Thanou, "Biodegradation, biodistribution and toxicity of chitosan," *Advanced Drug Delivery Reviews,* vol. 62, pp. 3-11, 2010.

[93] C. Chatelet, O. Damour, and A. Domard, "Influence of the degree of acetylation on some biological properties of chitosan films," *Biomaterials,* vol. 22, pp. 261-268, 2001.

[94] N. G. Schipper, K. M. Vårum, and P. Artursson, "Chitosans as absorption enhancers for poorly absorbable drugs. 1: Influence of molecular weight and degree of acetylation on drug transport across human intestinal epithelial (Caco-2) cells," *Pharmaceutical research,* vol. 13, pp. 1686-1692, 1996.

[95] J.-K. F. Suh and H. W. Matthew, "Application of chitosan-based polysaccharide biomaterials in cartilage tissue engineering: a review," *Biomaterials,* vol. 21, pp. 2589-2598, 2000.

[96] T. A. Khan, K. K. Peh, and H. S. Ch'ng, "Reporting degree of deacetylation values of chitosan: the influence of analytical methods," *J Pharm Pharmaceut Sci,* vol. 5, pp. 205-212, 2002.

[97] H. Zhang and S. H. Neau, "In vitro degradation of chitosan by a commercial enzyme preparation: effect of molecular weight and degree of deacetylation," *Biomaterials,* vol. 22, pp. 1653-1658, 2001.

[98] M. Huang, E. Khor, and L.-Y. Lim, "Uptake and cytotoxicity of chitosan molecules and nanoparticles: effects of molecular weight and degree of deacetylation," *Pharmaceutical research,* vol. 21, pp. 344-353, 2004.

[99] C.-M. Lehr, J. A. Bouwstra, E. H. Schacht, and H. E. Junginger, "In vitro evaluation of mucoadhesive properties of chitosan and some other natural polymers," *International journal of Pharmaceutics,* vol. 78, pp. 43-48, 1992.

[100] M. Liu, J. Zhang, X. Zhu, W. Shan, L. Li, J. Zhong, *et al.*, "Ef fi cient mucus permeation and tight junction opening by dissociable " mucus-inert " agent coated trimethyl chitosan nanoparticles for oral insulin delivery," vol. 222, pp. 67-77, 2016.

[101] L.-W. Hsu, Y.-C. Ho, E.-Y. Chuang, C.-T. Chen, J.-H. Juang, F.-Y. Su, *et al.*, "Effects of pH on molecular mechanisms of chitosan-integrin interactions and resulting tight-junction disruptions.," *Biomaterials,* vol. 34, pp. 784-93, 2013.

[102] I. F. Uchegbu, M. Carlos, C. McKay, X. Hou, and A. G. Schätzlein, "Chitosan amphiphiles provide new drug delivery opportunities," *Polymer International,* vol. 63, pp. 1145-1153, 2014.

[103] K. Sonaje, K.-J. Lin, M. T. Tseng, S.-P. Wey, F.-Y. Su, E.-Y. Chuang, *et al.*, "Effects of chitosan-nanoparticle-mediated tight junction opening on the oral absorption of endotoxins," *Biomaterials,* vol. 32, pp. 8712-8721, 2011.

[104] Y. Okamoto, R. Yano, K. Miyatake, I. Tomohiro, Y. Shigemasa, and S. Minami, "Effects of chitin and chitosan on blood coagulation," *Carbohydrate Polymers,* vol. 53, pp. 337-342, 2003.

[105] S. B. Rao and C. P. Sharma, "Use of chitosan as a biomaterial: studies on its safety and hemostatic potential," *Journal of biomedical materials research,* vol. 34, pp. 21-28, 1997.

[106] J. Yang, F. Tian, Z. Wang, Q. Wang, Y. J. Zeng, and S. Q. Chen, "Effect of chitosan molecular weight and deacetylation degree on hemostasis," *Journal of Biomedical Materials Research Part B: Applied Biomaterials,* vol. 84, pp. 131-137, 2008.

[107] Y. Ohshima, K. Nishino, Y. Yonekura, S. Kishimoto, and S. Wakabayashi, "Clinical application of chitin non-woven fabric as wound dressing," *European Journal of Plastic Surgery,* vol. 10, pp. 66-69, 1987.

[108] Y. Okamoto, K. Kawakami, K. Miyatake, M. Morimoto, Y. Shigemasa, and S. Minami, "Analgesic effects of chitin and chitosan," *Carbohydrate Polymers,* vol. 49, pp. 249-252, 2002.

[109] J. C. Fernandes, P. Eaton, H. Nascimento, M. S. Gião, Ó. S. Ramos, L. Belo, *et al.*, "Antioxidant activity of chitooligosaccharides upon two biological systems: Erythrocytes and bacteriophages," *Carbohydrate Polymers,* vol. 79, pp. 1101-1106, 2010.

[110] P.-J. Park, J.-Y. Je, and S.-K. Kim, "Free radical scavenging activities of differently deacetylated chitosans using an ESR spectrometer," *Carbohydrate Polymers,* vol. 55, pp. 17-22, 2004.

[111] R. Xing, S. Liu, Z. Guo, H. Yu, P. Wang, C. Li, *et al.*, "Relevance of molecular weight of chitosan and its derivatives and their antioxidant activities in vitro," *Bioorganic & medicinal chemistry,* vol. 13, pp. 1573-1577, 2005.

[112] Y. Kurita and a. Isogai, "Reductive N-alkylation of chitosan with acetone and levulinic acid in aqueous media," *International Journal of Biological Macromolecules,* vol. 47, pp. 184-189, 2010.

[113] Y. Kurita and a. Isogai, "N-Alkylations of chitosan promoted with sodium hydrogen carbonate under aqueous conditions.," *International journal of biological macromolecules,* vol. 50, pp. 741-6, 2012.

[114] B. E. Benediktsdóttir, T. Gudjónsson, Ó. Baldursson, and M. Másson, "N-alkylation of highly quaternized chitosan derivatives affects the paracellular permeation enhancement in bronchial epithelia in vitro," *European Journal of Pharmaceutics and Biopharmaceutics,* vol. 86, pp. 55-63, 2014.

[115] K. dos Santos Alves, R. R. Lima Vidal, and R. de Carvalho Balaban, "Chitosan derivatives with thickening properties obtained by reductive alkylation," *Materials Science and Engineering: C,* vol. 29, pp. 641-646, 2009.

[116] K. M. Varum, M. W. Anthonsen, H. Grasdalen, and O. Smidsrod, "Determination of the degree of N-acetylation and the distribution of N-acetyl groups in partially N-deacetylated chitins (chitosans) by high-field n.m.r. spectroscopy," *Carbohydrate Research,* vol. 211, pp. 17-23, 1991.

[117] I. Tsigos, A. Martinou, D. Kafetzopoulos, and V. Bouriotis, "Chitin deacetylases: New, versatile tools in biotechnology," *Trends in Biotechnology,* vol. 18, pp. 305-312, 2000.

[118] J. a. D. M. Delezuk, M. B. Cardoso, A. Domard, and S. P. Campana-Filho, "Ultrasound-assisted deacetylation of beta-chitin: influence of processing parameters," *Polymer International,* vol. 60, pp. 903-909, 2011.

[119] M. E. I. Badawy, E. I. Rabea, T. M. Rogge, C. V. Stevens, G. Smagghe, W. Steurbaut, *et al.*, "Synthesis and Fungicidal Activity of New N , O-Acyl Chitosan Derivatives," pp. 589-595, 2004.

[120] M. E. I. Badawy, E. I. Rabea, T. M. Rogge, C. V. Stevens, W. Steurbaut, M. Höfte, *et al.*, "Fungicidal and insecticidal activity of O-acyl chitosan derivatives," *Polymer Bulletin,* vol. 54, pp. 279-289, 2005.

[121] A. Pavinatto, A. L. Souza, J. a. M. Delezuk, F. J. Pavinatto, S. P. Campana-Filho, and O. N. Oliveira, "Interaction of O-acylated chitosans with biomembrane models: Probing the effects from hydrophobic interactions and hydrogen bonding," *Colloids and Surfaces B: Biointerfaces,* vol. 114, pp. 53-59, 2014.

[122] S. Hirano, Y. Yamaguchi, and M. Kamiya, "Novel N-saturated-fatty-acyl derivatives of chitosan soluble in water and in aqueous acid and alkaline solutions," *Carbohydrate Polymers,* vol. 48, pp. 203-207, 2002.

[123] S. Hirano, Y. Ohe, and H. Ono, "Selective N-acylation of chitosan.," *Carbohydrate research,* vol. 47, pp. 315-320, 1976.

[124] J. Desbrieres, C. Martinez, and M. Rinaudo, "Hydrophobic derivatives of chitosan: characterization and rheological behaviour," *International journal of biological macromolecules,* vol. 19, pp. 21-28, 1996.

[125] J. Desbrières, C. Martinez, and M. Rinaudo, "Hydrophobic derivatives of chitosan: Characterization and rheological behaviour," *International Journal of Biological Macromolecules,* vol. 19, pp. 21-28, 1996.

[126] M. Rinaudo, R. Auzely, C. Vallin, and I. Mullagaliev, "Specific interactions in modified chitosan systems," *Biomacromolecules,* vol. 6, pp. 2396-2407, 2005.

[127] M. Larsson, W.-C. Huang, M.-H. Hsiao, Y.-J. Wang, M. Nydén, S.-H. Chiou, *et al.*, "Biomedical applications and colloidal properties of amphiphilically modified chitosan hybrids," *Progress in Polymer Science,* vol. 38, pp. 1307-1328, 2013.

[128] V. Mourya and N. N. Inamdar, "Chitosan-modifications and applications: opportunities galore," *Reactive and Functional polymers,* vol. 68, pp. 1013-1051, 2008.

[129] K. Y. Lee, W. H. Jo, I. C. Kwon, Y.-H. Kim, and S. Y. Jeong, "Physicochemical Characteristics of Self-Aggregates of Hydrophobically Modified Chitosans," *Langmuir,* vol. 14, pp. 2329-2332, 1998.

[130] C.-G. G. Liu, K. G. H. DESAI, X.-G. G. Chen, and H.-J. J. Park, "Linolenic acid-modified chitosan for formation of self-assembled nanoparticles," *Journal of Agricultural and Food Chemistry,* vol. 53, pp. 437-441, 2005.

[131] Y. Hu, Y. Du, J. Yang, Y. Tang, J. Li, and X. Wang, "Self-aggregation and antibacterial activity of N-acylated chitosan," *Polymer,* vol. 48, pp. 3098-3106, 2007.

[132] G.-B. Jiang, D. Quan, K. Liao, and H. Wang, "Preparation of polymeric micelles based on chitosan bearing a small amount of highly hydrophobic groups," *Carbohydrate Polymers,* vol. 66, pp. 514-520, 2006.

[133] K. Kurita, "Controlled functionalization of the polysaccharide chitin," *Progress in Polymer Science (Oxford),* vol. 26, pp. 1921-1971, 2001.

[134] W. Sui, Y. Changqing, C. Yanjing, Z. Zhiguo, and K. Xiangzheng, "Self-assembly of an amphiphilic derivative of chitosan and micellar solubilization of puerarin," *Colloids and Surfaces B: Biointerfaces,* vol. 48, pp. 13-16, 2006.

[135] L. Martin, C. G. Wilson, F. Koosha, L. Tetley, A. I. Gray, S. Senel*, et al.*, "The release of model macromolecules may be controlled by the hydrophobicity of palmitoyl glycol chitosan hydrogels.," *Journal of controlled release : official journal of the Controlled Release Society,* vol. 80, pp. 87-100, 2002.

[136] C. Zhang, G. Qu, Y. Sun, X. Wu, Z. Yao, Q. Guo*, et al.*, "Pharmacokinetics, biodistribution, efficacy and safety of N-octyl-O-sulfate chitosan micelles loaded with paclitaxel," *Biomaterials,* vol. 29, pp. 1233-1241, 2008.

[137] M. Wiens, T. A. Elkhooly, H. C. Schroder, T. H. Mohamed, and W. E. Muller, "Characterization and osteogenic activity of a silicatein/biosilica-coated chitosan-graft-polycaprolactone," *Acta Biomater,* vol. 10, pp. 4456-64, Oct 2014.

[138] H. Tian, Z. Tang, X. Zhuang, X. Chen, and X. Jing, "Biodegradable synthetic polymers: Preparation, functionalization and biomedical application," *Progress in Polymer Science,* vol. 37, pp. 237-280, 2012.

[139] Y. Lu, L. Liu, and S. Guo, "Novel amphiphilic ternary polysaccharide derivates chitosan-g-PCL-b-MPEG: synthesis, characterization, and aggregation in aqueous solution," *Biopolymers,* vol. 86, pp. 403-8, Aug 5-15 2007.

[140] S. Zamani and S. Khoee, "Preparation of core–shell chitosan/PCL-PEG triblock copolymer nanoparticles with ABA and BAB morphologies: Effect of intraparticle interactions on physicochemical properties," *Polymer,* vol. 53, pp. 5723-5736, 2012.

[141] A. P. D. Elfick, "Poly(e-caprolactone) as a potential material for a temporary joint spacer," *Biomaterials,* vol. 23, pp. 4463–4467, 2002.

[142] T. Elzein, M. Nasser-Eddine, C. Delaite, S. Bistac, and P. Dumas, "FTIR study of polycaprolactone chain organization at interfaces," *J Colloid Interface Sci,* vol. 273, pp. 381-7, May 15 2004.

[143] A. J. Sawdon and C. A. Peng, "Ring-opening polymerization of epsilon-caprolactone initiated by ganciclovir (GCV) for the preparation of GCV-tagged polymeric micelles," *Molecules,* vol. 20, pp. 2857-67, 2015.

[144] S. Sahoo, A. Sasmal, D. Sahoo, and P. Nayak, "Synthesis and characterization of chitosan-polycaprolactone blended with organoclay for control release of doxycycline," *Journal of Applied Polymer Science,* vol. 118, pp. 3167-3175, 2010.

[145] L. S. Nair and C. T. Laurencin, "Biodegradable polymers as biomaterials," *Progress in Polymer Science,* vol. 32, pp. 762-798, 2007.

[146] D. L. Wise, *Encyclopedic Handbook of Biomaterials and Bioengineering: v. 1-2. Applications*: CRC Press, 1995.

[147] O. Coulembier, P. Degée, J. L. Hedrick, and P. Dubois, "From controlled ring-opening polymerization to biodegradable aliphatic polyester: Especially poly(ß-malic acid) derivatives," *Progress in Polymer Science,* vol. 31, pp. 723-747, 2006.

[148] D. Mondal, M. Griffith, and S. S. Venkatraman, "Polycaprolactone-based biomaterials for tissue engineering and drug delivery: Current scenario and challenges," *International Journal of Polymeric Materials and Polymeric Biomaterials,* vol. 65, pp. 255-265, 2016.

[149] R. F. Storey and A. Taylor, "Effect of stannous octoate concentration on the ethylene glycol-initiated polymerization of epsilon-caprolactone," in *ABSTRACTS OF PAPERS OF THE AMERICAN CHEMICAL SOCIETY*, 1996, p. 114.
[150] V. K. Thakur and M. K. Thakur, "Eco-friendly Polymer Nanocomposites," 2015.
[151] H. Yu, W. Wang, X. Chen, C. Deng, and X. Jing, "Synthesis and characterization of the biodegradable polycaprolactone-graft-chitosan amphiphilic copolymers," *Biopolymers,* vol. 83, pp. 233-242, 2006.
[152] S. C. Neves, L. S. M. Teixeira, L. Moroni, R. L. Reis, C. A. Van Blitterswijk, N. M. Alves, *et al.*, "Chitosan/Poly (ε-caprolactone) blend scaffolds for cartilage repair," *Biomaterials,* vol. 32, pp. 1068-1079, 2011.
[153] Z. Wang, L. Zheng, C. Li, D. Zhang, Y. Xiao, G. Guan, *et al.*, "A novel and simple procedure to synthesize chitosan-graft-polycaprolactone in an ionic liquid," *Carbohydr Polym,* vol. 94, pp. 505-10, Apr 15 2013.
[154] G. Cai, H. Jiang, Z. Chen, K. Tu, L. Wang, and K. Zhu, "Synthesis, characterization and self-assemble behavior of chitosan-O-poly (ε-caprolactone)," *European Polymer Journal,* vol. 45, pp. 1674-1680, 2009.
[155] C. Gu, V. Le, M. Lang, and J. Liu, "Preparation of polysaccharide derivates chitosan-graft-poly(varepsilon-caprolactone) amphiphilic copolymer micelles for 5-fluorouracil drug delivery," *Colloids Surf B Biointerfaces,* vol. 116, pp. 745-50, Apr 1 2014.
[156] H. Feng and C.-M. Dong, "Preparation and characterization of chitosan-graft-poly (ε-caprolactone) with an organic catalyst," *Journal of Polymer Science Part A: Polymer Chemistry,* vol. 44, pp. 5353-5361, 2006.
[157] L. Liu, Y. Wang, X. Shen, and Y. Fang, "Preparation of chitosan-g-polycaprolactone copolymers through ring-opening polymerization of epsilon-caprolactone onto phthaloyl-protected chitosan," *Biopolymers,* vol. 78, pp. 163-70, Jul 2005.
[158] R. A. Muzzarelli and R. Rocchetti, "Determination of the degree of acetylation of chitosans by first derivative ultraviolet spectrophotometry," *Carbohydrate Polymers,* vol. 5, pp. 461-472, 1985.
[159] R. Signini and S. P. Campana Filho, "Purification and characterization of commercial chitosan," *Polímeros,* vol. 8, pp. 63-68, 1998.
[160] M. R. Kasaai, "A review of several reported procedures to determine the degree of N-acetylation for chitin and chitosan using infrared spectroscopy," *Carbohydrate Polymers,* vol. 71, pp. 497-508, 2008.
[161] M. Wiens, T. A. Elkhooly, H.-C. Schröder, T. H. Mohamed, and W. E. Müller, "Characterization and osteogenic activity of a silicatein/biosilica-coated chitosan-graft-polycaprolactone," *Acta biomaterialia,* vol. 10, pp. 4456-4464, 2014.
[162] S. Nsereko and M. Amiji, "Localized delivery of paclitaxel in solid tumors from biodegradable chitin microparticle formulations," *Biomaterials,* vol. 23, pp. 2723-2731, 2002.
[163] T. Mosmann, "Rapid colorimetric assay for cellular growth and survival: application to proliferation and cytotoxicity assays," *Journal of immunological methods,* vol. 65, pp. 55-63, 1983.
[164] I. Aranaz, M. Mengíbar, R. Harris, I. Paños, B. Miralles, N. Acosta, *et al.*, "Functional characterization of chitin and chitosan," *Current Chemical Biology,* vol. 3, pp. 203-230, 2009.
[165] D. Liu, Y. Wei, P. Yao, and L. Jiang, "Determination of the degree of acetylation of chitosan by UV spectrophotometry using dual standards," *Carbohydrate research,* vol. 341, pp. 782-785, 2006.
[166] H. Y. Hsiao, C. C. Tsai, S. Chen, B. C. Hsieh, and R. L. Chen, "Spectrophotometric determination of deacetylation degree of chitinous materials dissolved in phosphoric acid," *Macromolecular bioscience,* vol. 4, pp. 919-921, 2004.
[167] S. C. Tan, E. Khor, T. K. Tan, and S. M. Wong, "The degree of deacetylation of chitosan: advocating the first derivative UV-spectrophotometry method of determination," *Talanta,* vol. 45, pp. 713-719, 1998.
[168] Z. Wang, L. Zheng, C. Li, D. Zhang, Y. Xiao, G. Guan, *et al.*, "A novel and simple procedure to synthesize chitosan-graft-polycaprolactone in an ionic liquid," *Carbohydrate polymers,* vol. 94, pp. 505-510, 2013.
[169] C. R. Huei and H.-D. Hwa, "Effect of molecular weight of chitosan with the same degree of deacetylation on the thermal, mechanical, and permeability properties of the prepared membrane," *Carbohydrate polymers,* vol. 29, pp. 353-358, 1996.

[170] A. Sionkowska, M. Wisniewski, J. Skopinska, C. Kennedy, and T. Wess, "Molecular interactions in collagen and chitosan blends," *Biomaterials,* vol. 25, pp. 795-801, 2004.
[171] P. Hendra, W. Maddams, I. Royaud, H. Willis, and V. Zichy, "The application of Fourier transform Raman spectroscopy to the identification and characterization of polyamides—I. Single number nylons," *Spectrochimica Acta Part A: Molecular Spectroscopy,* vol. 46, pp. 747-756, 1990.
[172] P. R. Griffiths and J. A. De Haseth, *Fourier transform infrared spectrometry* vol. 171: John Wiley & Sons, 2007.
[173] L. Mu and S. Feng, "A novel controlled release formulation for the anticancer drug paclitaxel (Taxol®): PLGA nanoparticles containing vitamin E TPGS," *Journal of controlled release,* vol. 86, pp. 33-48, 2003.
[174] F. Danhier, N. Lecouturier, B. Vroman, C. Jérôme, J. Marchand-Brynaert, O. Feron, *et al.*, "Paclitaxel-loaded PEGylated PLGA-based nanoparticles: *in vitro* and *in vivo* evaluation," *Journal of Controlled Release,* vol. 133, pp. 11-17, 2009.
[175] M. Garinot, V. Fiévez, V. Pourcelle, F. Stoffelbach, A. des Rieux, L. Plapied, *et al.*, "PEGylated PLGA-based nanoparticles targeting M cells for oral vaccination," *Journal of Controlled Release,* vol. 120, pp. 195-204, 2007.
[176] A. Potineni, D. M. Lynn, R. Langer, and M. M. Amiji, "Poly (ethylene oxide)-modified poly (β-amino ester) nanoparticles as a pH-sensitive biodegradable system for paclitaxel delivery," *Journal of Controlled Release,* vol. 86, pp. 223-234, 2003.
[177] Z. Wei, J. Hao, S. Yuan, Y. Li, W. Juan, X. Sha, *et al.*, "Paclitaxel-loaded Pluronic P123/F127 mixed polymeric micelles: formulation, optimization and *in vitro* characterization," *International journal of pharmaceutics,* vol. 376, pp. 176-185, 2009.
[178] T. Yang, M.-K. Choi, F.-D. Cui, J. S. Kim, S.-J. Chung, C.-K. Shim, *et al.*, "Preparation and evaluation of paclitaxel-loaded PEGylated immunoliposome," *Journal of Controlled Release,* vol. 120, pp. 169-177, 2007.
[179] C. Wang, Y. Wang, Y. Wang, M. Fan, F. Luo, and Z. Qian, "Characterization, pharmacokinetics and disposition of novel nanoscale preparations of paclitaxel," *International journal of pharmaceutics,* vol. 414, pp. 251-259, 2011.
[180] E. Raymond, A. Hanauske, S. Faivre, E. Izbicka, G. Clark, E. K. Rowinsky, *et al.*, "Effects of prolonged versus short-term exposure paclitaxel (Taxol (R)) on human tumor colonyforming units," *Anti-cancer drugs,* vol. 8, pp. 379-385, 1997.
[181] L. Zhang, Y. He, G. Ma, C. Song, and H. Sun, "Paclitaxel-loaded polymeric micelles based on poly (ε-caprolactone)-poly (ethylene glycol)-poly (ε-caprolactone) triblock copolymers: *in vitro* and *in vivo* evaluation," *Nanomedicine: Nanotechnology, Biology and Medicine,* vol. 8, pp. 925-934, 2012.
[182] R. Mo, X. Jin, N. Li, C. Ju, M. Sun, C. Zhang, *et al.*, "The mechanism of enhancement on oral absorption of paclitaxel by N-octyl-O-sulfate chitosan micelles," *Biomaterials,* vol. 32, pp. 4609-4620, 2011.
[183] U. K. Walle and T. Walle, "Taxol transport by human intestinal epithelial Caco-2 cells," *Drug metabolism and disposition,* vol. 26, pp. 343-346, 1998.
[184] E. Roger, F. Lagarce, E. Garcion, and J.-P. Benoit, "Lipid nanocarriers improve paclitaxel transport throughout human intestinal epithelial cells by using vesicle-mediated transcytosis," *Journal of Controlled Release,* vol. 140, pp. 174-181, 2009.
[185] Y.-H. Lin, F.-L. Mi, C.-T. Chen, W.-C. Chang, S.-F. Peng, H.-F. Liang, *et al.*, "Preparation and characterization of nanoparticles shelled with chitosan for oral insulin delivery," *Biomacromolecules,* vol. 8, pp. 146-152, 2007.
[186] N. Li, D. Wang, Z. Sui, X. Qi, L. Ji, X. Wang, *et al.*, "Development of an improved three-dimensional *in vitro* intestinal mucosa model for drug absorption evaluation," *Tissue Engineering Part C: Methods,* vol. 19, pp. 708-719, 2013.